



ΠΑΝΕΠΙΣΤΗΜΙΟ
ΙΩΑΝΝΙΝΩΝ

SCHOOL OF INFORMATICS AND TELECOMMUNICATIONS

DEPARTMENT OF INFORMATICS AND

TELECOMMUNICATIONS

MSc DEGREE IN INFORMATICS AND NETWORKS

MSc THESIS

MODELING OF ARTIFICIAL LIGHT PV CELL EVALUATION

SYSTEM

VASILIKI NASKARI

Supervisor: Gregory Doumenis

PhD EE, Assistant Professor

Arta, December 2022

Μοντελοποίηση Συστήματος Αξιολόγησης Φωτοβολταϊκών Στοιχείων

Approved by three-member examination committee

Arta, 6/12/2022

EXAMINATION COMITEE

1. Supervisor

Gregory Doumenis,

PhD EE, Assistant Professor

2. Committee member

Evipidis Glavas,

Department Dean, Professor

3. Committee member

Andreas Tsormpatzoglou,

PhD, Assistant Professor

© Naskari, Vasiliki, 2022.

Με επιφύλαξη παντός δικαιώματος. All rights reserved.

Non plagiarism statement

I declare responsibly and knowing the sanctions of Law 2121/1993 on Intellectual Property, that the present master's thesis is entirely the result of my own research work, is not a product of copying nor comes from assignment to third parties. All the sources used (of any kind, form, and origin) for its writing are included in the bibliography.

Naskari, Vasiliki

Signature

ACKNOWLEDGMENTS

First of all, I would like to thank Professor Gregory Doumenis for giving me the opportunity to perform this thesis and for the constant knowledge and experience sharing. I am thankful to all the time he spent with explanations and orientations, for his guidelines and constant support, which were essential to this work.

I am deeply grateful to the staff of the Autonomous Systems Laboratory, and more specifically to PhD student, Mr. Masklavanos, and to Postgraduate student, Mr. Koutsos, for helping me by providing the experimental device as well as helping me with the experimental procedure.

My heartfelt gratitude is expressed to my family, for their relentless support, understanding, and forbearing with me during the development of this thesis. Their contribution was essential to perform this work.

At last, but not least, I would like to thank all my friends for their support, patience and good company given. Their contribution has been important specially to lighten up the stress and to provide good leisure moments.

ΠΕΡΙΛΗΨΗ

Αντικείμενο της παρούσας εργασίας αποτελεί η εύρεση μαθηματικών μοντέλων με σκοπό την ορθή αξιολόγηση και προσδιορισμού των χαρακτηριστικών ενός συστήματος εξομοίωσης τεχνητών φωτεινών πηγών. Αρχικά, γίνεται αναφορά στις θεμελιώδεις έννοιες: της Ραδιομετρίας και της Φωτομετρίας, δίνοντας έμφαση στις φωτομετρικές ποσότητες. Έπειτα, παρουσιάζεται μία ανάλυση των LEDs ως φωτεινές πηγές. Στη συνέχεια, περιγράφεται μια τεχνική απεικόνισης που επιτρέπει την τρισδιάστατη αναπαράσταση της κατανομής της γωνιακής έντασης ακτινοβολίας ενός LED και παρέχεται μία μέθοδος υπολογισμού της ακτινοβολίας του φωτός που εκπέμπεται από ένα LED με χρήση ενός συστήματος αναλυτικών εξισώσεων. Επίσης, προτείνονται συνθήκες για τη μέτρηση ή τη μοντελοποίηση της διάδοσης του φωτός υπό συγκεκριμένες συστοιχίες LEDs, συναρτήσει της απόστασης, της γεωμετρίας, της διάταξης και του αριθμού των LEDs. Επιπρόσθετα, παρουσιάζεται μια μεθοδολογία εξαγωγής συμπερασμάτων (οδηγίες σχεδιασμού περιοχών φωτοβολίας) ικανή να μεγιστοποιήσει την ομοιομορφία. Επιπλέον, πραγματοποιείται προσομοίωση ενός τέτοιου συστήματος μέσω του περιβάλλοντος MATLAB και παρουσιάζονται τα αποτελέσματα για τοπολογίες LED (2x2, 4x4 και 6x6). Τέλος, τα ανωτέρω ευρήματα για τοπολογία 2x2 συγκρίνονται μέσω εργαστηριακών μετρήσεων χρησιμοποιώντας διάταξη αξιολόγησης φωτοβολταϊκών στοιχείων. Τα αποτελέσματα των προσομοιώσεων συγκρίνονται με τις εργαστηριακές μετρήσεις.

Λέξεις-κλειδιά: μοντελοποίηση, φωτοβολταϊκό στοιχείο εσωτερικού χώρου, LED, ραδιομετρία, φωτομετρία.

ABSTRACT

In this work we propose a mathematical modelling approach to properly determine and evaluate the characteristics of an artificial light source simulation system. First, fundamental concepts such as Radiometry and Photometry are stated, emphasizing the photometric quantities. An analysis of LEDs as light sources is presented. Subsequently, we present the three-dimensional representation of the angular intensity distribution of an LED and describe a method for calculating the irradiance of the light emitted by an LED using a system of analytical equations. Specific LED arrays topologies are investigated in terms of irradiance intensity as a function of spacing, geometry, arrangement, and number of LEDs. Additionally, an iterative methodology is presented for deriving optimal LED plane distance from the DUT surface -in terms of maximizing irradiance for given uniformity constraints. We implement the methodology into a MATLAB program and provide simulation results for practical LED topologies (2x2, 4x4 and 6x6). Finally, the above findings for the 2x2 topology were verified in the context of a laboratory experiment using a custom light simulator. The simulation results compare favorably with the obtained measurements.

Keywords: modeling, indoor photovoltaic cell, LED, radiometry, photometry.

TABLE OF CONTENTS

ACKNOWLEDGMENTS.....	iv
ΠΕΡΙΛΗΨΗ.....	v
ABSTRACT.....	vi
TABLE OF CONTENTS.....	vii
LIST OF TABLES.....	ix
LIST OF FIGURES.....	x
TABLE OF ABBREVIATIONS (ACRONYMS).....	xiii
INTRODUCTION.....	1
1 Natural and Artificial light sources.....	5
1.1 Nature of Light.....	7
1.2 Artificial light sources.....	13
1.3 Need for Light simulators.....	21
1.4 Architecture and characteristics of Light simulators.....	23
1.5 Radiometry & Photometry.....	26
1.6 Photometric Quantities.....	30
1.6.1 Color Space / White Color.....	30
1.6.2 MacAdam Ellipses.....	32
1.6.3 Correlated Color Temperature.....	33
1.6.4 Spectral Power Distribution.....	35
1.6.5 Color rendering.....	38
1.6.6 Characteristics of light sources.....	41
2 LEDs as light sources.....	43
2.1 Light Emitting Diode.....	43
2.2 Efficiency and Operating parameters.....	44
2.3 Types of LEDs.....	49
2.4 Advantages and disadvantages of LEDs.....	56

3	Modeling a multisource light simulator	60
3.1	Single LED light simulator model	60
3.1.1	FWHM	62
3.1.2	Convert Spherical coordinates to Cartesian	63
3.2	multi-LED light simulator model	64
3.2.1	Two (2) – LED Array	64
3.2.2	Circular Ring Array	67
3.2.3	Circular Ring Array with One LED in the Center	69
3.2.4	Linear Array	72
3.2.5	Square LED Array	74
3.2.6	Triangular LED Array	77
3.3	multi-LED light simulator design guidelines	80
4	Experimental Investigation	89
4.1	Experimental LED light simulator setup	90
4.2	Single LED measurements	93
4.3	2x2 matrix measurements	100
5	Evaluation and interpretation of results	105
5.1	Evaluation	105
5.1.1	Uniformity of illumination distribution	105
5.1.2	ΔE	105
5.1.3	R (Ratio)	106
6	Conclusion	107
7	Future Work	108
	APPENDIX	109
	BIBLIOGRAPHY	112

LIST OF TABLES

TABLE 1.1 Range of the visible spectrum	7
TABLE 1.2 Different types of light simulators along with their characteristics.....	18
TABLE 1.3 Light sources' Luminous Efficacy.	21
TABLE 1.4 Light simulators' field of applications.	22
TABLE 1.5 Solar Simulator's Classification according to the IEC 60904-9 standard.....	24
TABLE 1.6 Quantity Measured vs. Visible Light - Total Radiant Power.	36
TABLE 1.7 Comparison of electromagnetic spectrum.	37
TABLE 1.8 Light Sources – CRI [18].	40
TABLE 2.1 Wavelength - Typical Efficiency.....	47
TABLE 2.2 Semiconductor materials by wavelength.....	49
TABLE 3.1 Square LED topologies examination.....	82
TABLE 4.1 Light source's main characteristics.....	93
TABLE 4.2 System Variables.....	94
TABLE 4.3 Measured -Expected Illuminance - Single LED Topology.	97
TABLE 4.4 Measured -Expected Illuminance - Square LED Topology.	102

LIST OF FIGURES

Figure 1.1 Sun - the major natural source on Earth.....	5
Figure 1.2 The visible Spectrum	6
Figure 1.3 Solar spectrum	8
Figure 1.4 Solar spectrum and atmospheric absorbing gases from 240 nm to 2.5 μm wavelengths.....	9
Figure 1.5 The EM from lowest energy/longest wavelength (at the top).....	10
Figure 1.6 World map of surface downwelling solar radiation for the period 1981-2010.....	11
Figure 1.7 Starlight.....	12
Figure 1.8 Lightnings [14]	12
Figure 1.9 Incandescent Lamp	14
Figure 1.10 Halogen Lamp.....	15
Figure 1.11 Gas-discharge Lamp	16
Figure 1.12 RGB Light Emitting Diode.....	18
Figure 1.13 Solar Simulator [18].....	21
Figure 1.14 Color space	31
Figure 1.15 MacAdam Ellipses.....	33
Figure 1.16 Correlated Color temperature	34
Figure 1.17 Intensity - Wavelength.....	37
Figure 1.18 Typical Spectrum.....	38
Figure 1.19 Color Rendering Index [26].....	39
Figure 2.1 Light Emitting Diodes	43
Figure 2.2 LED VS Traditional Light Sources [28].....	44
Figure 2.3 LED lamp components	46
Figure 2.4 DIP LED	49
Figure 2.5 LED SMD.....	50
Figure 2.6 COB LED	51
Figure 2.7 RGB Common Clear Cathode LED.....	52
Figure 2.8 LED tube.....	53
Figure 2.9 High power LED.....	55
Figure 2.10 Graphene LED bulbs	56
Figure 3.1 Cartesian and Spherical coordinate system [33]	61
Figure 3.2 Full Width at Half Maximum [34].....	63
Figure 3.3 Schematic of a Two-LED array [36].	65
Figure 3.4 Two-LEDs array's uniform distribution [36].	66
Figure 3.5 Two-LEDs uniform distribution (with increased distance between LEDs) [36].	67

Figure 3.6 Schematic of a Circular Ring array [36].	67
Figure 3.7 Circular LED array's Irradiance pattern [36].	69
Figure 3.8 Circular LED array's normalized irradiance distribution along the x direction at y=0 [36].	69
Figure 3.9 Schematic of a Circular Ring array with one LED in the center [36].	70
Figure 3.10 Circular Ring array with one middle LED array's uniform Irradiance distribution [36].	71
Figure 3.11 Schematic of a Linear array [36].	72
Figure 3.12 Linear LED array's uniform Irradiance distribution [36].	74
Figure 3.13 Linear LED array's normalized irradiance distribution along the x direction at y=0 [35].	74
Figure 3.14 Schematic of a Square array [36].	75
Figure 3.15 Square LED array's uniform Irradiance distribution [36].	76
Figure 3.16 Square LED array's normalized irradiance distribution along the x direction at y=0 [36].	77
Figure 3.17 Schematic of a Triangular array [36].	77
Figure 3.18 Triangular LED array's uniform Irradiance distribution [36].	79
Figure 3.19 Triangular LED array's normalized irradiance distribution along the x direction at y=0 [36].	79
Figure 3.20 2x2 LED array's critical value.	83
Figure 3.21 Illuminance distribution - Critical_Value(0.081).	83
Figure 3.22 Illuminance heatmap - Critical_Value(0.081) (2).	84
Figure 3.23 4x4 LED array's Critical Value.	85
Figure 3.24 6x6 LED array's Critical Value.	87
Figure 3.25 Illuminance distribution - Critical_Value(0.019).	88
Figure 3.26 Illuminance distribution - Critical_Value (0.019) (2).	88
Figure 4.1 The Light Simulator used	90
Figure 4.2 Experimental setup, LED array's arrangement.	91
Figure 4.3 (a) Typical Angular Pattern of Radiant Power, (b) Forward Voltage vs. Forward Current.	92
Figure 4.4 LED's position	95
Figure 4.5 Simulated Illuminance	95
Figure 4.6 Comparison of Illumination curves. (a) Expected Illumination curve, (b) Measured Illumination curve.	98
Figure 4.7 Comparison of contour graphs. (a) Expected Irradiance contour graph, (b) Measured Irradiance contour graph.	99
Figure 4.8 LEDs positions.	100
Figure 4.9 Simulated Illuminance.	101
Figure 4.10 Comparison of Illumination curves for the 2x2 LED array. (a) Expected Illumination curve, (b) Measured Illumination curve.	103

Figure 4.11 Comparison of contour graphs for 2x2 LED array. (a) Expected Irradiance contour graph, (b) Measured Irradiance contour graph.....	104
Figure AI.1 Solid angle	109
Figure AI.2 Inverse Square Law [41].....	110
Figure AII.1 Turning Points	111

TABLE OF ABBREVIATIONS (ACRONYMS)

<i>Abbreviation</i>	<i>Definition</i>
AC	Alternating Current
AMOLED	Active-Matrix Organic Light Emitting Diode
ASTM	American Society for Testing and Materials
Br	bromine
CCT	Correlated Color Temperature
cd	candela
CFL	Compact Fluorescent Lamp
CIE	International Commission on Illumination (from Commission Internationale de l' Eclairage)
COB	Chop On Board
CRI	Color Rendering Index
DC	Direct Current
DIP	Dual in line Package
$E_{e,\Omega}$	Radiant Intensity
EM	Electromagnetic Spectrum
E_v	Illuminance
FWHM	Full Width at Half Maximum
HBLED	High Brightness Light Emitting Diode
HPS	High - Pressure sodium
I	iodine
I_e	Irradiance
IEC	International Electrotechnical Commission
IR	Infrared Radiation
IV	Current - Voltage
I_v	Luminous Intensity
$L_{e,\Omega}$	Radiance

LEC	Light emitting Electrochemical Cell
LED	Light Emitting Diode
lm	lumen
LPS	Low - Pressure sodium
LTI	Long - term instability
L_v	Luminance
OEL	Organic Electroluminescent
OLED	Organic Light Emitting Diode
PCB	Printed Circuit Board
PMOLED	passive matrix organic light emitting diode
PV	Photovoltaic
SMD	Surface Mount Device
SPD	Spectral Power Distribution
sr	steradian
SRC	Standard Reporting Condition
STI	Short - term instability
TFT	Thin Film Transistor
UHP	Ultra-High Pressure
UV	Ultraviolet
UVA	Ultraviolet A, 320-400nm
UVB	Ultraviolet B, 290-230nm
UVC	Ultraviolet C, 200-290nm
V	Volt
V_λ	luminous efficacy
W	tungsten
W	Watt
Xe	xenon
σ	standard deviation
Φ_e	Radiant Flux
Φ_v	luminous flux

INTRODUCTION

The energy demands of almost all countries around the world are steadily increasing, due to large-scale industrial expansion, increasing population, and continuous growth in energy consumption per capita. It should be emphasized that electricity makes up the majority of the needed energy. On the other hand, due to growing environmental concerns and a shortage of resources, the usage of fossil fuels for energy generation reached saturation levels [1].

Indeed, more environmentally friendly, cost-effective, and sustainable solutions must be discovered if today's society is to meet its energy needs. Thus, Renewable Energy Sources (RES) would fill any gaps between future demand and generation. The energy we receive through solar radiation and the energy from artificial light sources are the most promising types of renewable energy that have the potential to bridge the gap between production and consumption, given the significant advances in technology and cost reduction [2].

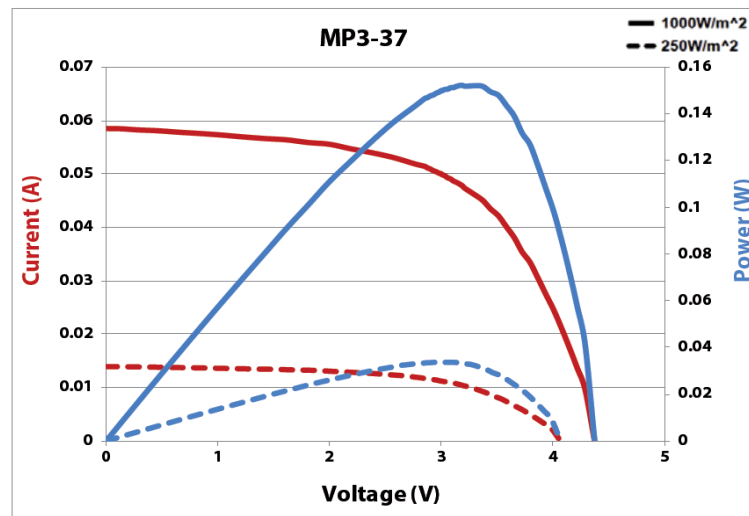
At the same time, the Internet of Things managed to invade the daily life of most of the world's population at an extremely fast pace. If we consider the important role that the Internet of Things plays in people's daily lives, we can claim that through the connectivity of many physical devices through the internet, it has brought new forms of communication. These new forms of communication have become possible between things and people as well as between things themselves, allowing the exchange of data for remote monitoring and control of devices from any location in the world with an internet connection [3].

As we already mentioned above, the most widely known energy harvested technique is photovoltaics. It is obvious - amid the great interest and findings of the research community - high power photovoltaic cells convert solar light into kW or MWs of electricity with an irradiance density of 1000W/m^2 (1 sun) in ideal weather conditions. Modern commercial photovoltaic cells can reach up to 20% conversion efficiency [4]. In contrast to solar light, the results of research concerning indoor lighting and their efficiency are dramatically reduced.

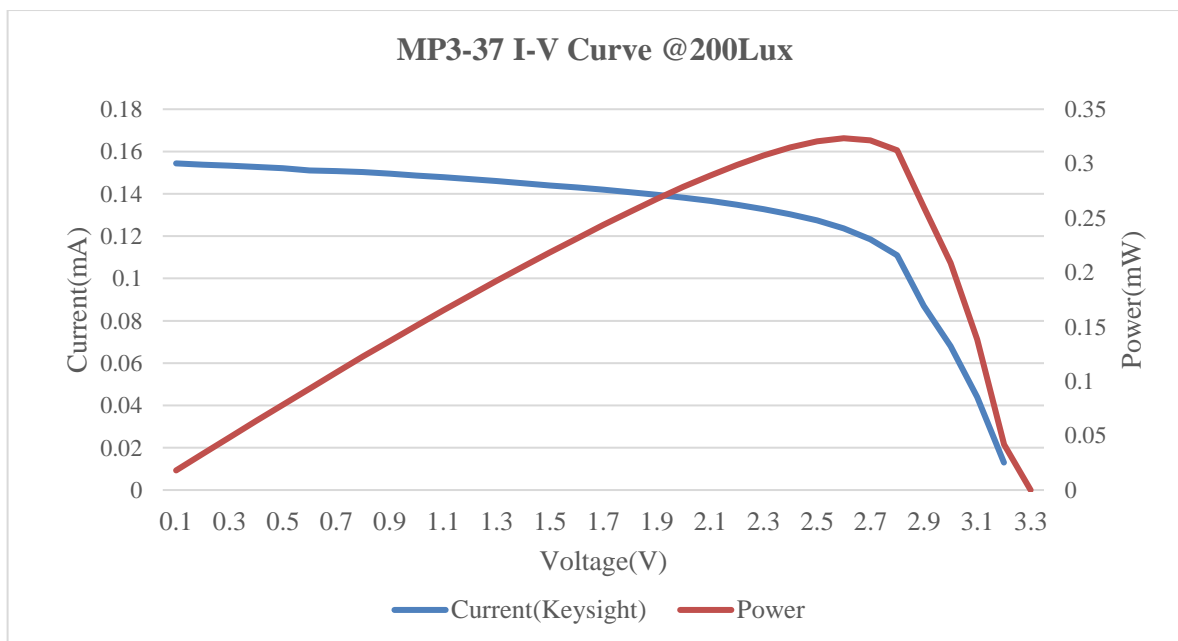
In recent years the demand for an accurate description of these specialized photovoltaic cells has been increased, due to the ever-increasing interest in utilizing indoor light as a power source for ultra-low-power Internet of Things devices. Most commercially available

PV cells are measured at an irradiance range between 1 and 0.25 suns. Their behavior in lower light irradiances is not properly documented, thus their actual performance cannot be guaranteed.

For example, during the evaluation of an indoor photovoltaic cell, deviations are observed compared to the values listed in datasheets and the values that are finally measured. As it is shown in the following graphs, when evaluating MP3-37 [5], I/V curves are given by the manufacturer for the standard 1 sun as well as the ¼ sun. Observing the second graph, we realize that in low Irradiance, we obtain 1000 less power and at a very different Voltage.



Graph 1 MP3-37 I/V curve [5]



Graph 2 MP3-37 I/V curve (measurements)

To better evaluate such devices, light simulators are used. These devices can simulate light under controlled conditions. They are used not only to evaluate the performance of photovoltaic cells, but also to evaluate cosmetics, electronic circuits, etc.

The coexistence of all the previous ones, led to the absolute need for the characterization of photovoltaic cells under artificial light or natural low light conditions. Unfortunately, most PV cell data are provided for “standard sun” exposures and/or with low resolution graphs in the datasheets, thus inappropriate to extrapolate low light behavior with reasonable accuracy. This has created needs in terms of validating photovoltaic cells in the aforementioned conditions.

However, despite the difficulties presented, a motive that triggered this work was the fact that despite the existence of light simulators - when they are available - they are extremely expensive. Therefore, because of the need created for the evaluation of indoor photovoltaic cells (not exclusively), this work can also both provide answers to questions of general interest regarding light sources, as well as provide solutions and design guidelines for light simulators.

More specifically, in the first chapter, natural and artificial light sources are analyzed. Emphasis is also placed on light simulators as well as the need for such devices, their architecture, and characteristics. Additionally, some of the most well-known photometric quantities are listed.

In the second chapter, LEDs are described as light sources. More specifically, the efficiency of LEDs and their operating parameters are analyzed, and their different types are presented as well as their advantages and disadvantages.

In the third chapter, the methodology followed to model a multi-source light simulator is described. First, the process by which a single LED is modeled is described and then possible topologies for multi-LEDs are described, such as linear, circular, square, triangular, etc. Also, design guidelines are provided to maximize uniformity as well as optimal illuminance of a test plane.

In the fourth chapter, reference is made to an experimental investigation, that contains the experimental setup of an LED light simulator, and measurements for both single LED arrays and 2x2 matrix measurements.

In the fifth chapter, all the information that was mentioned in the previous chapters is evaluated. The evaluation methods are described and then the interpretation of all the conclusions is made.

Chapters 6 and 7 conclude this thesis, referring to the conclusions drawn as well as the future work that follows this text.

1 Natural and Artificial light sources

It is a fact that there is the possibility to observe things that happening all around us due to the existence of light. There are numerous circumstances in which light is perceived, investigated, and used, hence there is no one definitive response to the seemingly simple question “What is light?”. The physical characteristics of light have been of interest to physicists, whereas enhance the properties of the visual world is of interest to artists. Light is a fundamental tool for understanding the world and interacting with it through the sense of sight.

The Sun’s light warms the Earth (Fig. 1.1), influences regional weather patterns, and initiates the process of photosynthesis that sustains life. At the most fundamental level, light’s interactions with matter have influenced the universe’s structure. Indeed, light offers a window through into universe at all scales, from the cosmic to the atomic. Electromagnetic radiation is the principal method of communication between the rest of the universe and Earth [6].

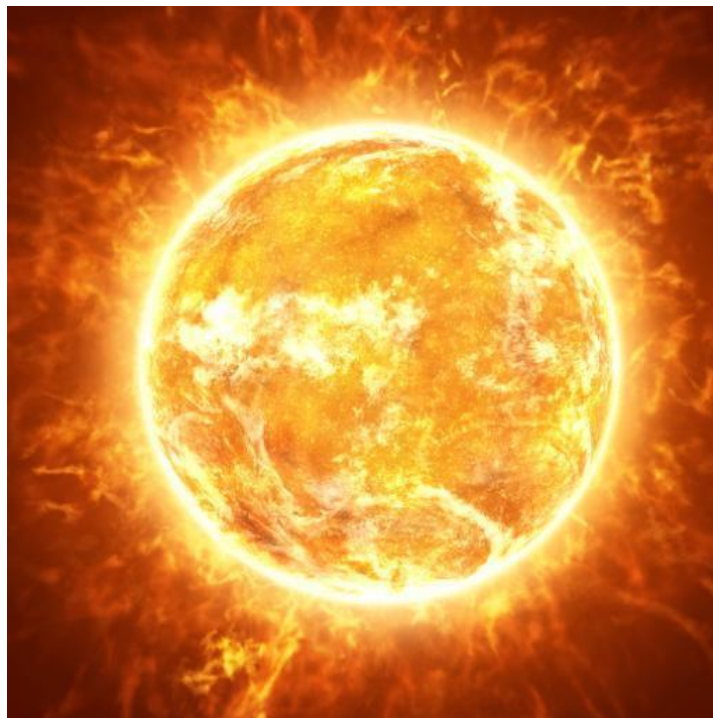


Figure 1.1 Sun - the major natural source on Earth

Light can emanate from a wide variety of sources. A body emits a distinctive spectrum of black body radiation at a specific temperature. Sunlight is a convenient thermal source because of the fact that when plotted in wavelength units, the radiation released by the Sun's chromosphere at about 6000 Kelvins (5730 degrees Celsius; 10340 degrees Fahrenheit) peaks in the visible portion of the electromagnetic spectrum and that the visible portion of sunlight that reaches the ground is about 44%.

Another instance is the energy output of incandescent light bulbs, which only emit around 10% of its energy as visible light and the rest as infrared (Fig. 1.2). The blazing solid particles in fires have historically been a common source of thermal light, although they primarily generate infrared radiation with a small amount of visible radiation.

For comparatively cool objects like people, the apex of the black body spectrum lies in the deep infrared, at a wavelength of around 10 micrometers (TABLE 1.1). The peak changes to shorter wavelengths as the temperature rises, first emitting a red glow, then a white glow, and finally a blue-white glow when the peak enters the ultraviolet region of the spectrum. The pure blue color usually seen in gas flames or welding torches [7].

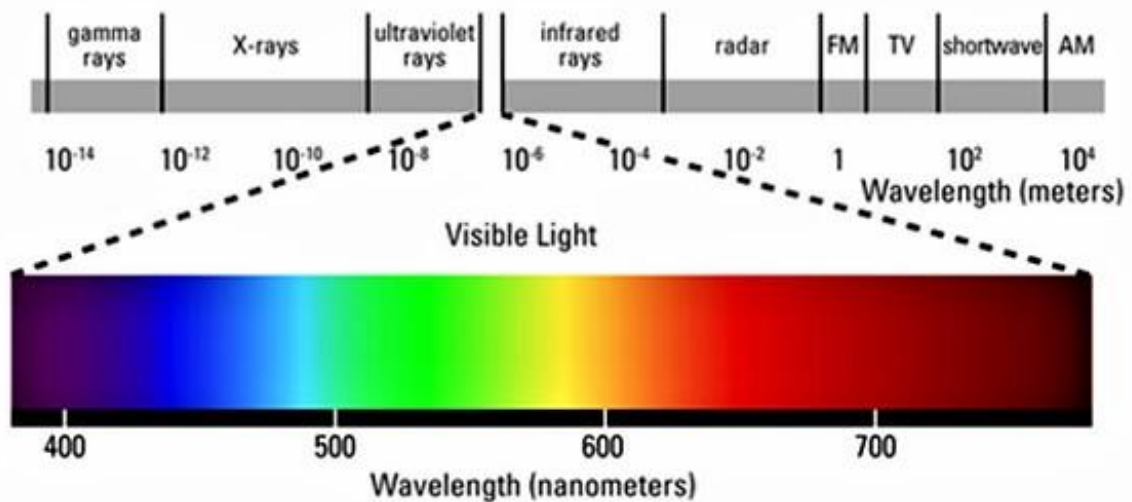


Figure 1.2 The visible Spectrum

Color*	Wavelength (nm)	Frequency (10¹⁴ Hz)	Energy (eV)
Red (limit)	700	4.29	1.77
Red	650	4.62	1.91
Orange	600	5.00	2.06
Yellow	580	5.16	2.14
Green	550	5.45	2.25
Cyan	500	5.99	2.48
Blue	450	6.66	2.75
Violet (limit)	400	7.50	3.10

TABLE I Range of the visible spectrum

1.1 Nature of Light

The region of the electromagnetic spectrum that the human eye perceives as light, or visible light, is made up of electromagnetic radiation. Typically, visible light is characterized as having wavelengths between 400 and 700 nanometers (nm) as shown in Fig 1.3 [8], or frequencies between 750 and 420 terahertz, which drop down between the longer wavelength infrared and the shorter wavelength ultraviolet (with shorter wavelengths).

The term “light” in physics has the potential to be used to describe electromagnetic radiation of any wavelength more broadly, whether visible or not. Gamma rays, X-rays, microwaves, and radio waves are all forms of light in this sense. Intensity, propagation direction, frequency or wavelength spectrum, and polarization are the four main characteristics of light. One of the basic constants of nature is the speed of light in a vacuum, which is 299.792.458 meters per second (m/s).

More specifically, the range of electromagnetic radiation's frequencies, along with their corresponding wavelengths and photon energies, is known as the electromagnetic spectrum.

The electromagnetic spectrum encompasses electromagnetic waves with frequencies in between Hertz and above 1025 Hertz, or wavelengths ranging thousands of kilometers and a significant subset of the size of an atomic nucleus.

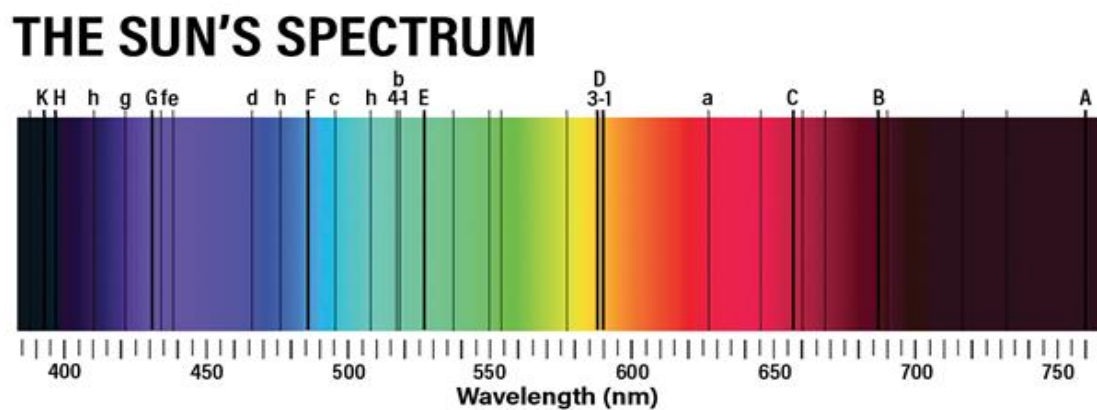


Figure 1.3 Solar spectrum

The electromagnetic waves observed within each of these bands are referred to by a different name; initiating at the low frequency (long wavelength) end of the spectrum, these are radio waves, microwaves, infrared, visible light, ultraviolet, X-rays, and gamma rays. This frequency range is divided into separate bands [9].

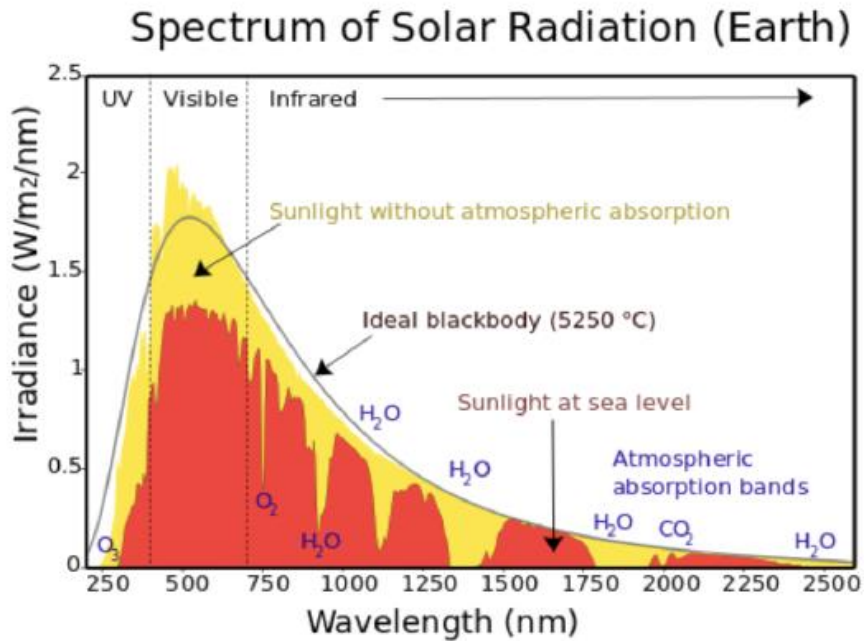


Figure 1.4 Solar spectrum and atmospheric absorbing gases from 240 nm to 2.5 μm wavelengths.

In terms of this generation, interactions with matter, and potential uses, the electromagnetic waves in each of these bands differ from one another. Both long and short wavelengths have no known limits.

Ionizing radiation includes the ultra-violet spectrum, soft X-rays, hard X-rays, and gamma rays because their photons are powerful enough to ionize atoms and cause chemical reactions. Exposure to ionizing radiation carries the potential for radiation sickness, cancer, and DNA damage. Longer wavelengths and visible light radiation are categorized as non-ionizing radiation, as their energies are insufficient to cause these effects.

Spectroscopy can be used to distinguish waves of varying frequencies across the majority of the electromagnetic spectrum, resulting in a spectrum of individual frequencies. The interactions of electromagnetic waves with matter are evaluated using spectroscopy. In the following Fig. 1.5, several instances in which we have the potential daily encounters with each region of the Electromagnetic Spectrum (EM) [10].

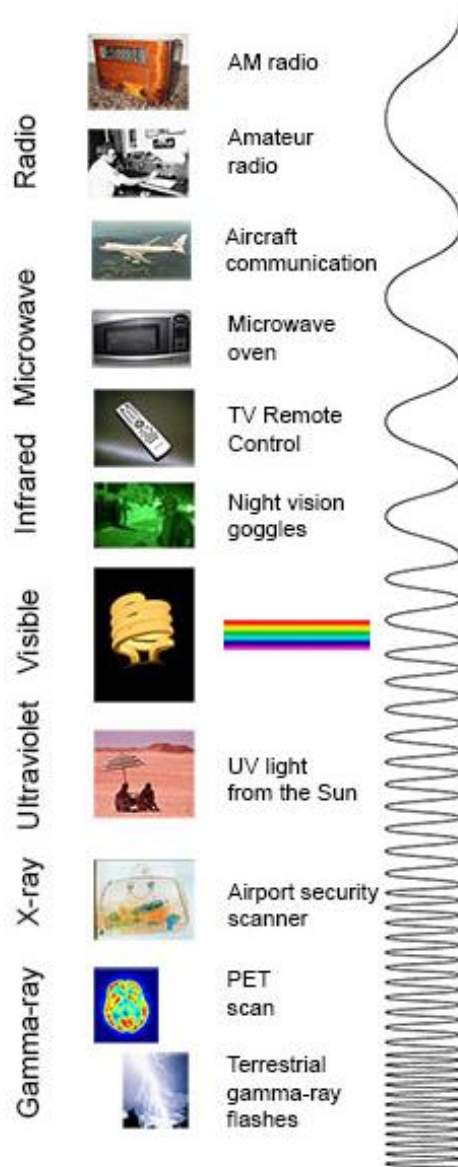


Figure 1.5 The EM from lowest energy/longest wavelength (at the top) to highest energy/shortest wavelength (at the bottom).

There are numerous things in our universe that produce their own light. The earth's surface can absorb some of the light from these sources. The following list contains elements that can emit light that have been found in nature [11].

- *Sun*

One of the main sources of light for our planet is the Sun. The Sun is depicted as a massive ball of fire that generates enormous amounts of energy through nuclear fusion at its core.

On Earth, sunlight is reflected and filtered by the atmosphere, and when the Sun is above the horizon, it is seen as daytime. Sunlight is a combination of bright light and radiant heat that results from direct solar radiation that is not obstructed by clouds.

Furthermore, it is dispersed when it is reflected off other objects or obstructed by clouds. According to sources, the average solar radiation received by each square meter on Earth during a 24-hour period ranges from 164 to 340 Watts according to NASA, this corresponds to around 25% of the average annual solar radiation received by the planet. In Fig. 6 [12], the global distribution of incoming shortwave solar radiation averaged over the years 1981-2010 from the CHELSA-BIOCLIM+ data set is represented.

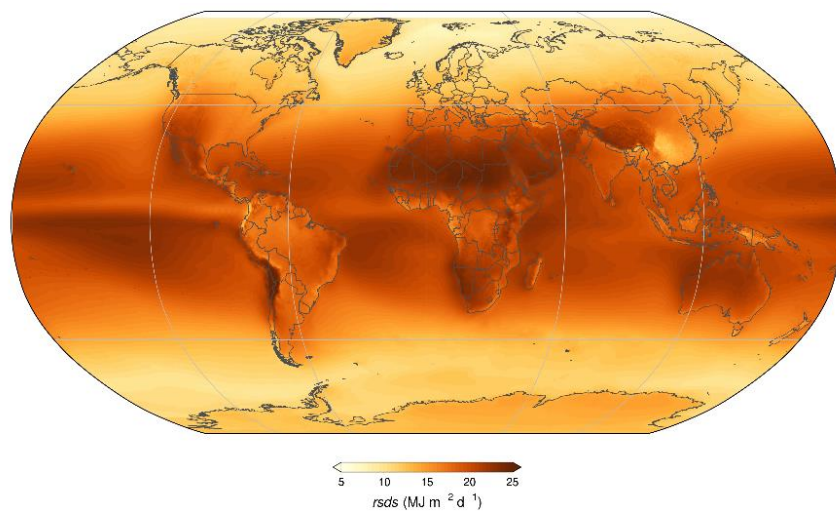


Figure 1.6 World map of surface downwelling solar radiation for the period 1981-2010

◦ Stars

Every star produces light (Fig. 1.7), nevertheless because of the immense distance that exists between Earth and these stars, only such a small amount -and occasionally none - of that light ever reaches the Earth's surface [13].



Figure 1.7 Starlight

◦ *Physical Phenomena*

Certain physical phenomena, such as volcanic eruptions or lightning (Fig. 1.8), also emit light.



Figure 1.8 Lightnings [14]

◦ *Living Organisms*

Several living organisms are also capable of generating their own light. They are known by the term of bioluminescence. Some of them are jellyfish, fireflies, light worms, etc.

1.2 Artificial light sources

In addition to natural sources, man-made sources can also produce light. Three categories can be used to categorize different artificial lights. These categories are incandescent sources, light sources, and gas discharge sources.

In the late 19th and early 20th centuries, electric energy sources were utilized to generate artificial lighting. The purpose of the technology innovations for artificial lighting is to achieve illumination that will approximate natural daylight (sunlight). The frequency range of an artificial light source and the amount of illumination, expressed in lumens, are the two metrics used to quantify and evaluate the artificial light.

Humanity's existence has been profoundly revolutionized by artificial electric light sources. It gives the ability for activities after dusk, altered workers' daily schedules, and extended the hours for leisure and social interaction. In the context of the continuously growing need, it offered enormous incentive in upgrading and extending energy supplies, that consequently led to help many countries' economies thrive globally.

Next, we refer to a list summarizing the types in which we can claim to distinguish the sources from which we can obtain artificial light, up to current technologies [15].

- First Generation

Incandescent Lamps

A typical contemporary incandescent lamp is mainly composed of a glass bulb that is vacuum filled with a metal wire filament comprised of tungsten (W). High electrical resistance is observed in the wire filament. When an electrical current flows through this wire filament, collisions between the wire's electrons and atoms cause the wire to become incandescent (i.e., glow), and emit light.

In order to increase the lamp's lifespan and maintain the quality of the light, the lamp is occasionally supplied with a noble gas (such as argon), that leads to slow evaporation of the wire filament. This occurs because over time, incandescence induces the atoms of the wire filament to evaporate.

A wide variety of sizes, voltages, and electric powers are available in the production of incandescent lights. Because of its low efficiency of about 4%, the incandescent lamp's basic standard form is regarded as an energy waster. The halogen lamp, the fluorescent lamp, and other more affordable light sources were created throughout time. Many nations have restricted or even banned the use of incandescent bulbs in recent years due to growing awareness of the need to conserve energy for both practical and environmental reasons.



Figure 1.9 Incandescent Lamp

Halogen lamps

An incandescent lamp characterized as a halogen lamp typically does indeed have a tungsten (W) filament and is filled with a halogen gas, such as iodine (I) or bromine (Br). Halogen gas increases the lifespan of the lamp and enhances the quality of the light by reducing the quantity of tungsten gas vapor released by the filament.

As a result, the lamp may function at greater temperatures than a typical incandescent lamp filled with noble gas, improving lighting, and making better use of electrical energy while also boosting the lamp's efficiency (by approximately 10%). This characteristic enables the integration of comparatively smaller halogen bulbs into small-footprint illumination fixtures like floodlights.

Visible light is produced by halogen lamps (Fig. 1.10). Only a minor portion of the radiation released is in the UV spectrum. It is best to avoid extended exposure to this spectrum of radiation surrounding halogen lamps since part of it is ionizing and can lead to burns or skin cancer.

The quartz in the glass bulb is typically optically thickened or doped with a small quantity of UV-absorbing material that lessens the possibility of exposure to UV radiation. Another strategy is to put the halogen light inside of a glass casing to lessen the chance of burns. UVB radiations from halogen lamps is purposely employed in science and medicine, including dental procedures.

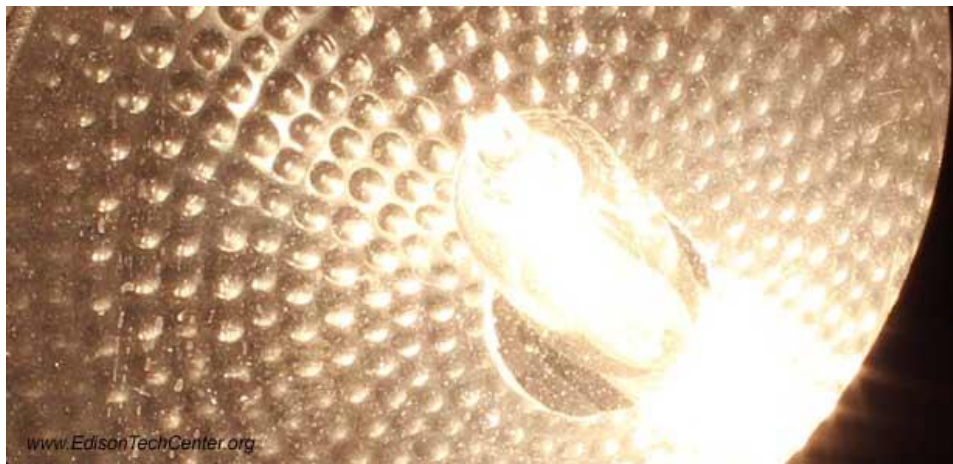


Figure 1.10 Halogen Lamp

- Second generation – gas discharge lamps.

To produce visible light, fluorescent lighting requires the electrical discharge of a gas (mercury) that releases high-energy photons (usually UV). These photons then interact with the fluorescent coating of the bulb.

The emission spectra of the atoms that comprises the gas, as well as the pressure of the gas, the current density, and other factors, affect the color of the light that has been generated. A variety of colors can be produced with gas discharge lamps (Fig. 1.11). Some of the light is emitted as UV radiation, which a fluorescent coating on the interior of the glass surface of the lamp transforms into visible light.

In addition to visible light, fluorescent tubes, and compact fluorescent lamps (CFLs) also emit a small amount of UV radiation with wavelengths between 315 and 380 nanometers (UVA) and even shorter wavelengths (but higher energy) with UVC. By maintaining the mercury containing CFL light sources at least 30 centimeters away from the viewer, UV radiation exposure could be prevented.

Gas-discharge lamps are more efficient than incandescent lamps, however they are more difficult to construct and most of them possess negative resistance, that causes the resistance on the plasma to diminish as the current flow rises.

The type of radiation emitted by fluorescent tubes and compact fluorescent lamps (CFL) include, in addition to visible light, a small amount of UV radiation in the UVA range (315-380 nanometers), and even shorter wavelengths (higher energy) in the UVC range.

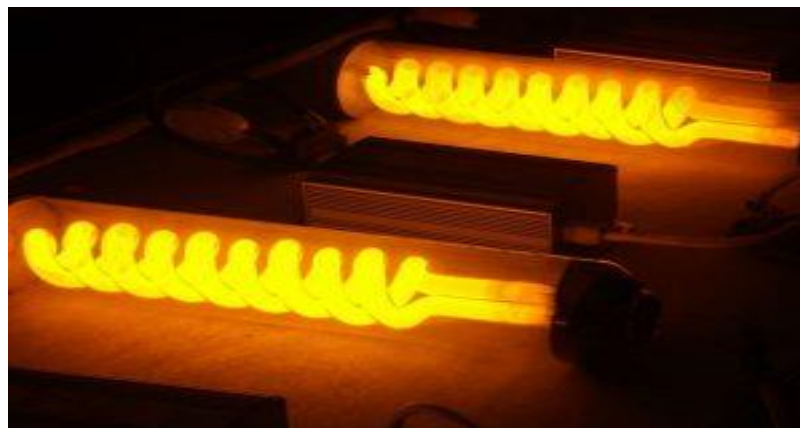


Figure 1.11 Gas-discharge Lamp

- Third generation – Light Emitting Diode (LED) lamps

The semiconductor utilized in a light-emitting diode (LED) has undergone doping¹. The atoms are excited to exceptionally high energies through an electric current

¹Doping: a technique where impurities are purposefully added to a semiconductor to increase its electrical conductivity (a semiconductor is a solid material that has intermediate electrical conductivity – between an insulator and a conductor).

flowing through the diode. Energy is released in the form of photons in the visible light spectrum when the atoms descend to lower energy levels.

More specifically, as it is known, an electric current can only flow in a single direction through a diode. At the meeting point of two different types of materials, a diode is produced (semiconductors). In what is described as a forward bias (directions), an alternating current is applied to the diode; in a reversed bias (directions), the current does not flow through the diode. When a direct electric current flows through the diode along its own bias, the diode also operates (direction).

Doped semiconductor is the main component of a light – emitting diode (LED). The semiconductor atoms in the diode undergo high – energy excitation when an electric current flows across it. The atoms release photons with visible light wavelengths as they naturally descend to lower levels. The characteristics of the materials that used to the construct the diode determine the wavelength of the light that is produced. LEDs don't always emit light in all directions.

Therefore, they must be placed together in a way that makes these functions possible. The diodes are embedded into a framework that resembles a regular incandescent bulb. LEDs generate significant lighting instantaneously in such a lamp. A fluorescent light does not turn on instantly, in comparison.

Despite the quality of LED bulbs has increased over time, their output and illuminating quality gradually deteriorate. LED bulbs are energy – sufficient and have longer lifespan (25,000 – 100,000 hours) (TABLE 1.2).

In today's world, CFLs and incandescent lamps are increasingly being replaced with white LED lighting. The switch to LED lighting will have a significant influence on worldwide energy saving because lighting accounts for nearly a quarter of all electricity usage.



Figure 1.12 RGB Light Emitting Diode

<i>Emission Technology</i>	<i>Spectral Match</i>	<i>Maximum Suns</i>	<i>Bulb Lifetime</i>	<i>Initial cost</i>	<i>Operating cost</i>
Xe	330-2500 nm	10,000	2,000	Medium	Medium
Metal Halide	300-1200nm	1,000	6,000	Medium	Medium
Tungsten Halogen	400-2500nm	25	2,000	Low	Medium
LED	300-1850nm	1.1	10,000+	High	Low

TABLE II Different types of light simulators along with their characteristics.

Light Efficiency

Artificial light sources are commonly evaluated based on their luminous efficacy, also known as wall – plug efficacy. This is the ratio of the total amount of input power (electrical, etc.) that a system utilizes to the total quantity of luminous flux that it emits.

The efficiency of the device is measured by the source's luminous efficacy, which accounts for the spectral response curve in the output (the luminosity function).

This quantity may be referred to as lighting efficiency, total luminous efficacy, or luminous efficiency of a source when presented in dimensionless form (for instance, as a percentage of the maximum potential luminous efficacy).

The major distinction between the luminous efficacy of radiation and that of a source is that the latter takes into account input energy that escapes the source as heat or in another manner other than electromagnetic radiation. A characteristic of the radiation that a source emits is its luminance efficiency.

The efficiency and luminous efficacy of various light sources are listed in the following table (TABLE 1.3) [16]. Unless otherwise stated, all lights that need an electrical or electronic ballast are listed without the associated losses, which lowers overall efficiency.

<i>Category</i>	<i>Type</i>	<i>Luminous Efficacy (lm/W)</i>
Combustion	candle	0.3
	Gas mantle	1-2
Incandescent	15, 40, 100W tungsten incandescent (230V)	8.0, 10.4, 13.8
	5, 40, 100W tungsten incandescent (120V)	19
Halogen incandescent	100, 200, 500W tungsten halogen (230V)	6.7, 17.6, 19.8
	2.6W tungsten halogen (5.2V)	19.2
	Halogen – IR (120V)	17.7-24.5
	Tungsten quartz halogen (12-24V)	24
	Photographic and projection lamps	35
Light – Emitting	LED screw base lamp (120V)	Up to 102

Diode	11W LED screw base lamp (230V)	138
	21.5W LED retrofit for T8 fluorescent tube (230V)	172
	Theoretical limit for a white LED with phosphorescence color mixing	260-300
Arc lamp	Carbon arc lamp	2-7
	Xenon arc lamp	30-50
	Mercury – xenon arc lamp	50-55
	Ultra – high – pressure (UHP) mercury – vapor arc lamp, free mounted	58-78
	Ultra – high – pressure (UHP) mercury – vapor arc lamp, with reflector for projectors	30-50
Fluorescent	32W T12 tube with magnetic ballast	60
	9-32W compact fluorescent (with ballast)	46-75
	T8 tube with electronic ballast	80-100
	PL-S 11W U-tube, excluding ballast loss	82
	T5 tube	70-104.2
	70-150W inductively – coupled electrodeless lighting system	71-84
Gas discharge	1400W sulfur lamp	100
	Metal halide lamp	65-115
	High – pressure sodium lamp	85-150
	Low – pressure sodium lamp	100-200
	Plasma display panel	2-10

Cathodoluminescence	Electron stimulated luminescence	30
Ideal sources	Truncated 5800 K black – body	251
	Green light at 450 THz (maximum possible luminance efficacy by definition)	683

TABLE III Light sources' Luminous Efficacy.

1.3 Need for Light simulators

By definition, a solar simulator or an artificial light simulator is a device that can achieve the provision of illumination by approximating natural sunlight or illumination under specific lighting conditions. More specifically, a light simulator is described as an equipment that uses a light source with a spectral distribution similar to natural sunlight (or a specific photo spectral response) used to primarily to evaluate the characteristics of (indoor or outdoor) photovoltaic devices [17].



Figure 1.13 Solar Simulator [18]

The light simulator's main role is to enable a controllable indoor testing environment under controlled lab circumstances. Light simulator (Fig. 1.13) can be utilized to evaluate any photosensitive procedures or substances, such as solar cells, sunscreen, cosmetics, plastics, aerospace materials, skin scare, bioluminescence, photosynthesis, water treatment, crude oil degradation, free radical production, etc.

The following table (TABLE 1.4) summarizes the range of field applications in which light simulators can be applied [17].

Field	Application
Energy Science	Performance testing of solar cells or PV modules New energy development
Biotechnology	Medical/Cosmetic research and application
Material Science	New material development and testing Photocatalyst
Architecture	Weathering Life Testing of Building Material Color study of coating/paint
Agriculture	Experiments and Tests of Agricultural, Forestry, Fisheries and Animal Husbandry
Environmental Engineering	Research of the interaction between humans and the environment

TABLE IV Light simulators' field of applications.

1.4 Architecture and characteristics of Light simulators

In a globalized world, every industry possesses standards that establish minimum requirements for reassuring the products they are associated with, are secure and capable of carrying out their intended purpose. The situation is no different for light simulation. Simulators that replicate sunshine, need to have standards that outline their operating conditions and provide requirements for determining if a light simulator is classified as Class AAA, Class ABA, Class CBC, etc.

Solar simulators are used extensively in the testing of solar cells, also known as photovoltaic devices. In real sense, when ASTM subcommittee EE44.09 was established in 1978, they comprehended that standardizing the metrics for solar (or in general light) simulators, was a crucial method for increasing confidence in photovoltaic efficiency measurements, so they authored “Specifications of Solar Simulators for Terrestrial Photovoltaics Testing” (which is the ASTM E927 standard). The measurement and classification of solar simulators were originally outlined in this standard.

The photovoltaic industry has expanded significantly over the previous 50 years, increasing by 40 times just from 2006 to 2014, and it is predicted that this expansion will continue. In that timeframe, acquisition of knowledge of photovoltaic materials and their physics has grown tremendously, resulting in far more effective materials and solar cell structures.

It should thus come as no surprise that new requirements regarding how to properly test photovoltaics arise with our increased expertise and knowledge of their capabilities given how closely solar simulators are related to photovoltaics research.

The modified standards in IEC 60904-9 are partly due to developments in photovoltaic technology. The addition of the Class A+ classification, that establishes the standard for the highest quality certification attainable by a solar simulator, is one of the most significant improvements in the new IEC 60904-9 standard.

Solar simulators have improved significantly in recent years in producing spectra that closely resemble those produced by the sun, just as there have been several breakthroughs in photovoltaic technology over the previous few decades.

The advancements in solar simulator technology in its entirety are reflected in the new Class A+ standard. Class A+ is twice as good as Class A in terms of three original standard criteria used to evaluate solar simulators – spectral match, non – uniformity, and temporal instability (Table 1.5, [19]).

Class	Minimum Wavelength Range to be Evaluated (nm)	Spectral match to all spectral bins (%)	Spatial non – uniformity (%)	Temporal instability	
				Short term instability (STI) %	Long term instability (LTI) %
A+	300 – 1200	87.5 to 112.5	1	0.25	1
A	400 – 1100	75 to 125	2	0.5	2
B	400 – 1100	60 to 140	5	2	5
C	400 - 1100	40 to 200	10	10	10

TABLE V Solar Simulator's Classification according to the IEC 60904-9 standard.

Where [17]:

- *Spatial Non – Uniformity*

Irradiance that is not uniformly distributed throughout a test area is called irradiance spatial non – uniformity. It can be measured by utilizing a photodiode or other irradiance detector for measuring the irradiance at various locations on the designated irradiation surface (the measuring g value is photocurrent) and then calculated by the following formula:

$$\text{Non – Uniformity}(\%) = \frac{[\text{MaxIrradiance} - \text{MinIrradiance}]}{[\text{MaxIrradiance} + \text{MinIrradiance}]} \times 100\% \quad (1)$$

It is also noticeable that, during the measurement, the step width of each movement of the detector should not be greater than one – fifth of the minimum dimension of the designed test area.

- *Temporal Instability*

This indicator measures stability. The output beam of the light simulator must maintain its illumination steady in order to guarantee the precision of measurements of photovoltaic cell efficiency. The following formula is the calculating formula:

$$\text{Instability}(\%) = \frac{[\text{MaxIrradiance} - \text{MinIrradiance}]}{[\text{MaxIrradiance} + \text{MinIrradiance}]} \times 100\% \quad (2)$$

According to the different IV measurement systems, the instability can be divided into two categories:

Short – term Instability (STI):

If spectral classification has been carried out in the constrained wavelength range of 400 nm to 1100 nm, or in the extended wavelength range of 300 nm to 1200 nm, the temporal instability is Class A or Class A+ for STI when there are three separate data input lines that simultaneously store values of irradiance, current, and voltage. It is

important to mention that there is a delay of less than 10 ns when the three multiple channels are simultaneously triggered.

Long – term Instability (LTI)

This value equals with the time required to obtain the I-V characteristic for a three channel I-V measurement (irradiance, current, and voltage) with a pulsed or steady – state solar simulator.

There is one further restriction on the Class A+ classification, which represents the requirements to accommodate the growing demands of photovoltaic researchers. The expanded range of 300 nm to 1200 nm must be examined for a solar simulator to receive the Class A+ classification in any of the three criteria (and its spectral match evaluated accordingly).

1.5 Radiometry & Photometry

In order to proceed with an analysis of the method developed for the modeling of photoemission, it is imperative to clarify some aspects or concepts. These concepts are intended to be the starting point of the entire modeling process and, more specifically, reference is to be made to used concepts of radiometry and photometry.

Radiometry is the measuring of electromagnetic radiation in the frequency range between 3×10^{11} Hz and 3×10^{16} Hz, known as optical radiation. The regions typically referred to by the terms ultraviolet, the visible, and the infrared are comprised of this range, which corresponds to wavelengths between 10 nm and 1000 nm.

The aforementioned radiometric measurements are often used: Watt (radiant flux), Watt per steradian (radiant intensity) Watt per square meter (irradiance), and Watt per square meter per steradian (radiance) [20], [21] .

- *Radiant flux* Φ_e : Radiant energy emitted, reflected, transmitted, or received per unit time, and is measured in watt (W). If we are dealing with an isotropic source (emitting equal amounts of energy per second in all directions) it is possible to determine the radiant flux measuring the energy arriving to a unit area perpendicular to the flux and dividing this amount by the time the process takes.

If, on the contrary, the flux is an anisotropic it is necessary to divide the illuminated field in areas small enough to consider the radiant flux $d\Phi_e$ as uniform, being the total flux the sum of its value over all the differential areas: $\Phi_e = \int_S d\Phi_e$.

- *Radiant Intensity* $E_{e,\Omega}$: Is the radiant flux emitted, reflected, transmitted, or received, per unit solid angle. As the suffix indicates, it is a directional quantity. It is measured in watt per steradian ($W \cdot sr^{-1}$). This unit is of paramount importance for defining the photometric units. The luminous flux of a source is a magnitude that characterizes it, though it could be increased or decreased by optical means: focusing the light of the source with convergent lenses will increase E_e .

The term is mostly applied with the approximation of a point source, i.e., in distances which are large to the extent of the source. In the SI system, radiant intensities are specified in units of W/sr (watts per steradian). Radiant intensity is a property of the light source and may not be relevant if the spatial distribution of radiation from the source is non-uniform. It is appropriate for point sources (and for close approximations, such as an LED intensity measurements), but not for collimated sources.

At a distance d from a source with radiant intensity I , an area element with its normal direction at an angle θ against the direction to the source receive an irradiance

$$E = I * \frac{\cos\theta}{d^2} \tag{3}$$

The total radiant flux of a source with uniform omnidirectional emission (i.e., and intensity not depending on the direction) is $\Phi = 4 * \pi * I$.

A related radiometric quantity is the spectral intensity, which is defined as the radiant intensity per unit optical frequency or wavelength interval. Generally, the radiant intensity depends on the observation direction, and the total radiant flux is obtained by integration over all directions. In case of isotropic radiation (i.e., with constant radiant intensity), the total radiant flux is simply 4π sr times the radiant intensity.

- *Irradiance* I_e : radiant flux received by a surface per unit area. Its unit is watt per square meter ($W \cdot m^{-2}$). However, because many sensor heads have a 1 cm^2 detector area, it is simpler to use watt/ cm^2 .

There are two ways to control the size of the detector area. The first is to use a sensor head with a known detector area. The second is to place an aperture with a known area between the source and the detector. When source radiation does not completely fill the detector, an aperture is the only reliable method of controlling detector area.

To compare the irradiance of different sources, one must consider the illuminating the walls or the field from different angles.

Irradiance function is approximated by a Gaussian function or the cosine function, which has the form [22]:

$$\int_{\theta_1}^{\theta_2} e^{-b_1(\theta-\alpha)^2} d\alpha \cong A e^{-b_2\theta^2} \quad (4)$$

And

$$\int_{\theta_1}^{\theta_2} [\cos(\theta - \alpha)]^{m_1} dA \cong \beta \cos^{m_2} \theta \quad (5)$$

- *Radiance* $L_{e,\Omega}$: radiant flux emitted, reflected, transmitted by a surface, per unit solid angle per unit projected area. Measured in watt per steradian per square meter ($W \cdot sr^{-1} \cdot m^{-2}$). If the source is not isotropic, the radiation field must be divided in differential solid angles, small enough to consider the radiance constant, and then integrate over all the illuminated regions.

To measure radiance, the definition of the area of the source needs to be measured. This is usually simulated utilizing an aperture and a positive lens in front of the detector. It is expressed as watts/cm²ster.

On the other hand, the measuring of light, that is referred to as electromagnetic radiation perceivable by the human eye, is known as photometry. As a result, it is constrained to the visible spectrum (wavelengths between 360 and 830 nm), and all the values are based on the eye's spectral response.

Either Spectro radiometry combined with the proper computations for weighting by the spectral response of the eye, or optical radiation detectors designed to imitate the spectrum response of the eye, are used in photometry. Lumens (luminous flux), candelas (luminous intensity), lux (illuminance), and candelas per square meter (luminance) are common photometric units.

- *Luminous Flux* Φ_v : measures the total amount of energy radiated per second from a light source in all directions. This parameter can be adjusted to reflect the changes in the sensitivity of the human eye with respect to different wavelengths of light. It is measured in lumens and used for describing the brightness of a projector.

One lumen defines the luminous flux of the uniform point light source having a luminous intensity of 1 candela. Luminous flux is the sum of power at all wavelengths in the visible band. The ratio of total luminous flux to the radiant flux is known as luminous efficacy. Flux is used as an objective measure of energy emitted by a light source in light bulb packaging applications.

For a monochromatic source producing light at a single wavelength, flux can be easily determined using the following relation:

$$\Phi_v = \Phi * V_\lambda * (683lm/W)$$

(6)

Where Φ_v is the luminous flux and V_λ is the luminous efficacy.

- *Luminous intensity* I_v : is a quantity in photometry for characterizing a light source. It is defined as the luminous flux per unit solid angle. The luminous

intensity takes into account the spectral response of the human eye - typically for photopic vision. The SI units of the luminous intensity are the candela which is equal to lumen per steradian ($\text{cd} = \text{lm}/\text{sr}$). One candela approximately corresponds to the luminous intensity of an ordinary candle.

- *Illuminance* E_v : is the total luminous flux incident on a surface, per unit area. It measures how much incident light illuminates the surface, wavelength – weighted by the luminosity function to correlate with human brightness perception.

Similarly, luminous emittance is the luminous flux per unit area emitted from a surface. Luminous emittance is also known as luminous exitance. In SI unit's illuminance is measured in lux (lx), or equivalently in lumens per square meter ($\text{lm}\cdot\text{m}^{-2}$).

- *Luminance* L_v : is defined as the intensity of light from the visible spectrum per unit area travelling in a given direction. The SI unit for luminance is candela per square meter (cd/m^2).

The difference between radiometry and photometry is that radiometry includes the entire optical radiation spectrum (and often involves spectrally resolved measurements), while photometry deals with the visible spectrum weighted by the response of the eye.

1.6 Photometric Quantities

1.6.1 Color Space / White Color

In monochromatic light sources, such as lasers, or near monochromatic, such as colored LEDs, the color of the light is a specified quantity. In white LEDs the spectrum is a continuous composition of different colors. Dramatically different spectra can all be considered white light.

The wavelength spectrum can be visualized as a point in a color space representing the resulting color, the (x, y) are called the color coordinates. In this RGB color space, a color is represented as a mixture of several amounts of red, green and blue. The colors in this chart are highly saturated (Fig. 1.14).

Below is a graphical representation of the CIE 1931 color space, charting all colors visible to the human eye. Numbers around the edge of the “horseshoe” are wavelengths of monochromatic light defining the boundaries of the color space. Inside the horseshoe, each perceptible color has a coordinate called CIE_x, CIE_y. Revisions to the original CIE color space were made in 1960 and 1976, but the 1931 version remains the most widely used version.

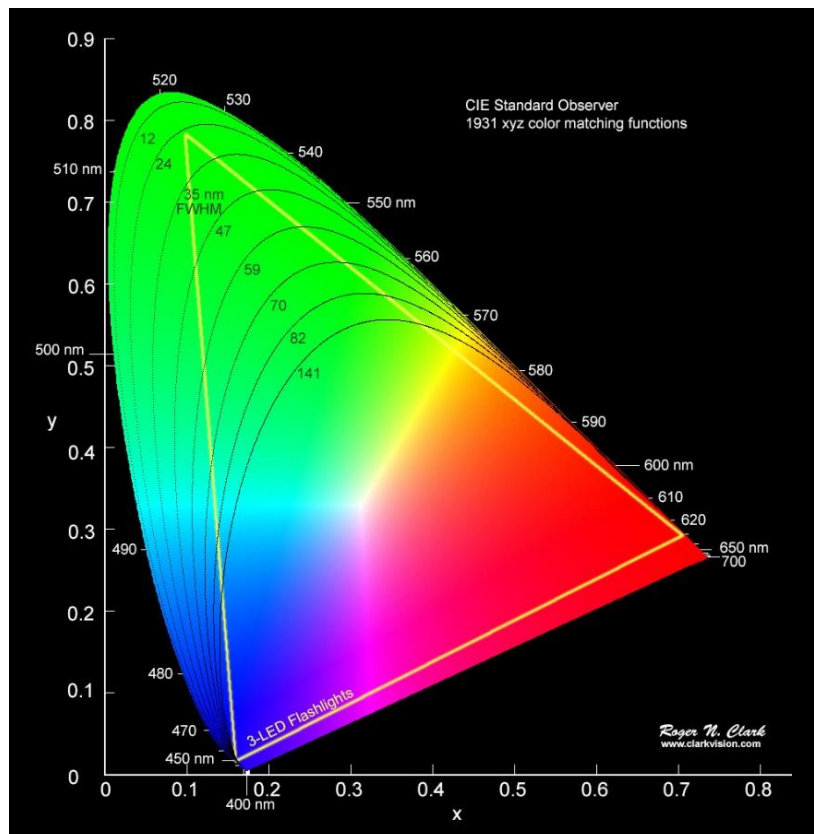


Figure 1.14 Color space

The CIE XYZ color matching functions can be approximated by a sum of Gaussian functions, as follows:

Let $g(x)$ denote a piecewise-Gaussian function, defined by [23]:

$$g(x; \mu, \sigma_1, \sigma_2) = \begin{cases} e^{\left(-\frac{1}{2}(x-\mu)^2/\sigma_1^2\right)}, & x < \mu \\ e^{\left(-\frac{1}{2}(x-\mu)^2/\sigma_2^2\right)}, & x \geq \mu \end{cases} \quad (7)$$

That is, $g(x)$ resembles a bell curve with its peak at $x = \mu$, a spread/standard deviation of σ_1 to the left of the mean and spread of σ_2 to the right of the mean. With the wavelength λ measured in nanometers, we then approximate the 1931 color matching functions:

$$\begin{aligned} \bar{x}(\lambda) &= 1.056g(\lambda; 599.8, 37.9, 31.0) + 0.362g(\lambda; 442.0, 16.0, 26.7) \\ &\quad - 0.065g(\lambda; 501.1, 20.4, 26.2) \\ \bar{y}(\lambda) &= 0.821g(\lambda; 568.8, 46.9, 40.5) + 0.286g(\lambda; 530.9, 16.3, 31.1) \\ \bar{z}(\lambda) &= 1.217g(\lambda; 437.0, 11.8, 36.0) + 0.681g(\lambda; 459.0, 26.0, 13.8) \end{aligned} \quad (8)$$

1.6.2 MacAdam Ellipses

David MacAdam, a scientist, conducted a series of experiments to understand human color discrimination—our perception of color differences—in the late 1930s and early 1940s (in LED lighting, these differences are measured as color temperature).

The result of this research was the eponymous MacAdam Ellipses, which Perley Nutting plotted on the CIE color space diagram as shown in the image below (Fig. 1.15). Each ellipse has an area that appears to be the same color to the human eye (although for illustration purposes, the ellipses are drawn 10 times their actual size). The "target" color is at the center of each ellipse (the starting point color value used in the experiments).

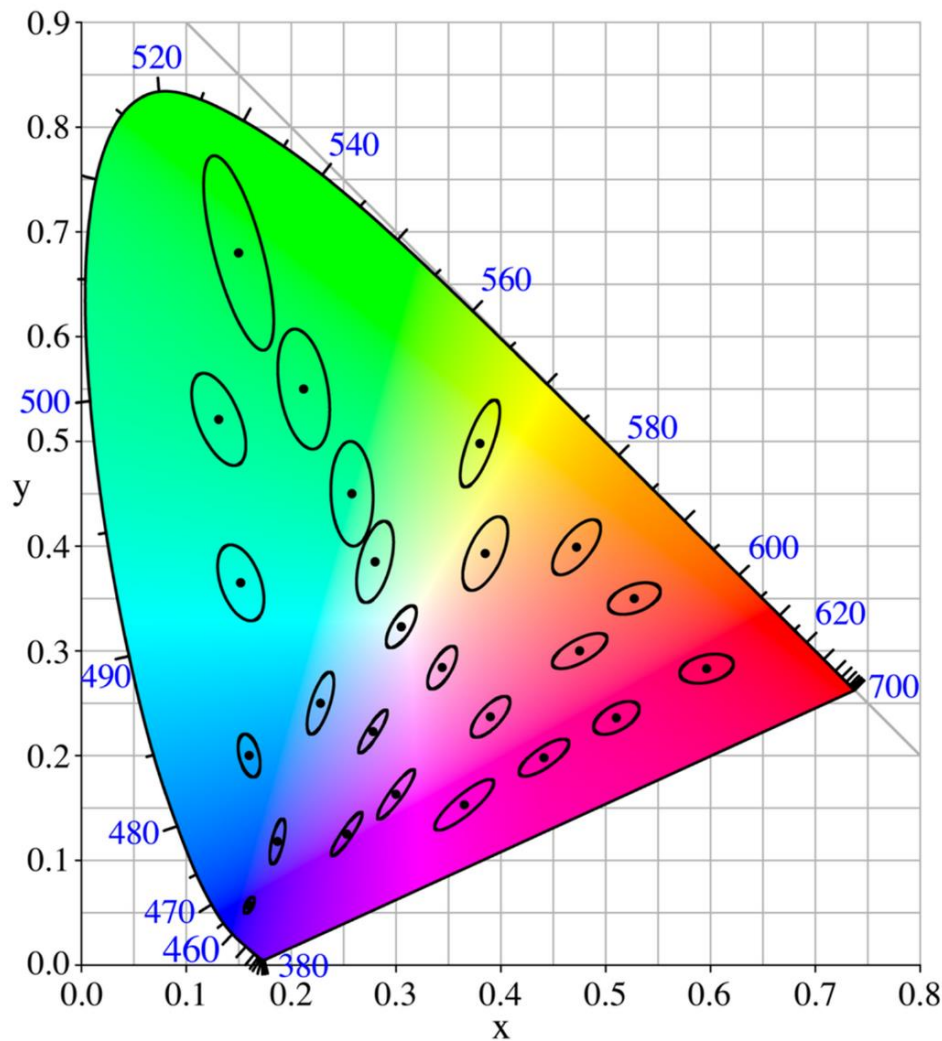


Figure 1.15 MacAdam Ellipses

The ellipses were supposed to have regular deviations and be entirely circular, as predicted by scientists. Apparently, there is a wide range in the ellipses' size, orientation, and shape. This revelation prompted the creation of various new versions of the CIE color space that would lessen apparent distortion and more accurately depict different facets of color perception.

1.6.3 Correlated Color Temperature

Correlated color temperature (CCT) is a way to characterize the color appearance of any white light source with a single number. Artificial white light can be produced using combinations of all the colors in the visible spectrum. Different amounts of each wavelength will cause the light to appear “cooler” (more blue/cyan wavelengths) or “warmer” (more yellow/orange wavelengths).

In the center of the color space is an area of generally white color where red, green, and blue are added equally. Reference point for white light is a black body. The black body will emit a different color light at different temperatures. Color temperatures between 2700K and 20000K are all perceived as white light by the human eye.

This constitutes the Planck locus and is depicted as a curved line at its center color space. Temperatures in Kelvin are referred to as color temperature. For example, the sun at noon in the equator has a color temperature of 6500 K. at dusk, the color temperature will be much lower and has a reddish color. The incandescent bulb has a temperature color around 2700 K, while a halogen incandescent lamp has 3000 K.

The diagram below (Fig. 16) compares the CCT of various light sources, including sunlight at different times of day and in different weather conditions, and various artificial light sources. Sunlight above the atmosphere is approximately 5900 K. Molecules in the atmosphere such as ozone absorb much of the UV and IR wavelengths, preventing us from receiving the full force of these damaging rays.

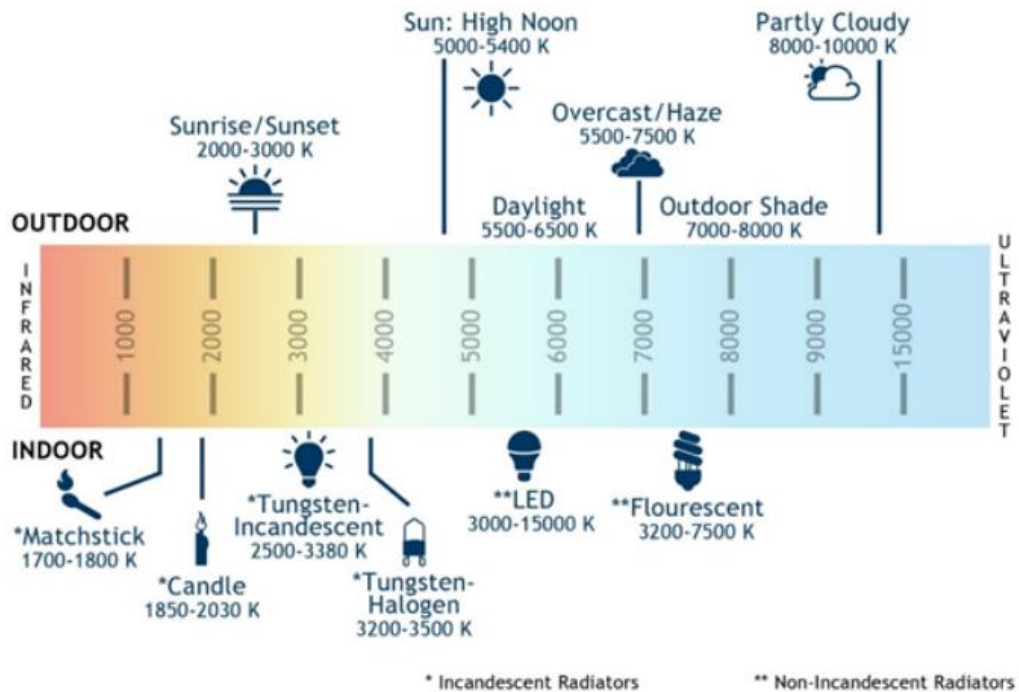


Figure 1.16 Correlated Color temperature

1.6.4 Spectral Power Distribution

One way to define light coming from any light source (a lightbulb, the sun, etc.) is by its spectral power distribution (SPD). SPD is a measurement of the energy (in Watts) that is output by the source as a function of wavelength. In other words, SPD describes how much optical power the light source emits within each wavelength band (as measured by a spectrometer).

Just as visible light wavelengths are described with terms like luminance, illuminance, and luminous flux, the entire electromagnetic output of a source is described in terms of radiance – energy output. The terms radiance, irradiance, and radiant flux have parallel meanings [24]:

Quantity Measured	Visible Light	Total Radiant Power
Total light (energy) output	Luminous flux. Measured in lumens (lm)	Radiant flux. Measured in Watts (W)
Light from a direction	Luminous intensity, measured in candela (cd). 1 cd = 1 lumen/steradian	Radiant intensity. Watts per steradian (W/sr)
Light incident on a surface	Illuminance = lux. 1 lux = 1 lumen/meter	Irradiance. Measured as Watts per square meter (W/m ²)

Brightness	Luminance. Measured in candela per square meter (cd/m ²) or nits. 1 nit = 1 cd/m ²	Radiance. Measured as Watts per square meter per steradian (W/sr·m ²)
-------------------	--	--

TABLE VI Quantity Measured vs. Visible Light - Total Radiant Power.

The total power is referred to as the radiant flux of the source. The radiant flux characteristics of light sources are typically represented with an SPD graph: wavelengths (in nanometers, nm) are on the X-axis, and spectral power (radiant flux) is distributed on the Y-axis. It is measured in Watts per nanometer, W/nm but is commonly normalized as an arbitrary unit such as intensity, normalized intensity, relative sensitivity, or similar [25].

	Source	Wavelength	Frequency	Photon energy
<i>Extremely low frequency</i>	Power lines	km	30 – 300 Hz	Pico eV (10 – 12 eV)
<i>Radiowaves</i>	AM and FM radios	cm to km	20 kHz to 30 MHz	Nano to micro eV
<i>Microwaves</i>	Microwave oven	mm to m	300 MHz to 300 GHz	Micro to milli eV
<i>Infrared</i>	Radiant heat	Microns to mm	300 GHz to 300 THz	Milli eV to eV
<i>Visible light</i>	Sun	400 – 700 nm	430 to 750 THz	1.8 to 3 eV
<i>Ultraviolet</i>	Arc welding	400 to 100 nm	750 to 3000 THz	3 to 12 eV

<i>X – rays</i>	X – ray	100 to 10 ⁻³ nm	3000 THz to 10 ²⁰ Hz	keV to MeV
<i>Gamma rays</i>	Radioactive sources	100 to < 10 ⁻³ mm	3000 THz to > 10 ²⁰ Hz	keV to > MeV

TABLE VII Comparison of electromagnetic spectrum.

Refer to the black body locus shown on the CIE graph above – we mentioned that artificial white light sources have color coordinates that reside on or very near the black-body curve. But it’s important to understand that the spectral power distributions (SPDs) of “white” light sources can include many combinations of wavelengths. Their SPDs do not always resemble the smooth curves associated with a black-body source, as seen in the image below of three black body radiators (Fig. 1.17) [24]:

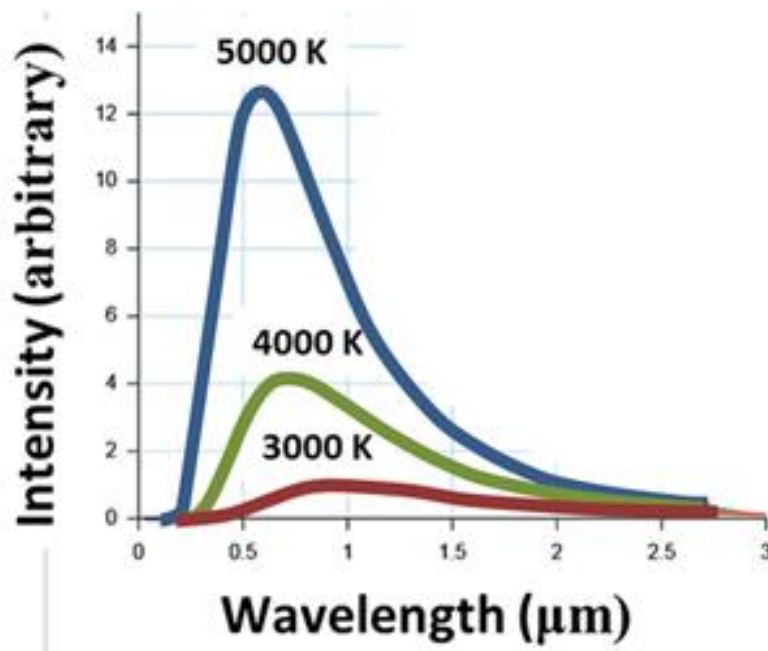


Figure 1.17 Intensity - Wavelength

The graph below, however, displays the SPDs of a Luminus white LED product series, which exhibits variations across the spectrum. It features two peaks at approximately 450

nm (in the blue region of the visible spectrum) and in the approximately 525 – 625 nm (in the green – yellow area of the visible spectrum).

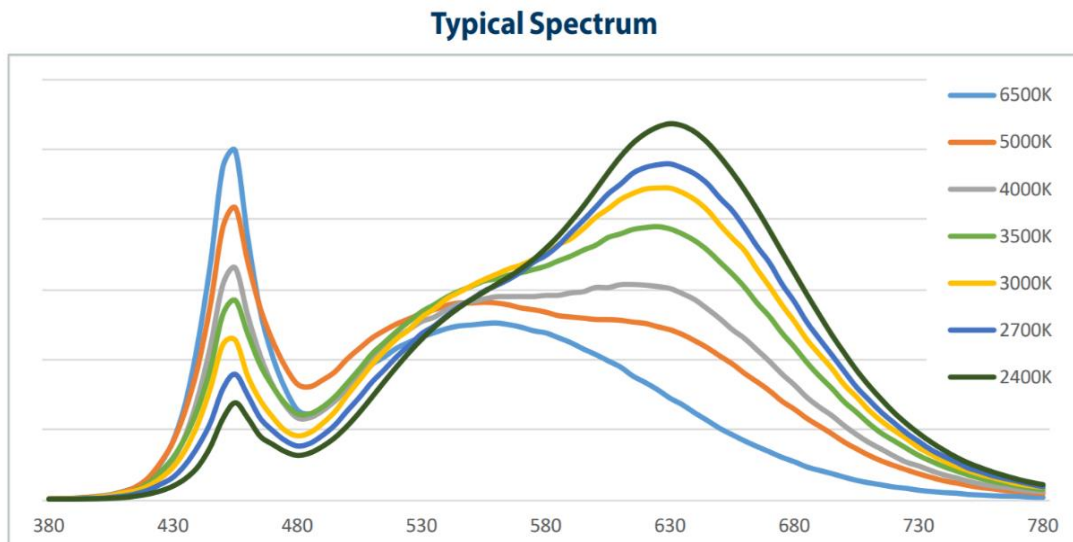


Figure 1.18 Typical Spectrum

1.6.5 Color rendering

Light sources with different color temperatures all appear white, but the objects being illuminated may appear very different. All light sources appear white to the eye because the brain interprets them that way. Even the limited spectrum of thorium light appears white because the eye is essentially a three-carrier sensor.

The perceived color of the illuminated object depends on the spectral distribution of the light source. The object can only reflect the colors present in the light source. The color rendering index (CRI) is a quantitative measure of a light source's ability to render the color of objects relative to an ideal or natural light source. The International Committee on Illumination CIE (1995) defined the original test color samples.

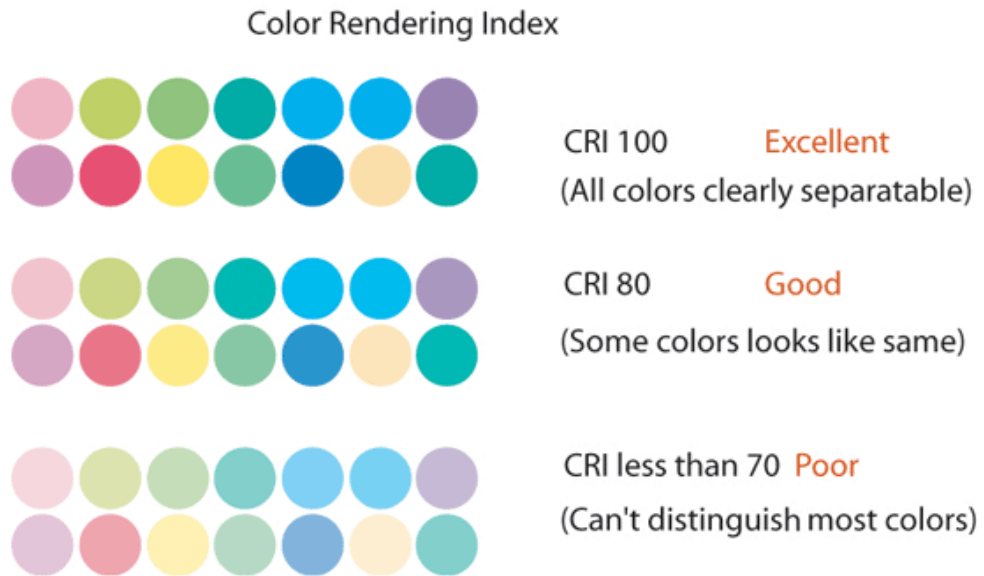


Figure 1.19 Color Rendering Index [26]

In the following table (TABLE 1.8), indicative values of CRI in various light sources are displayed.

Light Source	CCT (K)	CRI
Low pressure sodium – vapor (LPS/SOX)	1800	-44
Mercury vapor	6410	17
High pressure sodium (HPS/SON)	2100	24
Coated mercury-vapor	3600	49

Halo phosphate warm-white fluorescent	2940	51
Halo phosphate cool-white fluorescent	4230	64
Tri-phosphor warm-white fluorescent	2940	73
Halo phosphate cool-daylight fluorescent	6430	76
"White" SON	2700	82
Standard LED Lamp	2700-5000	83
Quartz metal halide	4200	85
Tri-phosphor cool-white fluorescent	4080	89
High-CRI LED lamp (blue LED)	2700-5000	95
Ceramic discharge metal-halide lamp	5400	96
Ultra-high-CRI LED lamp (violet LED)	2700-5000	99
Incandescent/halogen bulb	3200	100

TABLE VIII Light Sources – CRI [18].

1.6.6 Characteristics of light sources

Light sources – including LEDs, fluorescent lamps, halogen lamps and incandescent lamps – possess similar properties. Therefore, they have their advantages and disadvantages. In fact, there are several types of light sources used around the world. None of them has proven particularly effective in all applications. The main characteristics of light sources are distinguished in [27]:

- *Light Quality:*

The quality of the light generated is vital. Through the quality of light, it can be seen how good a light source really is. In general, two simple measures are considered under the light quality characteristic. They include Correlated Color Temperature (CCT) and Color Rendering Index (CRI). These measures offer a broad overview of most light source. The CCT explains the color temper of light sources.

- *Efficacy:*

Another important factor for the characterization of light sources is the efficacy. This is mainly related to their efficiency and how much light they generate regarding their energy input. When it comes to efficacy, the incandescent lamps are at the lowest ebb. They simply serve as resistors. A typical incandescent bulb of 60W produced 830 lumens. Higher incandescent bulbs are also more efficient than the low-capacity ones.

On the other hand, fluorescent bulbs are known to be higher in efficacy when compared to the incandescent lamps but requires a ballast to convert power.

- *Timing:*

Timing is yet another vital characteristic of light sources. It covers the flicker and turn on time. When it comes to turn on time, incandescent bulbs are known to be very simple. When power is applied to them, they can easily turn on immediately. They simply glow to the full brightness. On the other hand, fluorescent bulbs require extra timing. They can be very complex as well.

In most cases, a fluorescent bulb may take some minutes before coming up. The filament is usually preheated before the plasma arc is created to ensure the longevity of the tube. The preheat time usually takes up to 700msec. When the tube is put on eventually, it may take

some minutes before coming to full brightness. This delay is actually one of the major flaws of most fluorescent bulbs.

- *Dimming:*

Most of the light sources usually have dimming problems. Incandescent bulbs for instance drop their CCT levels as they dim. This usually makes them to look redder in color.

Fluorescent tubes also turn off when they become dim. They usually perceive the missing voltage as a blatant decrease in the average line voltage. Again, if the voltage applied to the ballast of a fluorescent tube is reduced, the arc current and the filament power will also be reduced. This shortens the lifetime of the tube. LEDs also have dimming issues although some series are designed to dim.

- *Aging:*

Aging issues also occur in most of the light sources. If one of multiple incandescent bulbs is replaced in a fixture, this can indicate that the older bulbs have worn out over time. The same scenario is also seen in fluorescent bulbs and LEDs.

However, there's a difference on aging duration for all the light sources. An incandescent bulb has a lifetime of 100 hours of usage. Fluorescent bulbs have complex lifetime since their lifetime depends on how many hours they are used as well as the on/off cycles used. Basically, their lifetime stands at 10,000 hours of usage.

LEDs have longer lifetimes. This is because they are made of semiconductors that last for years. LEDs can serve for thousands of hours. Their average lifetime stands at 50,000 hours

2 LEDs as light sources

2.1 Light Emitting Diode

The fundamental distinction between conventional incandescent and fluorescent lighting and LED lighting is efficiency. Due to energy loss throughout their manufacturing process, LED lights require 25% to 80% less direct power than incandescent lights (the standard light bulb) or fluorescent lights (tubular lights or bulbs).

Since they emit a small fraction of the heat that incandescent lights generate, LED lights are frequently safer. Compared to incandescent or fluorescent lighting, LED lights have a significantly longer lifespan.

Electricity is used in incandescent bulbs to heat a metal filament to a white-hot state, which is referred to as incandescence. In consequence of this, incandescent lamps emit 90% of their energy as heat. For fluorescent lighting to function, mercury vapor must first be ionized in a glass tube or globe.

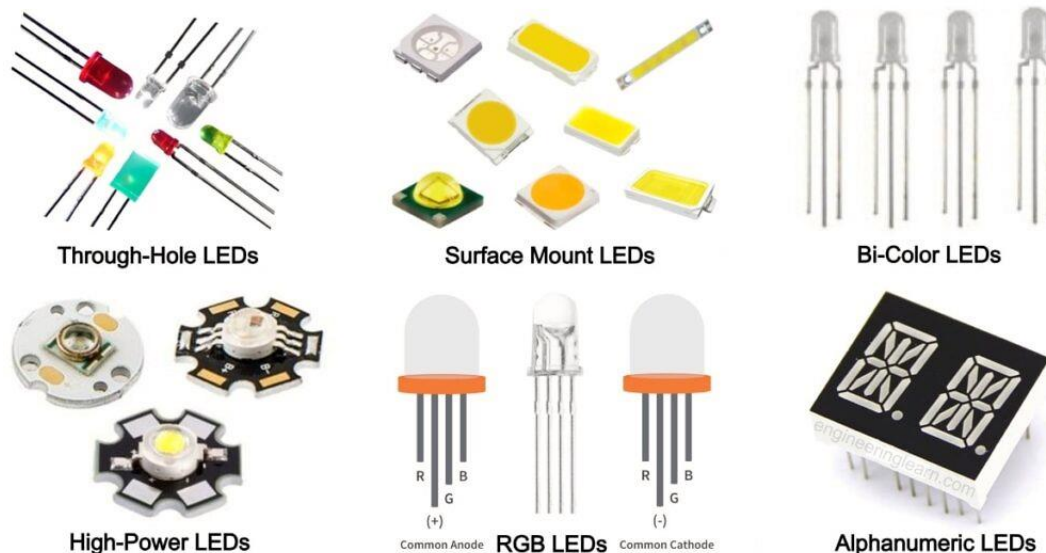


Figure 201 Light Emitting Diodes

This enables the generated gas's electrons to release photons with UV frequencies, and the UV light is then filtered via the phosphor coating on the inside to produce visible light. Due to their procedure, incandescent and fluorescent lighting lose efficiency.

As power flows through the diode, LEDs (semiconductor) emit light. All LED lights require DC power, which must be converted from our AC power sources via a converter (like a standard 5V,1A DC adapter). Some bigger LED replacement lights come with built-in transformers or drivers. A 12 V DC transformer is available from us in 1 Amp or 5 Amp capacities.

Since the majority of the electrical energy is used to produce light, the amount of power needed is greatly reduced. In contrast to incandescent and CFL light sources, which produce light and heat in all directions, LEDs also generate light in a single direction. This implies that LEDs can use light and energy more effectively in a variety of applications.

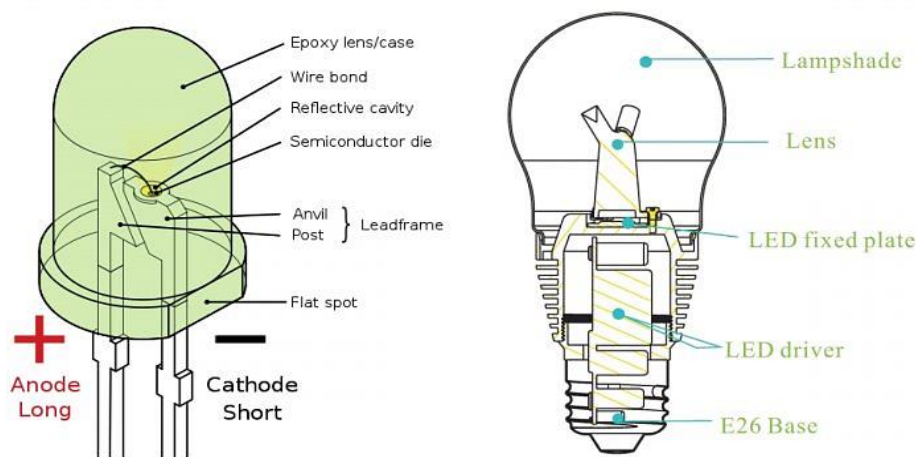


Figure 212 LED VS Traditional Light Sources [28]

2.2 Efficiency and Operating parameters

The most crucial issue in the field of energy is efficiency. To improve energy efficiency, numerous studies in the field of energy are used. Compared to traditional lighting, LED lamps are differentiated by their energy efficiency.

Monochrome light sources (narrowband): Because the light is in the proper wavelength range, no color separators such as prism or color filter are required. The term "light efficiency" refers to the proportion of light produced by lamps to electric energy used.

Its unit is the lumen/Watt. Values of Lumen/Watt for various light sources [29]:

- The luminous efficiency in incandescent lamps is 12-15 lm/W,
- For halogen lamps, 18-22 lm/W,
- For compact fluorescent lamps: 60 lm/W,
- Fluorescent lamps: 55-104 lm/W

The lumen/watt values for LEDs vary according to the LED's color. The red color has the highest efficiency of 60 lm/W, 55 lm/W for yellow 35 lm/W for green and 18 lm/W for blue. White light is the most important color used in lighting. The efficiency for white LED is around 85 lm/W depending on the manufacturer and the light efficiency is steadily increased.

Regarding LED light values, it's important to be aware of light angles. The light values are expressed in candelas because LEDs are directed lights. One of the key components of solid-state lighting is altering the light's angle, directing it, distributing it, and utilizing the LED light for a limited amount of time.

LEDs only emit single color of light. While one color can be utilized in ornamental lighting, combining different colored LED lights can provide intermediate colors. Theoretically, if each color is DIMMED by 255 steps (third power of 255) 16 million colors can be obtained.

LEDs used when creating LED array should have the same or similar wavelength. Differences of 5-10 nm are especially perceived by the eye in green and yellow colors. The components of the LED lamp are shown in Figure 2.3.

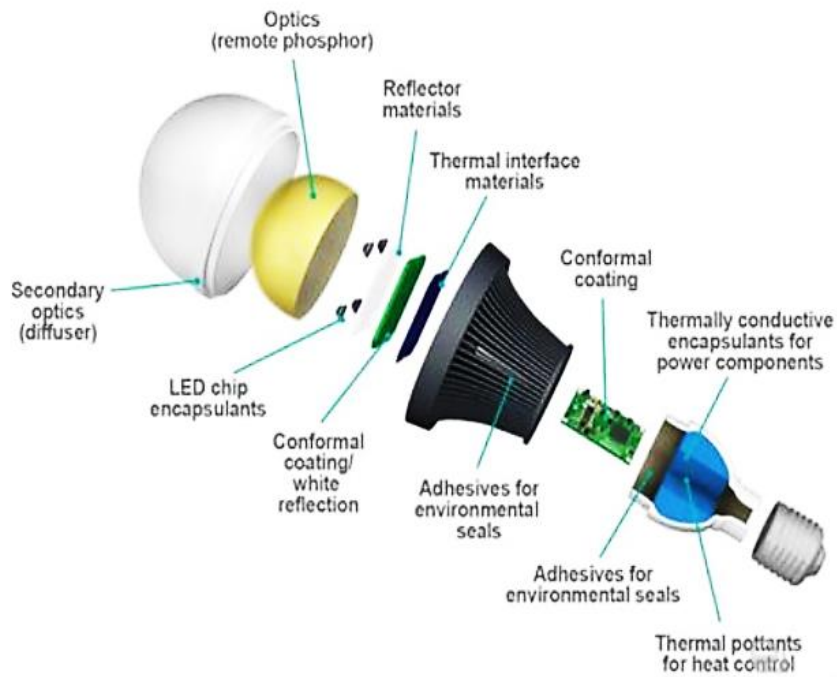


Figure 223 LED lamp components

Typical indicator LEDs are designed to operate on no more than 30-60 milliwatts (mW) of electricity. Around 1999, Philips Lumileds introduced LEDs capable of continuous use at one watt. These LEDs use much larger semiconductor sizes to handle the large input power. Also, the semiconductors were placed on a piece of metal to allow the heat to be removed from the LED. One of the main advantages of LED light sources is the high light output. White LEDs quickly surpassed the efficiency of standard incandescent lighting systems. In 2002 Lumileds offers a light output of 18-22 lumens per watt (lm/W) for five-watt LEDs. In comparison, a conventional 60-watt incandescent lamp emits about 15 lm / W and standard fluorescent lamps emit up to 100 lm / W [30].

Color	Wavelength Range (nm)	Typical Efficiency
Red	$620 < \lambda < 645$	72

Orange	$610 < \lambda < 620$	98
Green	$520 < \lambda < 550$	93
Cyan	$490 < \lambda < 520$	75
Blue	$460 < \lambda < 490$	37

TABLE IX Wavelength - Typical Efficiency.

In addition, as shown in the TABLE 2.2, the wavelength range in comparison with the semiconductor material is given [30].

Color	Wavelength (nm)	Semiconductor Material
Infrared	$\lambda > 760$	Gallium arsenide (GaAs)
		Aluminium gallium arsenide (AlGaAs)
Red	$610 < \lambda < 760$	Aluminium gallium arsenide (AlGaAs)
		Gallium arsenide phosphide (GaAsP)
		Aluminium gallium indium phosphide (AlGaInP)
		Gallium (III) phosphide (GaP)
Orange	$590 < \lambda < 610$	Gallium arsenide phosphide (GaAsP)
		Aluminium gallium indium phosphide (AlGaInP)
		Gallium (III) phosphide (GaP)
Yellow	$570 < \lambda < 590$	Gallium arsenide phosphide (GaAsP)

		Aluminium gallium indium phosphide (AlGaInP)
		Gallium(III) phosphide (GaP)
Green	$500 < \lambda < 570$	Traditional Green:
		Gallium(III) phosphide (GaP)
		Aluminium gallium indium phosphide (AlGaInP)
		Aluminium gallium phosphide (AlGaP)
		Pure green:
		Indium gallium nitride (InGaN) / Gallium (III) nitride (GaN)
Blue	$450 < \lambda < 500$	Zinc selenide (ZnSe)
		Indium gallium nitride (InGaN)
		Silicon carbide (SiC) as substrate
		Silicon (Si) as substrate - under development
Violet	$400 < \lambda < 450$	Indium gallium nitride (InGaN)
Purple	multiple types	Dual blue/red LEDs
		blue with red phosphor
		or white with purple plastic
Ultraviolet	$\lambda < 400$	Diamond (235 nm)
		Boron nitride (215 nm)
		Aluminium nitride (AlN) (210 nm)
		Aluminium gallium nitride (AlGaN)
		Aluminium gallium indium nitride (AlGaInN) -- down to 210 nm
Pink	multiple types	Blue with one or two phosphor layers:
		yellow with red, orange or pink phosphor added afterwards

		or white with pink pigment or dye
White	Broad spectrum	Blue/UV diode with yellow phosphor

TABLE X Semiconductor materials by wavelength

2.3 Types of LEDs

- LED DIP

A dual in-line package (DIP or DIL) (Fig. 2.4) is an electronic component package with a rectangular housing and two parallel rows of electrical connecting pins. The package may be through-hole mounted to a printed circuit board (PCB) or inserted in a socket.

A DIP is usually referred to as a DIPn, where n is the total number of pins.

Common packages have as few as three and as many as 64 leads. Many analog and digital integrated circuit types are available in DIP packages, as are arrays of transistors, switches, light emitting diodes, and resistors.

Also, DIP LEDs have a cylindrical shape with a sphere on top, which improves the light's projection. The interior contains a single cell with the semiconductor crystal that emanates light with a continuous flow of electricity.

By having a single-color cell, DIP LEDs can only produce a single color. That's why DIP led screens are combined in a 3 DIP pixel, each capable of emitting a particular color (Red, green and blue).



Figure 23 DIP LED

- SMD LED

SMD LED (acronym for Surface-Mount-Device, Light-Emitting-Diode) (Fig. 2.5) is a type of LED characterized by having a 3 in 1 encapsulation, meaning that it integrates all 3 colors (Red, Green, Blue) in a single system.

The assembly on the circuit board is done by a polarization process on the front of the LED module. It is important to mention that this process is carried out with high-quality equipment in order to avoid future problems such as loose or non-functioning LEDs.

SMD LEDs are rectangular in shape and consist of three cells. These cells contain a luminescent element (semiconductor crystal) that produces light when current flows through it. To protect the SMD cells, resins are used to completely cover the upper part. These resins for SMD are available in various colors and shades.

Depending on the number of cells in the SMD led, it will have a certain number of contacts for welding. For a single-color LEDs, one of them is always the anode (+) and the other will be the cathode (-).



Figure 24 LED SMD

- COB LED

Chip-on-Board or “COB” (Fig. 2.6) refers to the mounting of a bare LED chip in direct contact with a substrate (such as silicon carbide or sapphire) to produce LED arrays. COB LEDs has a number of advantages over older LED technologies, such as Surface Mounted Device (“SMD”) LEDs or Dual In-line Package (“DIP”) LEDs. Most notably, COB technology allows for a much higher packing density of the LED array, or what light engineers refer to as improved “lumen density”.

For example, using COB LED technology on a 10mm x 10mm square array results in 38 times more LEDs compared to DIP LED technology and 8.5 times more LEDs compared to SMD LED technology (see diagram below). This results in higher intensity and greater uniformity of light.

Alternatively, using COB LED technology can greatly reduce the footprint and energy consumption of the LED array while keeping light output constant.

Although there are different forms of the COB chip, they can offer a much higher number of lumens per watt which can often be well over 100.



Figure 25 COB LED

- RGB

RGB LEDs (Fig. 2.7) consist of three LEDs. Each LED consists of one red, one green and one blue light LED. These three-color LEDs are capable of producing any color and white. Because the function needs electronic circuits to control the mixing and diffusion of the different colors, and because each individual color LED usually has a slightly different emission pattern (resulting in color variation with direction), even if they are made as a single unit, RGB LEDs are rarely used to produce white lighting. Nevertheless, this method is widespread in many uses because of the flexibility in mixing different colors, and mainly because this mechanism has a higher quantum efficiency in the production of white light. There are several types of white multi-color LEDs: bi-color, tricolor and tetra-color LEDs. Many key factors are factored in between these different methods, such as color fastness, color rendering ability, and bright performance.

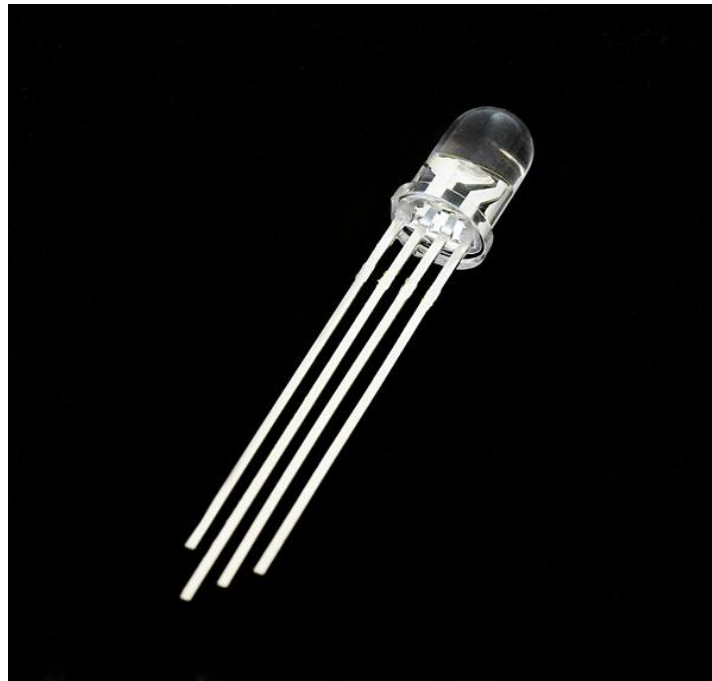


Figure 26 RGB Common Clear Cathode LED

- LED Tubes

LED tube lights (Fig. 2.8) are long, linear lamps designed to operate in traditional fluorescent fixtures. The most common type of LED tube light is the T8 4-ft LED tube light, designed to replace 4-ft fluorescent lamps.

The most common LED tube light types include: T8 LED tube (1 inch diameter), T12 LED tube (1.5-inch diameter), and T5HO LED tube (5/8-inch diameter). The number after the letter “T” indicates the diameter of the tube, in eighths of an inch. A T8 lamp, therefore, has a diameter of 8 eighths of an inch (8/8 inch), or exactly 1 inch. Each of these LED tube light types can be found in a variety of lengths, ranging from 1-ft (30 cm) to 8-ft (240 cm).



Figure 27 LED tube

- Traditional and Inorganic LEDs

Inorganic LEDs are light-emitting diodes (LEDs) made from a crystalline semiconductor. The optical emission wavelength can be selected by varying material composition. Example active regions include germanium, gallium arsenide, gallium nitride and indium phosphide.

The fibers are extremely small, typically they are 1/10th of the width of a human hair enabling manufacturers to deposit them as pixel arrays on a substrate in order to make a display.

Using these very small LEDs to create subpixels, depending on how light from the subpixels is mixed (generally made up of one green, one red and one blue), they can produce any given color, not dissimilar to display technologies already in existence.

- **Organic LED**

An organic light-emitting diode (OLED or organic LED), also known as organic electroluminescent (organic EL) diode, is a light-emitting diode (LED) in which the emissive electroluminescent layer is a film of organic compound that emits light in response to an electric current.

This organic layer is situated between two electrodes; typically, at least one of these electrodes is transparent. OLEDs are used to create digital displays in devices such as television screens, computer monitors, and portable systems such as smartphones and handheld game consoles. A major area of research is the development of white OLED devices for use in solid-state lighting applications.

There are two main families of OLED: those based on small molecules and those employing polymers. Adding mobile ions to an OLED creates a light-emitting electrochemical cell (LEC) which has a slightly different mode of operation. An OLED display can be driven with a passive-matrix (PMOLED) or active-matrix (AMOLED) control scheme. In the PMOLED scheme, each row (and line) in the display is controlled sequentially, one by one, whereas AMOLED control uses a thin-film transistor (TFT) backplane to directly access and switch each individual pixel on or off, allowing for higher resolution and larger display sizes [31].

- **HBLEDs**

High brightness LEDs (Fig. 2.9), also known as HBLEDs or high-power LEDs, are being used increasingly for lighting applications.

These high-power LEDs or high brightness LEDs provide much higher levels of light output than the traditional indicator LEDs. This places new challenges on the technology, although they are able to provide high levels of performance: greater efficiency than other forms of lighting technology and a much longer lifetime.

High brightness LED HBLED:

One HBLED definition is that it is a light emitting diode that produces over 50 lumens (1 candela = 12.75 lumens).

High power LED:

Generally, a high-power LED is defined as consumes more than 1 watt in power. Although high power LEDs and high brightness LEDs, HBLEDs may normally be one and the same, the two definitions refer to different characteristics or parameters.



Figure 28 High power LED

- Graphene LED

Graphene is a modified version of carbon, and while it has a history in physics since the middle of the 20th century, it was in 2004 that it was discovered and produced under lab conditions, by two Russian scientists at The University of Manchester, Andre Geim and Konstantin Novoselov, who went on to win the Nobel Prize in Physics.

Graphene has a vast number of applications in industry, particularly in electronics, energy storage, and photovoltaics. It is reported to be around 100 times stronger than steel by weight and is hugely efficient at conducting both heat and electricity. It is light, durable, and almost transparent.

Adding graphene to an LED bulb helps to dissipate heat – this makes them much brighter, meaning a lower wattage bulb will have the same effect as a traditional LED bulb – effectively reducing energy use for the same result.

With LED, graphene helps to dissipate heat from the bulbs which make them brighter, meaning a lower wattage bulb will have the same effect – effectively reducing energy use for the same result [32].



Figure 29 Graphene LED bulbs

2.4 Advantages and disadvantages of LEDs

Advantages

- *Long lifespan*

Long lifespan is undoubtedly the main advantage of LED lights. Compared to energy-saving lights, which have a lifespan of less than a year, the LEDs used in this type of lighting have high work productivity and can last up to 11 years. For example, LEDs that work 8 hours a day will last for about 20 years under normal administration, and only after that will we need to replace the light source with a new one.

- *Productivity*

Nowadays, LEDs are the most energy-efficient lighting source, using between 80 and 90 percent less energy (power) than conventional lighting sources such as mercury, metal halide, fluorescent and incandescent. Accordingly, 80% of the energy supplied to the device is converted into light, while 20% is wasted and converted into heat. Bright light efficiency is between 5 and 10%. precisely that much of the supplied energy is converted into light.

- *Protection from effect and temperature*

The advantage of LED lighting over conventional lighting is that it does not contain fibers or glass components, which are quite vulnerable to knocks and blows. In most cases, high-quality plastics and aluminum parts are used in the production of high-quality LED lighting, making the latter more durable and vibration- and low-temperature resistant.

- *Heat dissipation*

Due to their superior efficiency, LEDs generate significantly less heat than conventional lights. 90% of this energy production is managed and converted into light, allowing direct human contact with the LED light source without the risk of consumption even after a long period of use. In addition, the risk of fire, which can occur in spaces where traditional lighting is used and heats up to several hundred degrees, is only a small risk. As a result, LED lighting is preferable for equipment or products that are very sensitive to temperature.

- *Environmentally friendly*

In contrast with energy-saving lights, LEDs do not contain harmful pollutants such as mercury or other climate-threatening metals and are 100% recyclable, which helps reduce carbon dioxide emissions. This is another advantage of LED lighting. They contain artificial compounds that are harmless to the environment and are responsible for the phosphor in its light, which gives it its color.

- *Color*

We now have access to every illuminating light tone thanks to LED innovation. Although the three primary colors are red, green, and blue, we also may obtain any tone thanks to the latest technological advancements. Three segments make up each individual RGB LED framework, and each of these segments emits a different color from the RGB spectrum (red, green, and blue).

- *Design Flexibility*

LEDs also have wide range of applications including aquarium illumination, traffic signals, car or boat lights, and residential and commercial property applications. Due to their relatively small size, they may be used singly, in groups, or strung together to create a conventional bulb.

Disadvantages

- *Cost*

In contrast to a conventional light source, LED lighting is more expensive. In any case, it is important to keep in mind that this type of lighting has a life expectancy that is significantly higher (north of 10 years) than that of regular lights while also using a less amount of energy.

- *Temperature responsiveness*

Ambient temperature has a significant impact on how well diodes illuminate. The leakage current limits of semiconductor components alter at high temperatures, which can cause the LED module to wear out prematurely. Only the areas and surfaces exposed to highly rapid temperature changes or extremely high temperatures are affected by this problem (steel plants).

- *Light quality*

The majority of cool white LEDs have spectra that fundamentally differ from those of the sun or other dark heat sources such as incandescent lights. Due to metamerism, which is a phenomenon where red surfaces are rendered more severely by common cool-white phosphor-based LEDs, the peak at 460 nm and plunge at 500 nm can make the shade of objects clearly visible under cool-white LED lighting despite daylight or bright sources. But the ability of standard fluorescent lamps to transmit color is often inferior to that of white LEDs currently available in excellent manufacturing conditions.

- *Voltage responsiveness*

It is recommended to supply LED module with voltage that is above the limit and current that is below the nominal value. Series resistors or current-controlled power supply fall within this category.

3 Modeling a multisource light simulator

In this chapter, the approximation of the irradiance distribution will be studied. First, the irradiance distribution will be studied at a level of illumination, when it is illuminated by a single source, an LED.

Because the goal is to achieve the best uniformity, which is not going to be achieved no matter how much we reduce or increase the intensity of the luminous flux, it is recommended to use a greater number of LEDs.

Based on these arrangements, the irradiance distribution will be studied respectively for the following LED arrays: two (2) LEDs, linear, circular and circular with one LED in the center, square and triangular.

3.1 Single LED light simulator model

This specific approximation can determine the illuminance distribution as well as the lighting uniformity. The distance of the observer from the target field, the incident angle of the illuminating beam, the background brightness, the target reflectivity, the target pattern, and the target color all affect how homogeneous the perceived illumination is.

In this study, only the irradiance distribution across a flat region is examined. This flat region is parallel to the surface of the LED array in order to produce an appropriate design tool for uniform lighting.

In order to proceed with the modeling of both the radiant flux and luminous flux, emitted by a light source, we ought to make some general assumptions that will ensure the validity of the calculations.

Initially, the most significant assumption made in this work is that the illuminated surface is a flat and smooth surface, without examining (in this particular case) possible roughness and other surface irregularities.

In accordance with the research in light sources mentioned above and considering their significant advantages in their use, during this design and modeling, Light Emitting Diodes

were selected to be utilized as light sources. Additionally, every LED is modeled as an imperfect Lambertian² emitter.

Also, in this approach it is assumed that there is no addition for optical diffusion (optical diffusers) and the variation of the irradiance is approximated according to the Inverse Square Law for a point source (Appendix I).

As shown in Fig. 3.1, without loss of generality, we set the position of an LED at the point of intersection of the x, y, z axes that corresponds to the point in three – dimensional space (0, 0, 0).

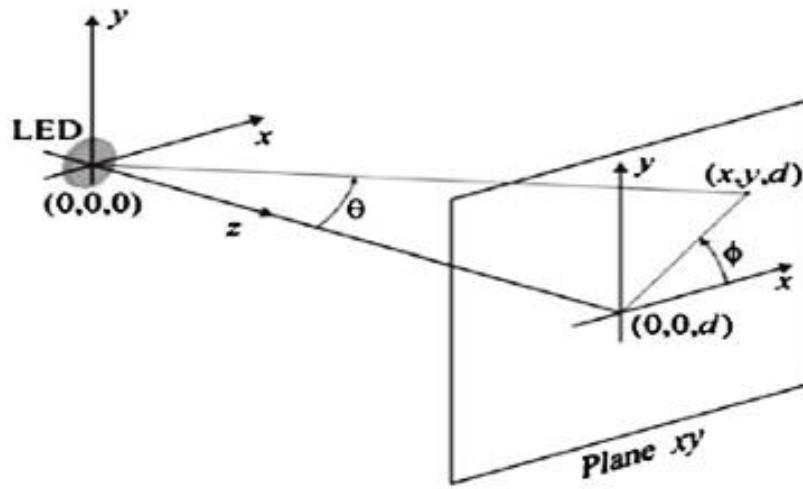


Figure 30 Cartesian and Spherical coordinate system [33]

Subsequently, the Irradiance pattern for an LED, which is placed in a point (x_0, y_0, z_0) , is represented by the following system of equations, expressed in spherical coordinates.

$$x_0 = R * \sin \theta \cos \varphi$$

$$y_0 = R * \sin \theta \sin \varphi$$

$$z_0 = R * \cos \theta$$

(9)

² A Lambertian source is defined as an area in which the brightness (or luminance) is independent of angle, in other words the off – axis luminance is the same as on – axis. Such a source has an intensity vs. angle profile that falls off as the cosine of the angle.

In the previous equation we assume that it is on the outer surface of a sphere of radius R in terms of Cartesian coordinates x, y, z , where r stands for radius ($r \in [0, \infty)$), θ for inclination ($\theta \in [0, \pi)$), and φ ($\varphi \in [0, 2\pi)$), for azimuthal angle.

In such situation, the Irradiance of an LED, with an intensity distribution given by:

$$\begin{aligned}
 & E(x, y, z; R, \theta, \varphi) \\
 &= A_{LED} L_{LED} \frac{[(x - R \sin\theta \cos\varphi) \sin\theta \cos\varphi + (y - R \sin\theta \sin\varphi) \sin\theta \sin\varphi + (z - R \cos\theta) \cos\theta]^m}{[(x - R \sin\theta \cos\varphi)^2 + (y - R \sin\theta \sin\varphi)^2 + (z - R \cos\theta)^2]^{\frac{m+3}{2}}}
 \end{aligned}
 \tag{10}$$

Where:

L_{LED} : is the radiance which is measured in $W \cdot m^{-2} \cdot sr^{-1}$ (value which depends on the LED chip)

A_{LED} : is the emitting area of the LED (m^2)

m : is a constant, the value which depends on the characteristics of the LED and specifically on the FWHM (Full Width at Half Maximum) which is analyzed below.

$$m = \frac{-\ln 2}{\ln \left(\cos\theta_{\frac{1}{2}} \right)}
 \tag{11}$$

3.1.1 FWHM

Full Width at Half Maximum (FWHM) is the difference between the two values of the independent variable at which the dependent variable is equal to half of its maximum value (Fig. 3.2). In other words, it is the width of a spectrum curve measured between those points on the y-axis which are half the maximum amplitude.

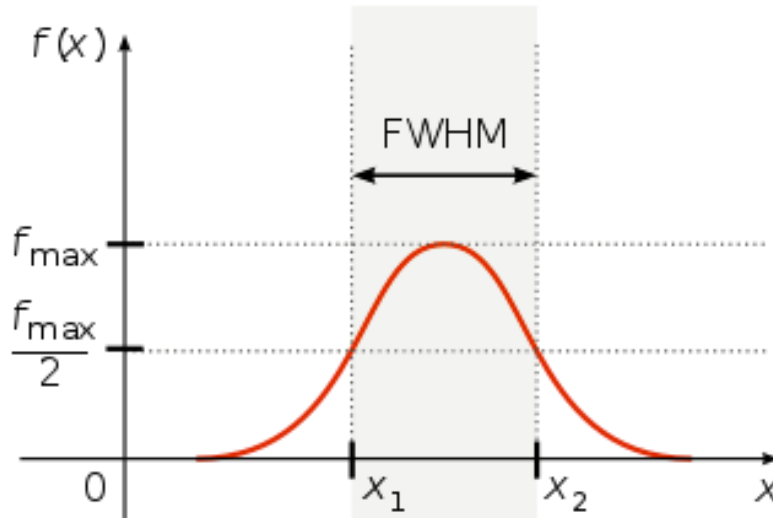


Figure 31 Full Width at Half Maximum [34]

If the considered function is the density of a normal distribution of the form (as it happens in this case):

$$f(x) = \frac{1}{\sigma * \sqrt{2\pi}} * e^{-\frac{(x-x_0)^2}{2\sigma^2}}.$$

(12)

Where σ is the standard deviation and x_0 is the expected value, then the relationship between FWHM and the standard deviation is:

$$FWHM = 2\sqrt{2 \ln 2} \sigma \approx 2,355 \sigma.$$

The corresponding area within this FWHM accounts to approximately 76%. The width does not depend on the expected value x_0 ; it is invariant under translation.

3.1.2 Convert Spherical coordinates to Cartesian

To investigate the Irradiance in a plane, Cartesian coordinates (x, y, z) are usually used. The Irradiance distribution of an LED given that the LED is placed at position $(X, Y, 0)$ and converting the spherical coordinates to Cartesian (x, y, z) can now be expressed as follows:

$$E(x, y, z) = \frac{z^m L_{LED} A_{LED}}{[(x - X)^2 + (y - Y)^2 + z^2]^{\frac{m+3}{2}}} \quad (13)$$

Also, if the product $L_{LED} A_{LED}$ is replaced with I_{LED} , where I_{LED} : LED Intensity (W/sr) the equation describing the Irradiance is given by:

$$E(x, y, z) = \frac{z^m I_{LED}}{[(x - X)^2 + (y - Y)^2 + z^2]^{\frac{m+3}{2}}} \quad (14)$$

3.2 multi-LED light simulator model

As was already established, the irradiance distribution from a light source can be represented by the sum of Gaussian distributions. Therefore, when we refer to an arrangement of light sources -in accordance with the principle of superposition- the irradiance at every point of the illuminated surface is calculated based on the sums of the irradiance received from each light source.

One of the main parts of this research was the study of relatively possible geometric topologies. The primary target was to achieve the best possible uniformity in combination with the increase of the maximum value for the irradiance. Subsequently, the topologies in which the LEDs can be arranged are listed [35].

3.2.1 Two (2) – LED Array

The first topology that was studied was the simplest arrangement according to which two LEDs should be arranged on the light beam surface (Fig. 3.3). In this specific case, the

Irradiance E can be calculated considering that it is the sum of the Irradiances from the two LEDs.

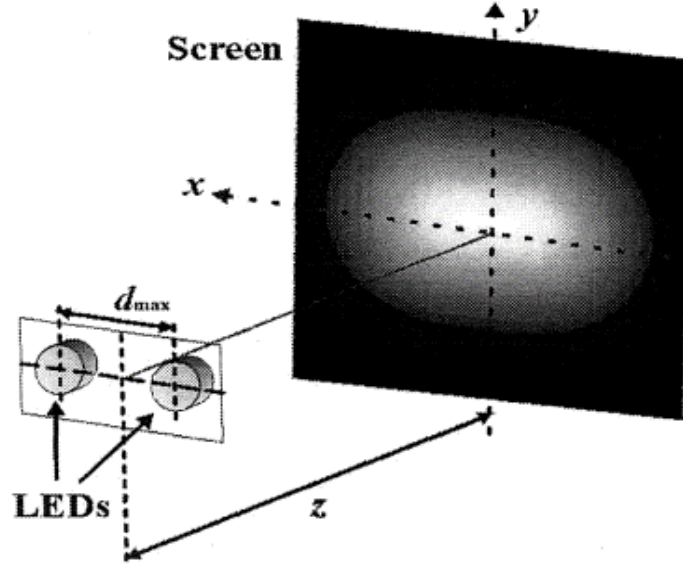


Figure 32 Schematic of a Two-LED array [36].

The distance between these LEDs is referred to as d. The formula through which we can calculate the Irradiance is given by [35]:

$$E(x, y, z) = z^m I_{LED} \left\{ \left[\left(x - \frac{d}{2} \right)^2 + y^2 + z^2 \right]^{-\frac{(m+2)}{2}} + \left[\left(x + \frac{d}{2} \right)^2 + y^2 + z^2 \right]^{-\frac{(m+2)}{2}} \right\} \quad (15)$$

A wider area than the uniform region covered by a single LED can provide Irradiance that is substantially uniform by adjusting the separation d. in a comparable pattern, we could modify the distance of the LEDs from each other to ensure that the second – order term of the previously given equation no longer in existence.

As a result, the maximally flat condition is obtained by differentiating E twice and setting $d^2E/dx^2 = 0$ at $x = 0$ and $y = 0$:

$$d_0 = \sqrt{\frac{4}{m+3}} * z$$

(16)

In the following graphs, the uniform irradiance distribution, along the x direction at $y=0$ for $m=80.7$ and $d=d_0=0.219$ (Fig. 3.4) and the corresponding pattern when the separation between LEDs is slightly increased (Fig. 3.5), is represented.

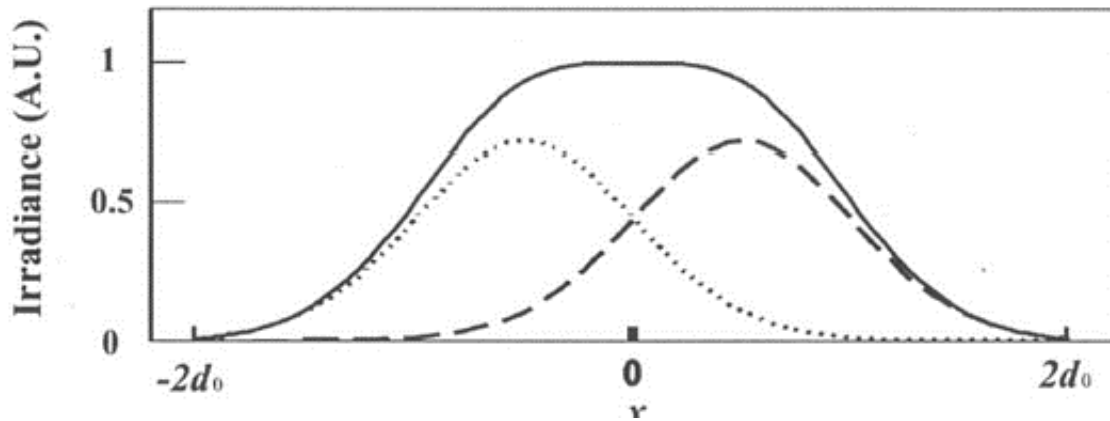


Figure 33 Two-LEDs array's uniform distribution [36].

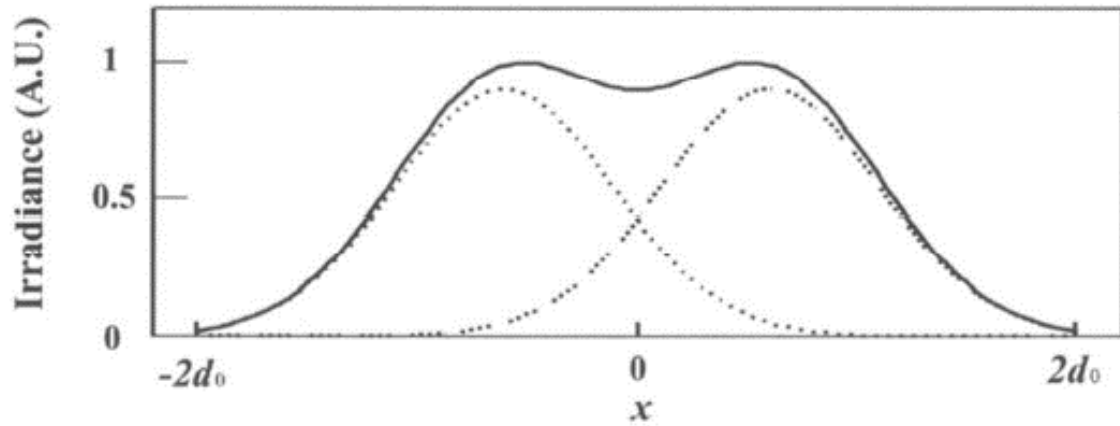


Figure 34 Two-LEDs uniform distribution (with increased distance between LEDs) [36].

3.2.2 Circular Ring Array

The case where the LEDs are arranged in a circular array with a defined radius r is the next case we investigate (Fig. 3.6). It needs to be noted, that this arrangement is intended for an array of more than four LEDs.

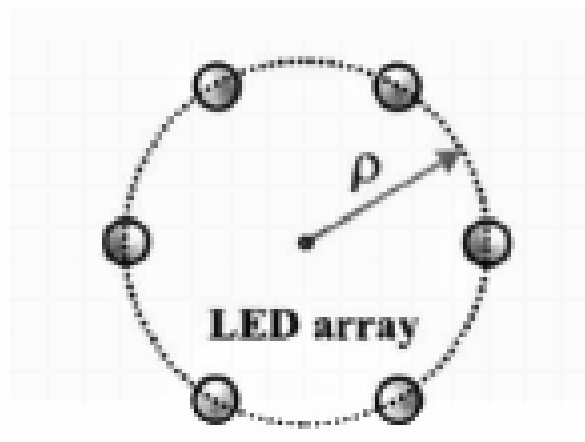


Figure 35 Schematic of a Circular Ring array [36].

The Irradiance for each point (x, y, z) of the plane from a circular arrangement of the LEDs can be calculated according to the following formula [36]:

$$E(x, y, z) = z^m I_{LED} \sum_{n=1}^N \left\{ \left[x - \rho \cos \frac{2\pi n}{N} \right]^2 + \left[y - \rho \sin \frac{2\pi n}{N} \right]^2 + z^2 \right\}^{-(m+2)/2} \quad (17)$$

The radius of the circular ring array can be changed to almost uniformly illuminate a central area of the surface. Similar to the two – LED arrangement, the radius of the ring can be changed in order to eliminate the second – order part in the previous equation.

Due to the symmetry, the problem reduces to a single dimension, allowing us to calculate the maximum planar state along a single axis connecting two LEDs, such as the y axis when $x = 0$.

Then, for each pattern pair, the separation is maximized to remove the minimum among the maximum from these designs. At some point, the maximum flat condition is obtained by differentiating E twice and setting $d^2E/dy^2 = 0$ at $y = 0$ and $x = 0$:

$$\rho_{max} = \sqrt{\frac{2}{m+2}} z \quad (18)$$

In the following graphs, the uniform irradiance distribution of the circular (ring) array with $N=6$, when $m=30$ and $\rho=\rho_0=0,25$ (Fig 3.7) and the corresponding normalized irradiance pattern along the x direction at $y=0$ (Fig 3.8), is represented.

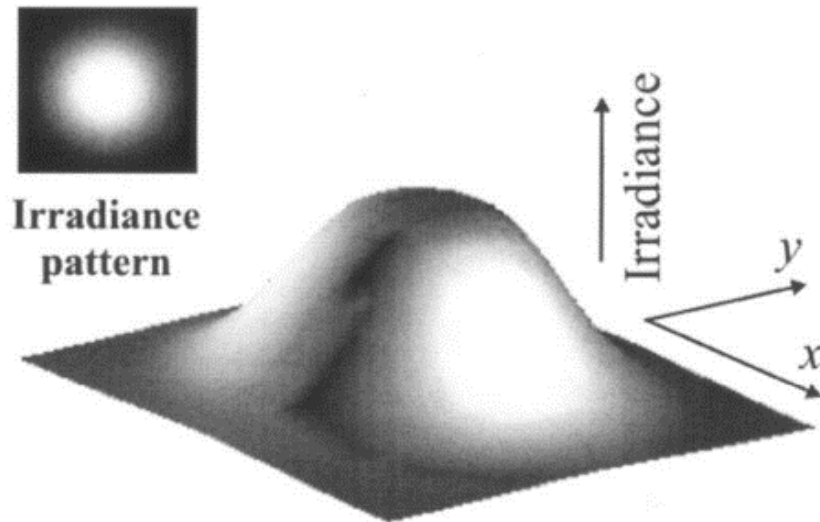


Figure 36 Circular LED array's Irradiance pattern [36].

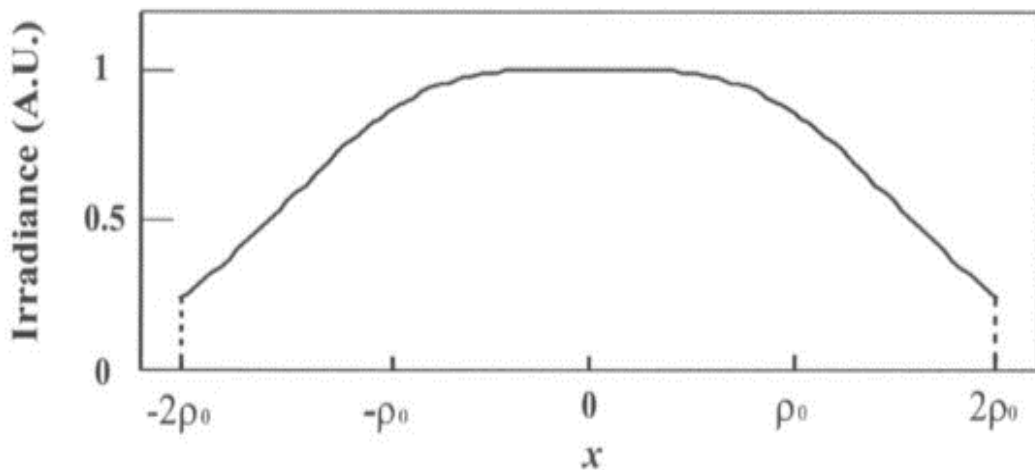


Figure 37 Circular LED array's normalized irradiance distribution along the x direction at $y=0$ [36].

3.2.3 Circular Ring Array with One LED in the Center

One LED is positioned in the center of a circular ring in LED lanterns used mostly for medical illumination, such as the curing LED lamps used by dentists. Therefore, designers and researchers take into account an N – LED circular ring array with one LED in the middle (Fig. 3.9).

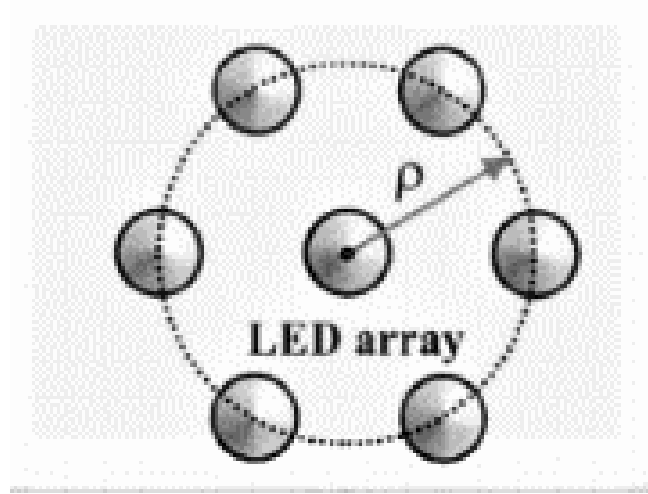


Figure 38 Schematic of a Circular Ring array with one LED in the center [36].

When using this type of array, the relative power of the middle LED must be adjusted in order to obtain a flat pattern.

The sum of the Irradiances for $(N + 1) \geq 4$ LEDs yields the Irradiance E [36].

$$E(x, y, z) = z^m I_{LED} \left(\sum_{n=1}^N \left\{ \left[x - \rho \cos \left(\frac{2\pi n}{N} \right) \right]^2 + \left[y - \rho \sin \left(\frac{2\pi n}{N} \right) \right]^2 + z^2 \right\}^{-(m+2)/2} + \varphi \{x^2 + y^2 + z^2\}^{-(m+2)/2} \right) \quad (19)$$

Where φ is the relative flux ($\varphi = \Phi_{\text{center}} / \Phi_{\text{ring}}$) of the middle LED (Φ_{center}) with respect to the power (Φ_{ring}) of one LED over the ring. Differentiating the Equation _, twice and setting $d^2x E / dx^2 = 0$ at $x = 0$ and $y = 0$ eventually gives the condition for uniform irradiance:

$$\rho_0 = \sqrt{\frac{4}{m+2}} z \quad (20)$$

In the following graphs, the uniform irradiance distribution of the circular (ring) array of six LEDs with one middle LED, when $m=30$, $z=1$, $\rho=\rho_0=0.354$ and $\varphi_0=0.72$ (Fig 3.10) and the resulting irradiance pattern along the x direction at $y=0$ (Fig 3.11), is represented.

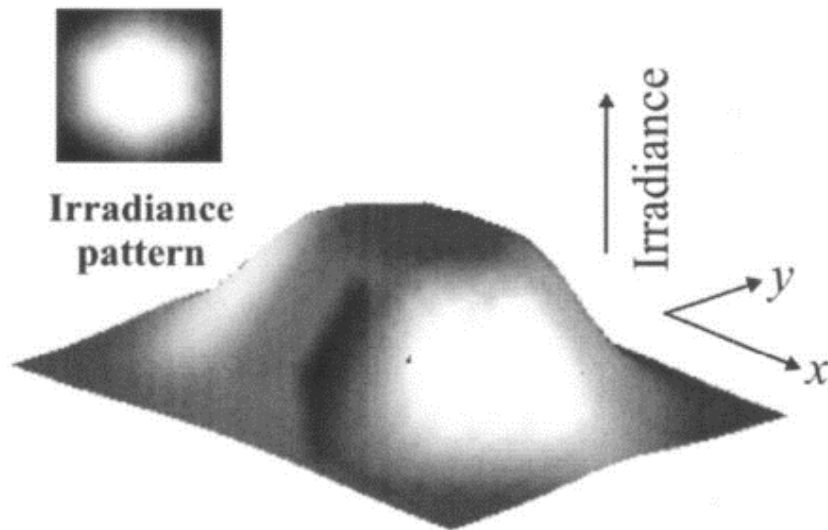


Figure 39 Circular Ring array with one middle LED array's uniform Irradiance distribution [36].

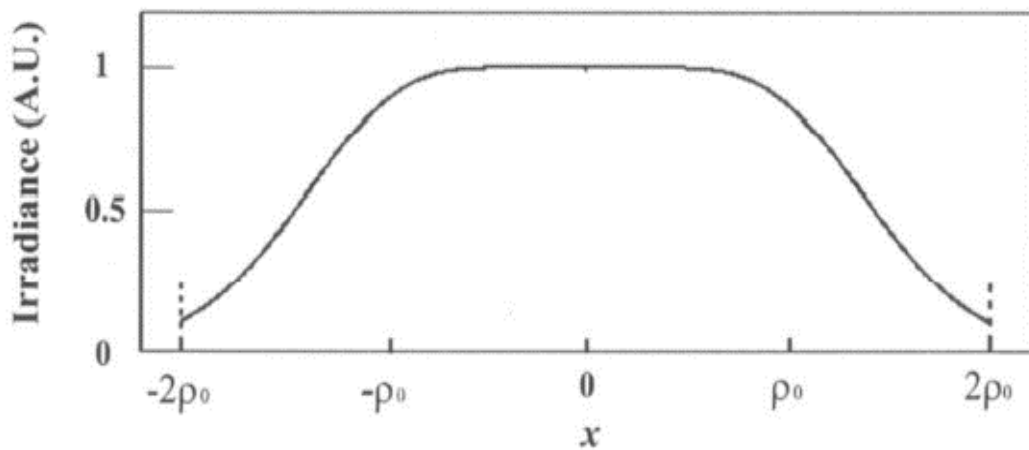


Figure 3.11 Circular Ring array with one middle LED array's normalized irradiance distribution along the x direction at $y=0$ [36].

3.2.4 Linear Array

The most commonly used LED source for structured lighting is a linear array of LEDs. It must be taken into consideration a linear array with a d LED – to – LED distance (Fig. 3.11).



Figure 401 Schematic of a Linear array [36].

In this instance, Irradiance E is determined by adding the Irradiances of N LEDs.

$$E(x, y, z) = z^m I_{LED} \sum_{n=1}^N \{ [x - (N + 1 - 2n)(d/2)]^2 + y^2 + z^2 \}^{-(m+2)/2} \quad (21)$$

The maximally flat condition obtained by differentiating E twice and setting $d^2x/dx^2 = 0$ at $x = 0$ and $y = 0$ eventually gives the expression,

$$f(D) = \sum_{n=1}^N [(N + 1 - 2n)^2(D^2/4) + 1]^{-(m+6)/2} * [1 - (m + 3)(N + 1 - 2n)^2(D^2/4)] \quad (22)$$

This results in d (where $D=d/z$) as a function of m and N satisfying the maximum flat condition. The zero cross of the f function defines $D=d/z$ as the maximum flat condition when N is even.

The minimum of the aforementioned equation, when applied to N odd, gives the maximum flat condition. These common cases presented challenges to analyze. The answer could,

however, be easily achieved with any mathematical software when numerical values for m and N are given.

The middle LED's relative flux is required to be adjusted in order to obtain a flat pattern. The maximum flat condition is provided by twice differentiating E and setting $d^2E/dx^2 = 0$ at $x = 0$ and $y = 0$:

$$d_0 = \sqrt{\frac{12}{m+3}}z \quad (23)$$

In the case of linear array of LEDs, we distinguish two (2) cases:

- For N odd number of LEDs:

$$E(x, y, z) = z^m I_{LED} \sum_{n=\frac{-(N-1)}{2}}^{\frac{(N-1)}{2}} [(x - nd)^2 + y^2 + z^2]^{-\frac{(m+2)}{2}} \quad (24)$$

- For N even number of LEDs:

$$E(x, y, z) = z^m I_{LED} \sum_{n=\frac{-(N-2)}{2}}^{\frac{N}{2}} \left[\left(x - (2n-1)\frac{d}{2} \right)^2 + y^2 + z^2 \right]^{-\frac{(m+2)}{2}} \quad (25)$$

In the following graphs, the uniform irradiance distribution of the linear array of seven LEDs, when $m=80.7$ and $d=d_0=0.135$ (Fig 3.12) and the resulting irradiance pattern along the x direction at $y=0$ (Fig 3.13), is represented.

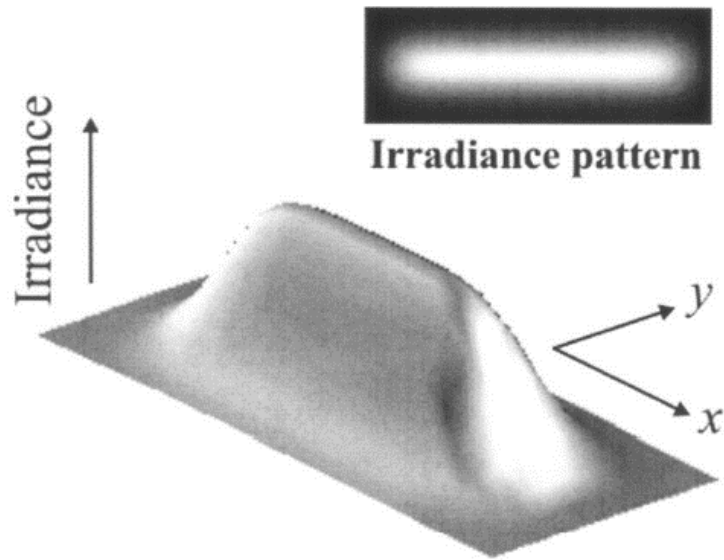


Figure 412 Linear LED array's uniform Irradiance distribution [36].

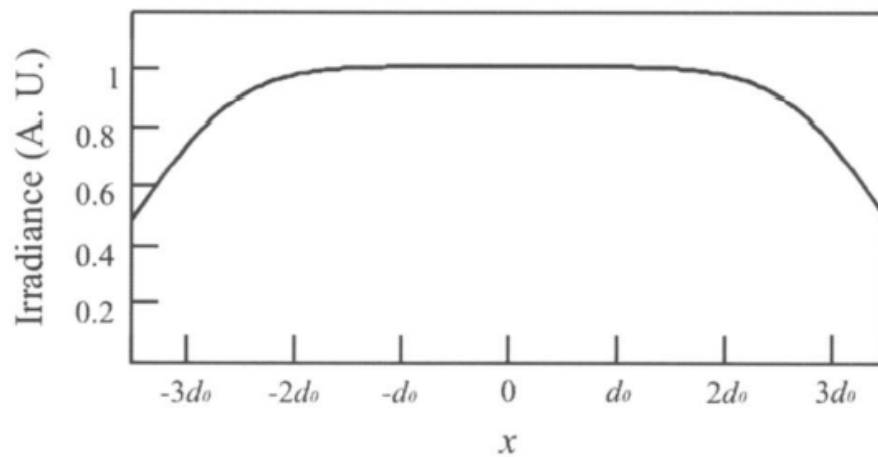


Figure 423 Linear LED array's normalized irradiance distribution along the x direction at $y=0$ [35].

3.2.5 Square LED Array

The square extended LED array is the most widely used (Fig. 3.14), for particular in operating illumination, in terms of assembly needs.

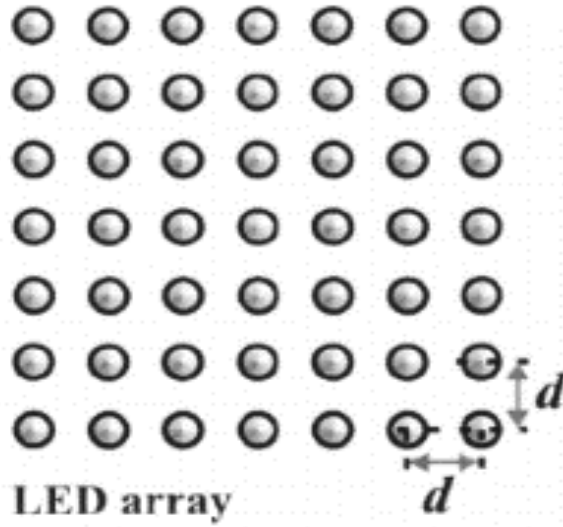


Figure 434 Schematic of a Square array [36].

The irradiance E for a square array of LEDs is derived by adding the irradiances of a matrix of $N \times M$ LEDs, which is given by:

$$E(x, y, z) = z^m I_{LED} \times \sum_{i=1}^N \sum_{j=1}^M \{ [x - (N + 1 - 2i)(d/2)]^2 + [y - (M + 1 - 2j)(d/2)]^2 + z^2 \}^{-(m+2)/2} \quad (26)$$

Differentiating the previous equation twice and setting $d^2E/dx^2 = 0$ at $x = 0$ and $y = 0$ gives the following expression:

$$f(D) = \sum_{i=1}^N \sum_{j=1}^M \{ [(N + 1 - 2i)^2 + (M + 1 - 2j)^2] (D^2/4) + 1 \}^{-(m+6)/2} \{ 1 - [(m + 3)(N + 1 - 2i)^2 - (M + 1 - 2j)^2] (D^2/4) \} \quad (27)$$

Which yields the maximally flat condition for d (where $D=d/z$) as a function of m , N , and M . When both N and M are even numbers, the maximally flat condition, $D=d_0/z$, is given by the zero cross of the f function.

If both N and M are odd, the maximally flat condition is provided by the minimum of the Equation 27. For all other possibilities, the maximally flat condition is given by the zero cross or the first minimum of f(D).

Especially, for the specific cases:

- For 2x2 LED Array:

$$d_0 = \sqrt{\frac{4}{m+2}} z \quad (28)$$

- For 4x4 LED Array:

$$d_0 = \sqrt{\frac{1.2125}{m-3.349}} z \quad (29)$$

In the following graphs, the uniform irradiance distribution of the linear array of seven LEDs, when $m=50$ and $d=d_0=0.17$ (Fig 3.15) and the resulting irradiance pattern along the x direction at $y=0$ (Fig 3.16), is represented.

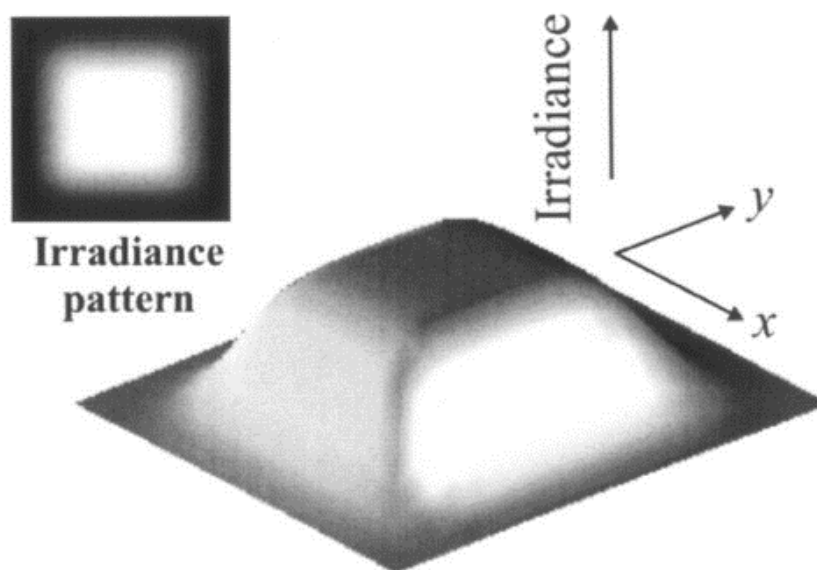


Figure 445 Square LED array's uniform Irradiance distribution [36].

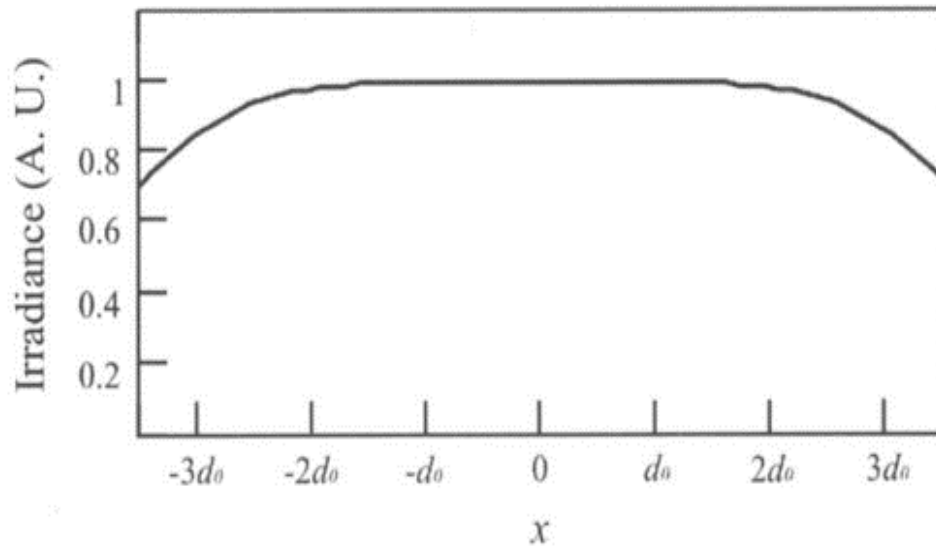


Figure 456 Square LED array's normalized irradiance distribution along the x direction at $y=0$ [36].

3.2.6 Triangular LED Array

Due to its compact advantages, the triangular array, also known as the hexagonal (Fig. 3.17), is a prevalent arrangement of LED sources.

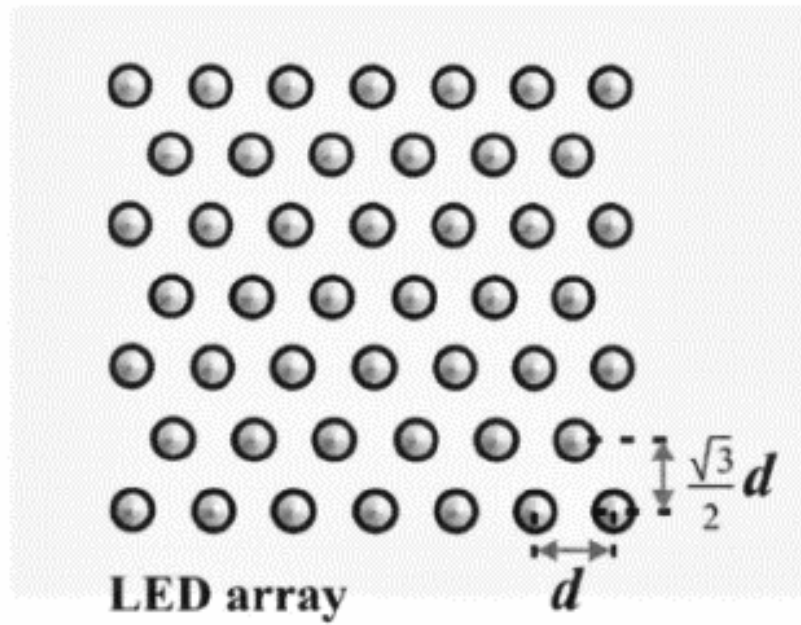


Figure 467 Schematic of a Triangular array [36].

Irradiance E for a triangular array is determined by the total of the irradiances for an array of S LEDs:

$$\text{Where: } S = \{(N \times M) - 0.25 [2M + (-1)^M - 1]\} \quad (30)$$

The Irradiance E given by:

$$E(x, y, z) = z^m I_{LED} \sum_{j=1}^M \sum_{i=1}^{N_-} \left\{ \left[x - (N_+ - 2i) \left(\frac{d}{2} \right) \right]^2 + \left[y - (M + 1 - 2j) \left(\frac{\sqrt{3}d}{4} \right) \right]^2 + z^2 \right\}^{-\frac{m+2}{2}} \quad (31)$$

$$\text{where: } N_{\pm} = N + \frac{[(-1)^j \pm 1]}{2}$$

The maximally flat condition obtained by differentiating E twice and setting $d^2E/dx^2 = 0$ at $x = 0$ and $y = 0$ eventually gives the expression:

$$f(D) = \sum_{j=1}^M \sum_{i=1}^{N_-} \left\{ \left[(N_- + -2i)^2 + 3/4 (M + 1 - 2j)^2 \right] (D^2 / 4) + 1 \right\}^{-(m+6/2)} \left\{ 1 - \left[(m+3)(N_- + -2i)^2 - 3/4(M + 1 - 2j)^2 \right] (D^2 / 4) \right\} \quad (32)$$

Which yields the maximally flat condition for d (where $D=d/z$) as a function of m, N, and M. when both N and M are even numbers, the maximally flat condition, $D=d_0/z$, is given by the zero cross of the f function.

If both N and M are odd, the maximally flat condition is provided by the minimum of the previous equation. The zero cross or the first minimum of “f” function provides the maximally flat condition in all other circumstances.

In the following graphs, the uniform irradiance distribution of the linear array of seven LEDs, when $m=50$ and $d=d_0=0.192$ (Fig 3.18) and the resulting irradiance pattern along the x direction at $y=0$ (Fig 3.19), is represented.

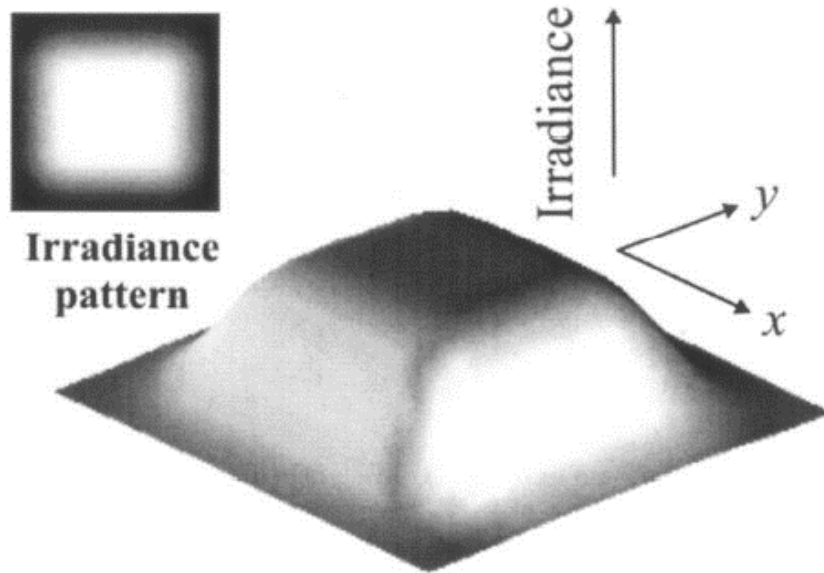


Figure 478 Triangular LED array's uniform Irradiance distribution [36].

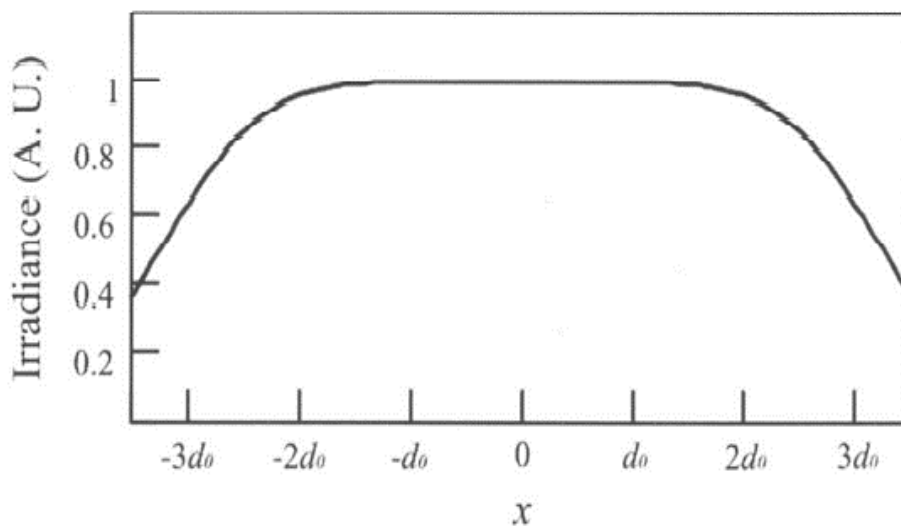


Figure 4819 Triangular LED array's normalized irradiance distribution along the x direction at $y=0$ [36].

3.3 multi-LED light simulator design guidelines

As we have already mentioned, the need for light simulators nowadays has become imperative. The search for light simulators leads to a particularly large number of results, when it comes from a search for the case of solar simulators.

Also, an object of the present work, was the finding of design guidelines. These guidelines seek - for a specific topology, height between the surfaces, available number of LEDs as well as possibly other limitations that can be taken into account - to reduce non-uniformity to the minimum possible degree (in the best case).

As this is obvious, given that we were dealing with equations that include several parameters, in order to approximate the solution to the problem we seek to solve, we must stabilize certain parameters.

The starting point of this process is the study of Irradiance along a random testing plane.

We assume that the Irradiance distribution can calculate from a formula of the form:

$E(x, y, z)$, where x and y are the dimensions of the testing plane, therefore $x \in [\alpha, \beta]$ and $y \in [\gamma, \delta]$.

Stabilizing z , at each step of the process, results to: $E(x, y)$, which corresponds to a matrix of $x*y$ values, all of which have positive values strictly.

Therefore, we consider the metric space (\mathbb{R}, E) , where $E: \mathbb{R} \times \mathbb{R} \rightarrow [0, +\infty)$.

The most important value (critical) that we must examine is that of non-uniformity, so it appears:

$$\text{Critical Value} = \frac{\sup_{x \rightarrow [\alpha, \beta]} (E(x, y)) - \inf_{x \rightarrow [\alpha, \beta]} (E(x, y))}{\sup_{x \rightarrow [\alpha, \beta]} (E(x, y)) + \inf_{x \rightarrow [\alpha, \beta]} (E(x, y))}$$

(33)

If the corresponding procedure assumes that it takes place in the three-dimensional space \mathbb{R}^3 , we found that there is an interval subset of the domain definition of the function Critical Value, in which the function appears to vary monotonically.

This interval determines the appropriate height of placing the luminous surface in a specific range of distances from the surface where the light sources are arranged. Several different arrangements were tested, and the best results in terms of uniformity were achieved by arrays in which the LEDs are arranged squarely.

During this process, that area is approached with the appropriate heights at which the best uniformity is achieved compared to the smallest possible height. This is a fact that allows better radiation of the surface (higher irradiance; W/m^2) with better uniformity.

For a better understanding of what was mentioned, then a practical application of all the previous ones is made through graphic representations.

Due to the previous study, the arrangement that showed greater interest because of the best results it provided, was that of the square arrangement, which was chosen.

Through the MATLAB environment an algorithm was developed which calculates the irradiance distribution over a test plane, and an interval for the height between the surfaces.

The same algorithm also, through the same process, extracts the turning point - which is the key factor for the specific case - as well as an analytical graphical representation of the function Critical Value (z), (Appendix II).

The following test were carried out, as shown in the Table 3.1.

<i>Topology</i>	<i>Distance between LEDs (m)</i>	<i>Z₀ (m)</i>
2x2	0.18	0.081
4x4	0.06	0.031
6x6	0.036	0.019

TABLE XI Square LED topologies examination.

The upper table contains the results obtained through the developed algorithm. In more detail, the graphic results are presented below for each case examined.

❖ Case 1: Analysis of 2x2 LED array.

During the study, given that the available number of light sources was chosen to be equal to four LEDs, the algorithm extracts the optimal topology as well as the best possible distance between them, in accordance with the limitations set for the testing plane.

Then, after the baselines have been set, the critical value function is approached. Thus, by analyzing the above function, the turning point is found.

Finally, replacing the turning point in the illuminance (or the irradiance) distribution calculation algorithm, we also extract the graphical representation of the plane test, for the calculated conditions.

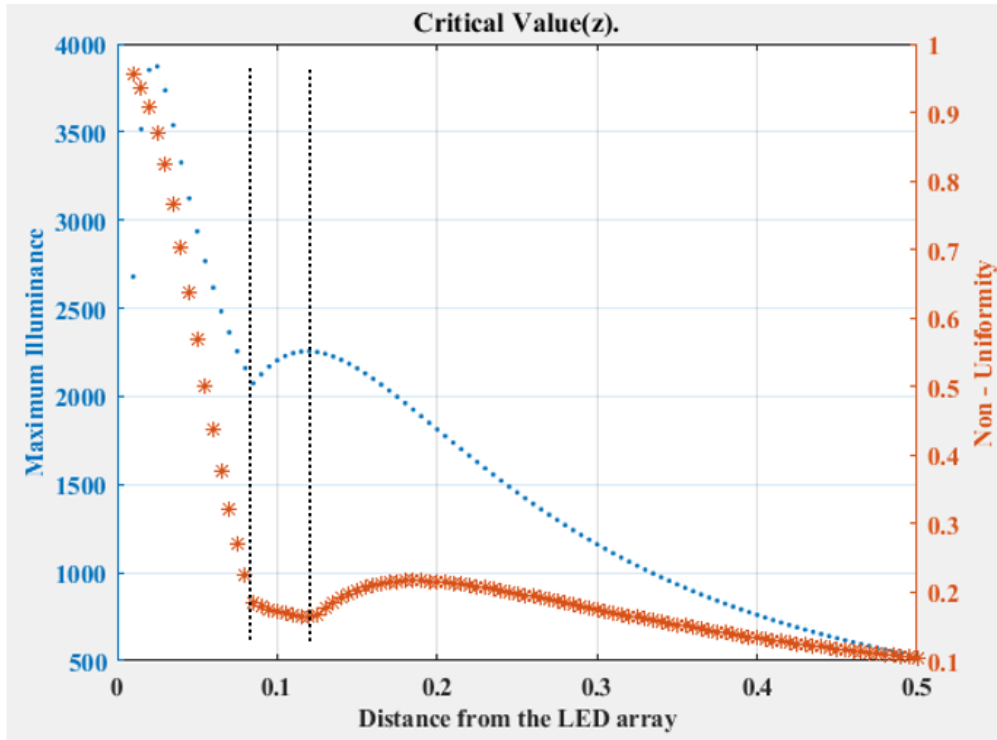


Figure 490 2x2 LED array's critical value.

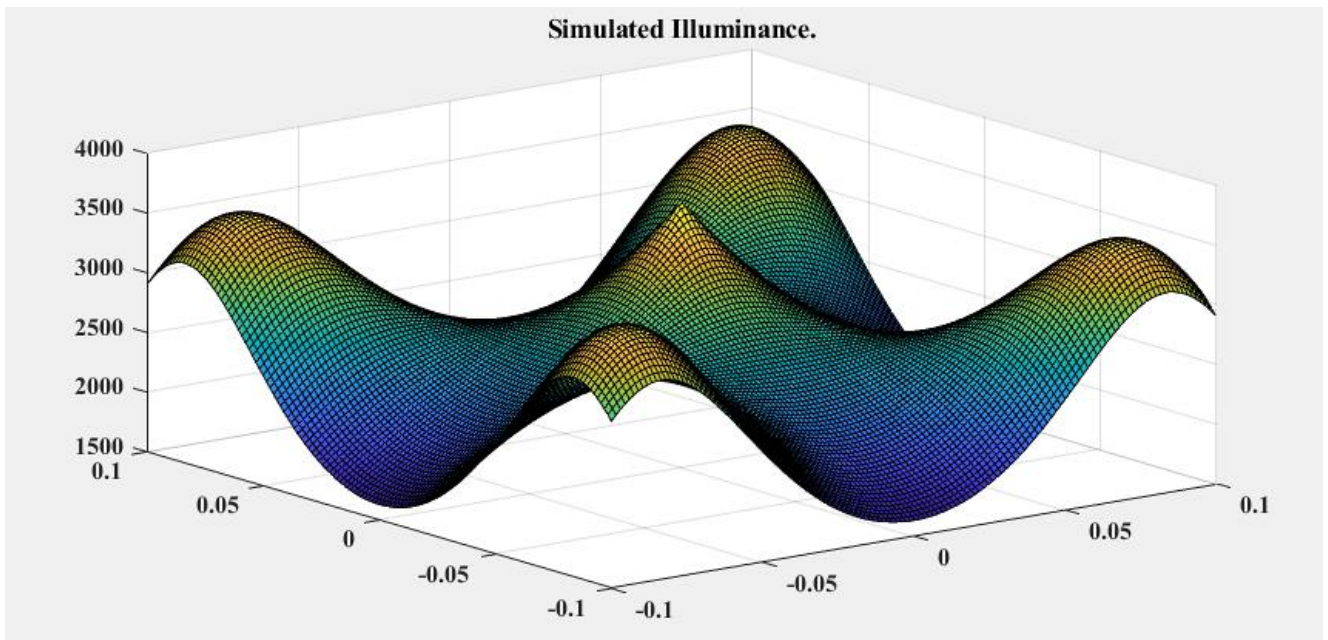


Figure 501 Illuminance distribution - Critical_Value(0.081)

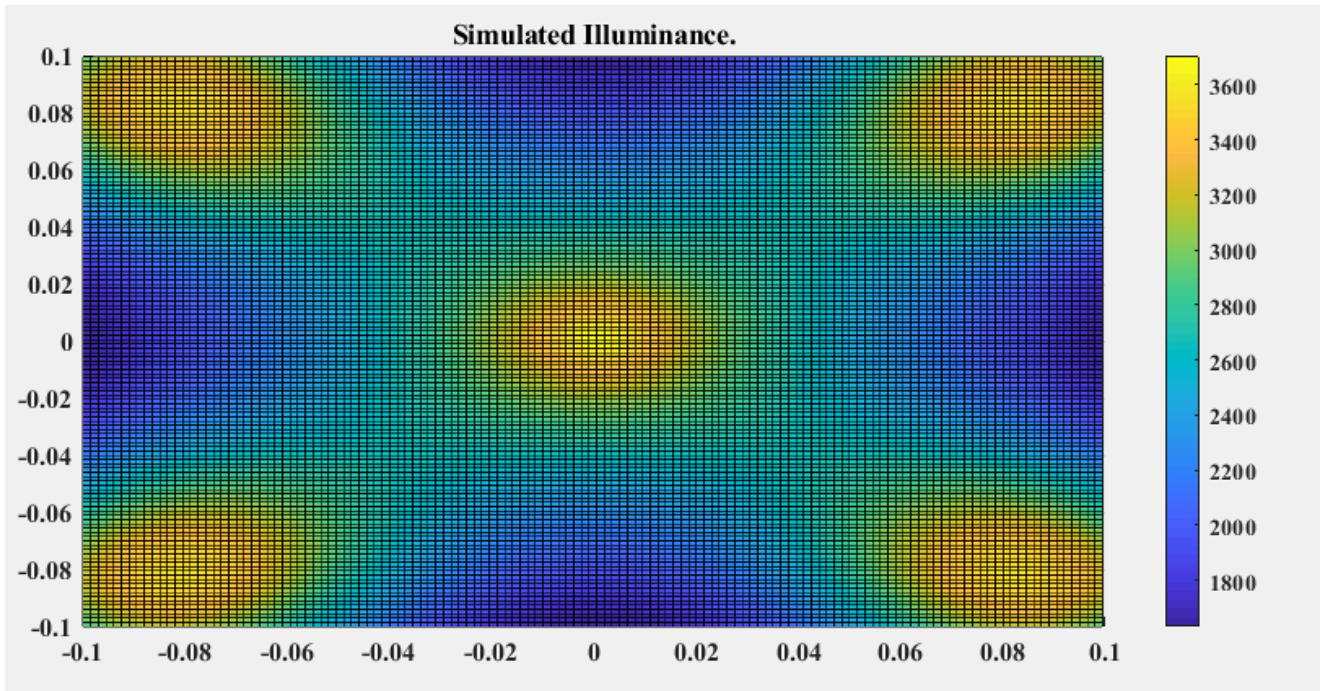


Figure 512 Illuminance heatmap - Critical_Value(0.081) (2)

❖ Case 2: Analysis of 4x4 LED array.

During the study, given that the available number of light sources was chosen to be equal to sixteen LEDs, the algorithm extracts the optimal topology as well as the best possible distance between them, in accordance with the limitations set for the testing plane.

Then, after the baselines have been set, the critical value function is approached. Thus, by analyzing the above function, the turning point is found.

Finally, replacing the turning point in the illuminance (or the irradiance) distribution calculation algorithm, we also extract the graphical representation of the plane test, for the calculated conditions.

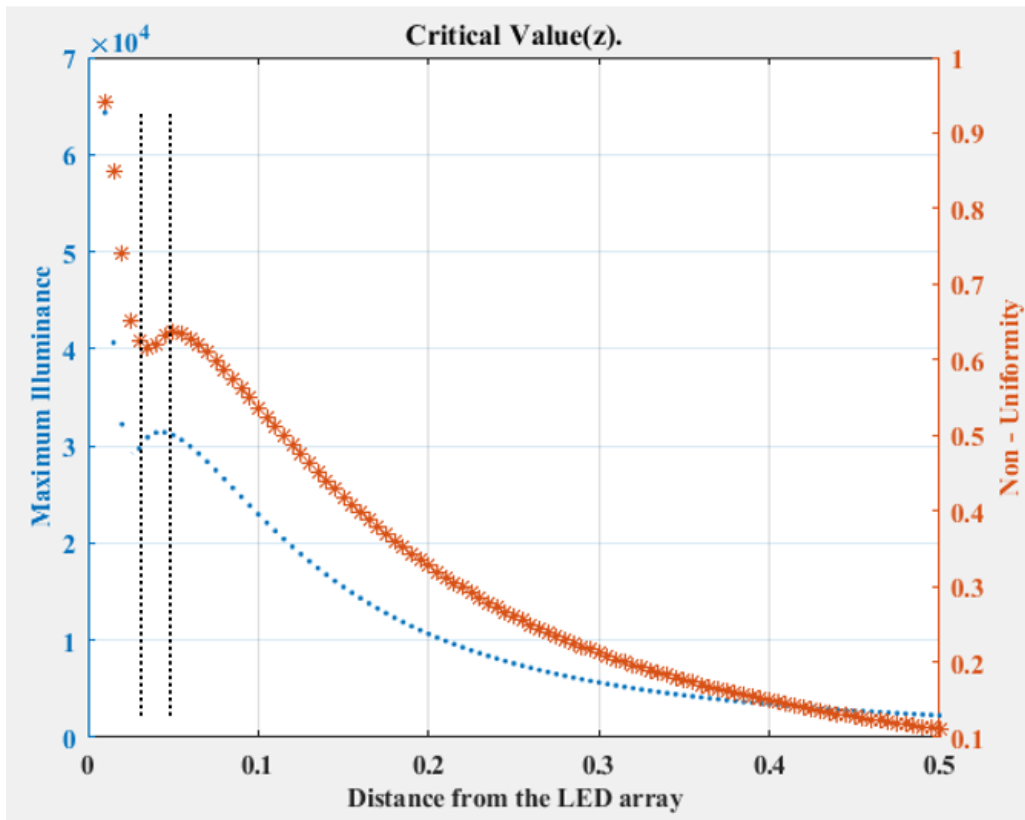


Figure 523 4x4 LED array's Critical Value.

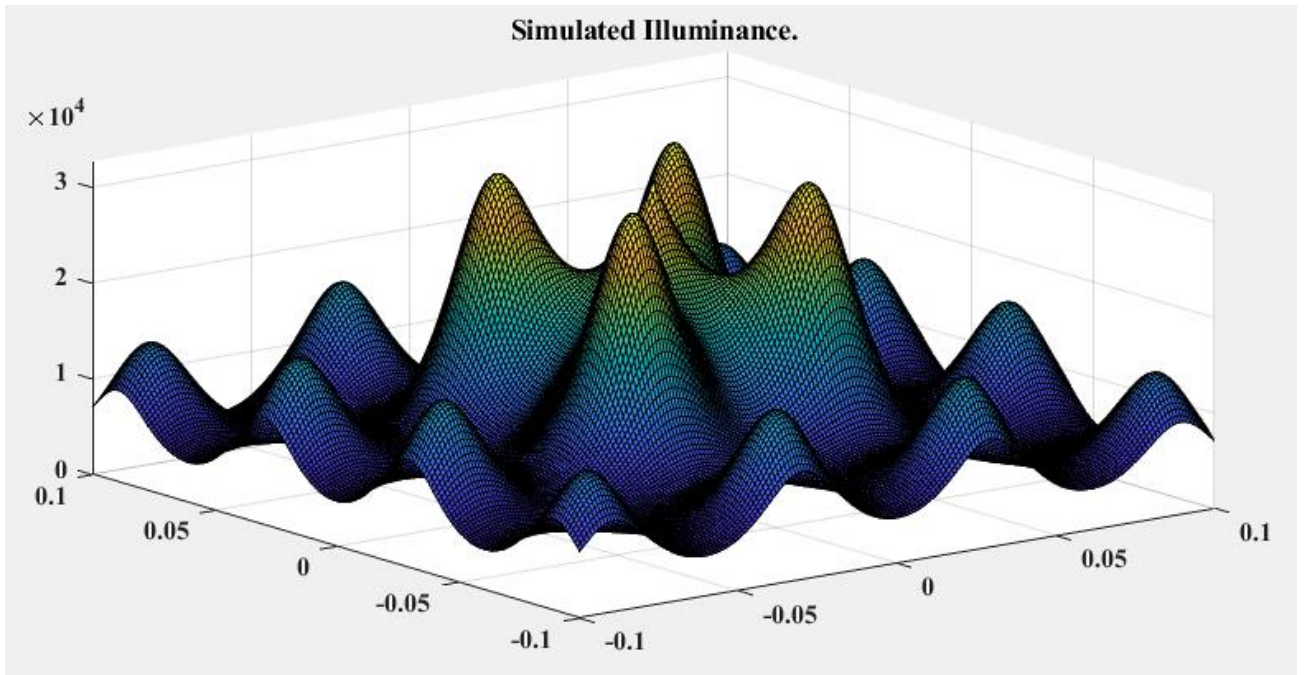


Figure 3.24 Illuminance distribution - Critical Value (0.031)

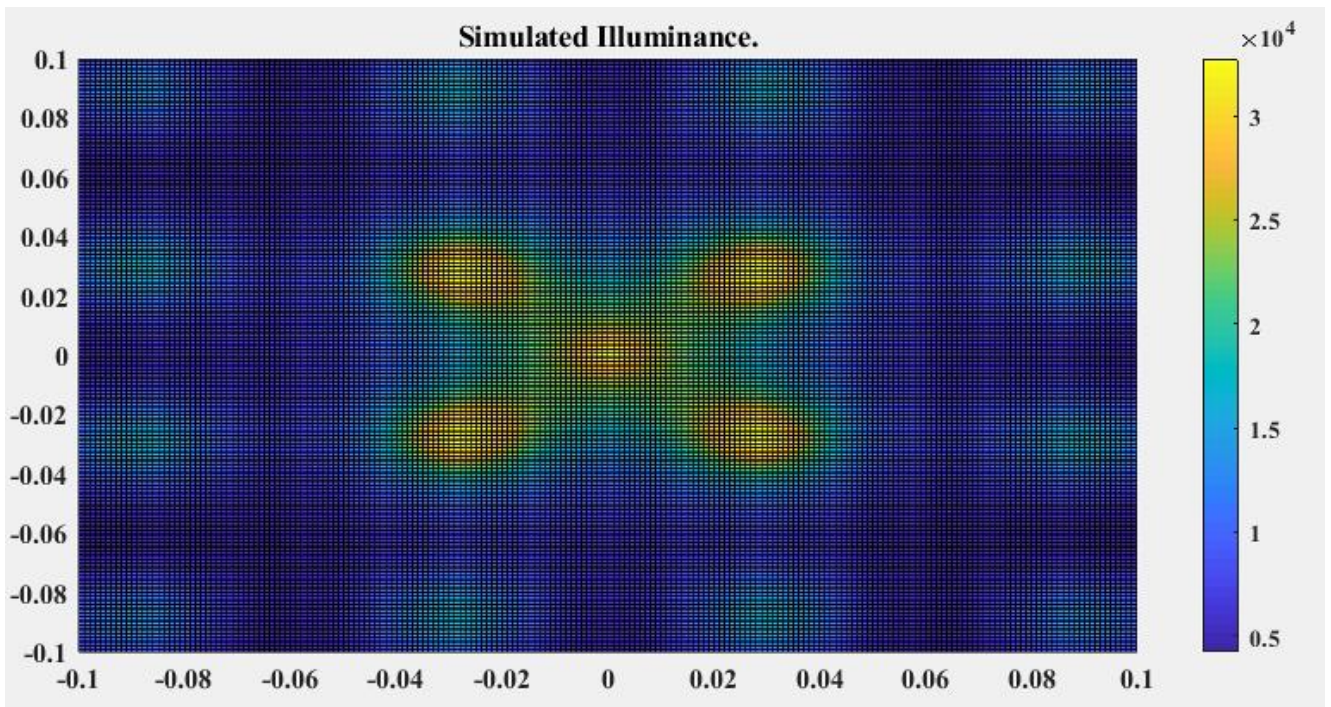


Figure 3.25 Illuminance distribution - Critical Value (0.031) (2)

❖ Case 3: Analysis of 6x6 LED array.

During the study, given that the available number of light sources was chosen to be equal to thirty-six LEDs, the algorithm extracts the optimal topology as well as the best possible distance between them, in accordance with the limitations set for the testing plane.

Then, after the baselines have been set, the critical value function is approached. Thus, by analyzing the above function, the turning point is found.

Finally, replacing the turning point in the illuminance (or the irradiance) distribution calculation algorithm, we also extract the graphical representation of the plane test, for the calculated conditions.

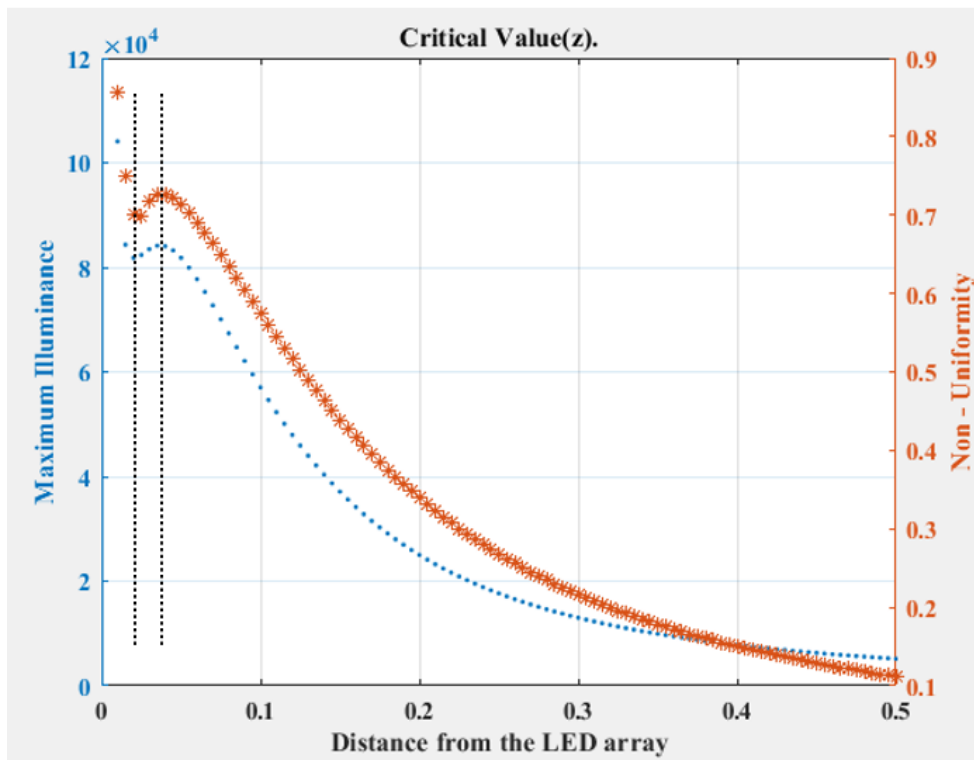


Figure 534 6x6 LED array's Critical Value.

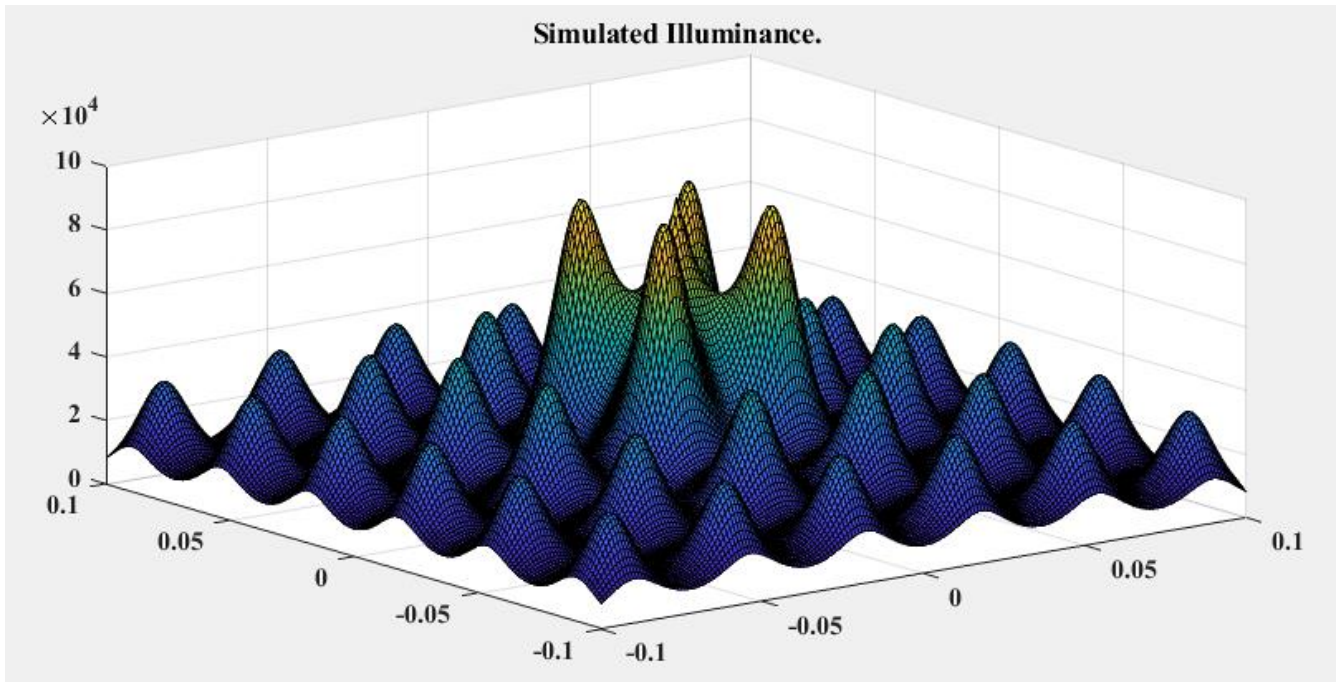


Figure 54 Illuminance distribution - Critical_Value(0.019)

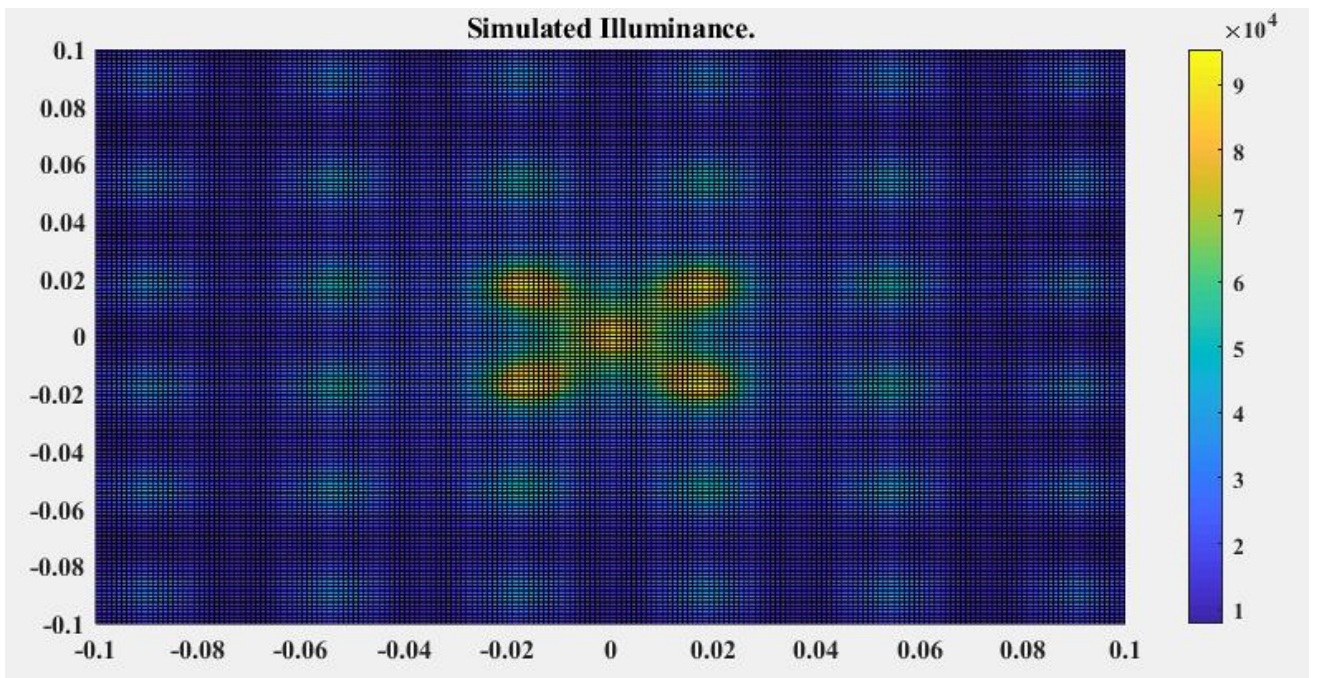


Figure 55 Illuminance distribution - Critical_Value (0.019) (2)

As shown in the figures above, in all cases an optimal square area was created which is interesting, due to the beneficial combination of low Non-uniformity - High Irradiance performance.

4 Experimental Investigation

The aim of the study mentioned in the previous chapters, was to create the basic knowledge regarding the light sources, their characteristics, their mode of operation and other basic parameters.

Firstly, the goal of this thesis is to find a technique needed in order to be able of lighting an area, with the lowest possible cost, both in terms of economic benefit due to the reduction of sources, as well as construction cost.

Using this knowledge, we will be able to surpass in quality compared to those, which are already in circulation, thanks to the results obtained and their interpretation based on the specifications considered.

In this chapter, the experimental measurements will be represented, and their results will be interpreted. The procedure started with the development of the algorithms that were used for determining the values of the quantities of interest, such intensity, irradiance, and illuminance [37].

next, the development of an algorithm that is capable of deciding the arrangement for a given number of LEDs, the dimensions of the surface on which the user can place the LEDs, the dimensions of the luminous surface and the distance between them and their positions in the surface, based on uniformity.

In the case where the algorithm is asked to choose between two or more arrangements with the same – or significantly similar – uniformity, then choose the arrangement with the smallest number of LEDs, because priority is given to the cost.

Restrictions can also be placed (e.g., for uniformity, maximum or minimum irradiance), where based on them, the algorithm must extract the corresponding result. Unless the assumptions defined by the user are not satisfied with any arrays, then it extracts the closest result based on the requirements. All the algorithms developed as well as the results obtained in the MATLAB environment.

A very common mathematical process in different disciplines of science and technology is fitting equations to data. A corresponding procedure was followed to approximate the

irradiance distribution, initially of the single LED and then its adaption to the square arrangement was made, by Curve Fitting Tool from MATLAB.

4.1 Experimental LED light simulator setup

In the context of this thesis, a device for evaluating indoor photovoltaic cells by the Autonomous Systems Laboratory was used [38]. This device has a movable bed that can be placed in a range of heights between 5 and 31 cm from the surface where the LEDs are placed (Fig 4.1).

Furthermore, this experimental device has such a design that can support a variety of array geometries, because of the fact that each LED is supplied separately. More concretely, it supports from single up to five LEDs light sources (Fig 4.2). The bed is also enclosed to prevents external light interference i.e., blocks incoming light from environment.

Also, both the dimensions of the surface on which the LEDs are placed, and the illuminated area are 18 x 18 cm.



Figure 56 The Light Simulator used

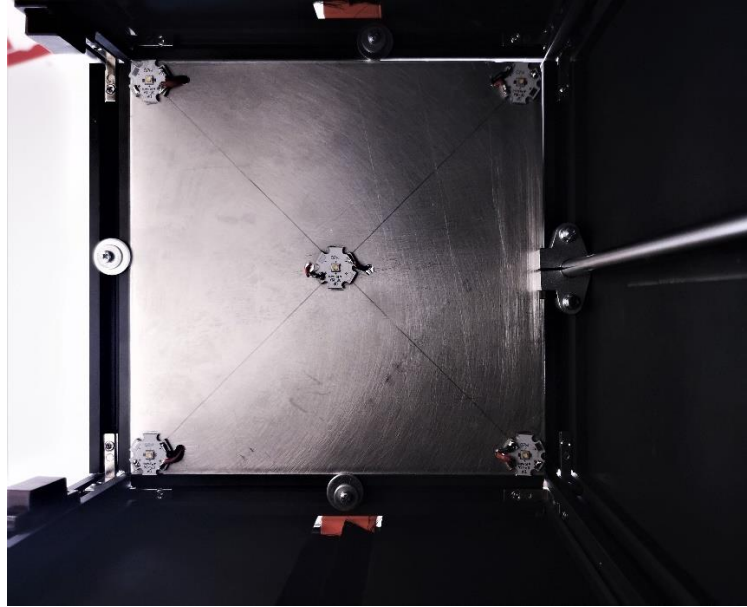
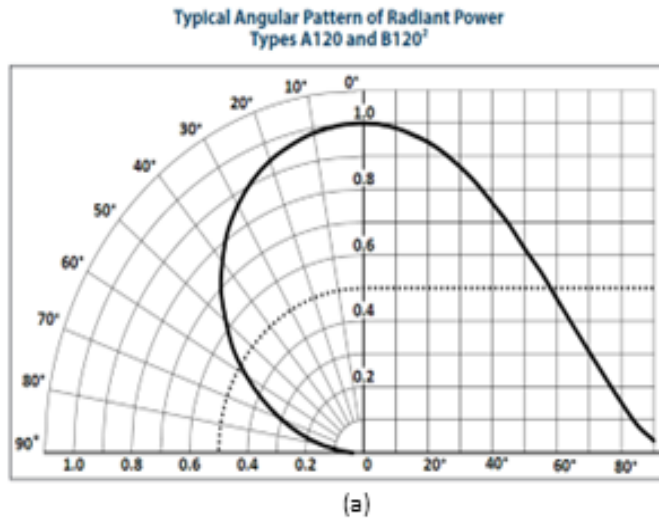


Figure 57 Experimental setup, LED array's arrangement.

As for the light source, the LED used is LST1 – 01G03 – 4095 – 01, from Luminus. As shown in Fig. 4.3 (a) & Fig. 4.3 (b), both optical and electrical characteristics are displayed, and the TABLE 4.1 shows its main characteristics [39].



Forward Voltage vs. Forward Current

$V_f(I_f)$ Single Pulse 20ms $T_j = 85^\circ\text{C}$

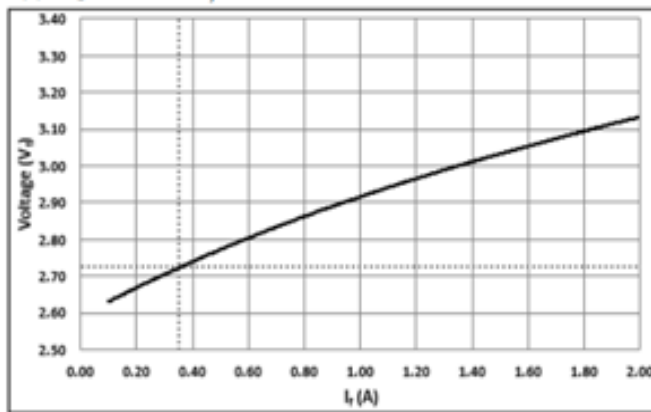


Figure 58 (a) Typical Angular Pattern of Radiant Power, (b) Forward Voltage vs. Forward Current

<i>Parameter</i>	Symbol	Value	Unit
<i>Forward Current at test</i>	I_f	350	mA
<i>Forward Voltage</i>	V_f	2.73	V

<i>Luminous Flux</i>	Φ_v	107	lm
<i>Radiometric Flux</i>	Φ_e	442	mW
<i>Viewing angle</i>	$2\theta_{1/2}$	120	Degrees
<i>Color Rendering Index</i>	CRI	95 (minimum)	-

TABLE XII Light source's main characteristics.

Due to the lack of a generally acknowledged standard reporting condition (SRC) for indoor photovoltaic measurements or of calibrated reference cells for low light measurements, many researchers have been obliged to employ illumination meters to measure irradiance and report values in lux ($lx = lm/m^2$) [37].

Therefore, to evaluate the experimental device, illuminance measurements were carried out. To measure the illuminance, we use the commercially available instrument E – SUN LX – 101, whose measurement range is from 1 up to 50,000 Lux and accuracy $\pm 5\%$.

4.2 Single LED measurements

Initially, an algorithm was developed that can approximate – simulate all the quantities of interest. More specifically, this program is able, taking as input the dimensions of the illuminated surface, the distance from the surface to the light source as well as the FWHM, to extract the expected maximum and minimum values of the Irradiance and Illuminance.

Furthermore, it can calculate overall the Non – Uniformity of Irradiance along the entire irradiated surface and it can identify the dimensions of the surface that can be illuminated for specific values for non – uniformity.

The latter mentioned is a basic criterion for the characterization – classification of light simulators. It can also extract a graphical representation of the distribution of Irradiance and Illuminance for all the aforementioned cases.

The following graphs show the results obtained from a simulation made considering that the LED was placed in the center of a surface of dimensions 18 x 18 cm, for an illuminated surface of dimensions 14 x 14 cm, and the distance of 31 cm between them.

In summary, the data used for the following simulations are summarized in the following table.

Dimensions of Illuminated Surface (m)	
x axis	[-0.07, 0.07]
y axis	[-0.07, 0.07]
Height (m)	
z axis	0.31
LED array's dimensions (m)	
x axis	[-0.09, 0.09]
y axis	[-0.09, 0.09]
Radiometric Flux (mW)	
φ_e	442
Viewing angle (Degrees)	
$2 \vartheta_{/2}$	120

TABLE XIII System Variables.

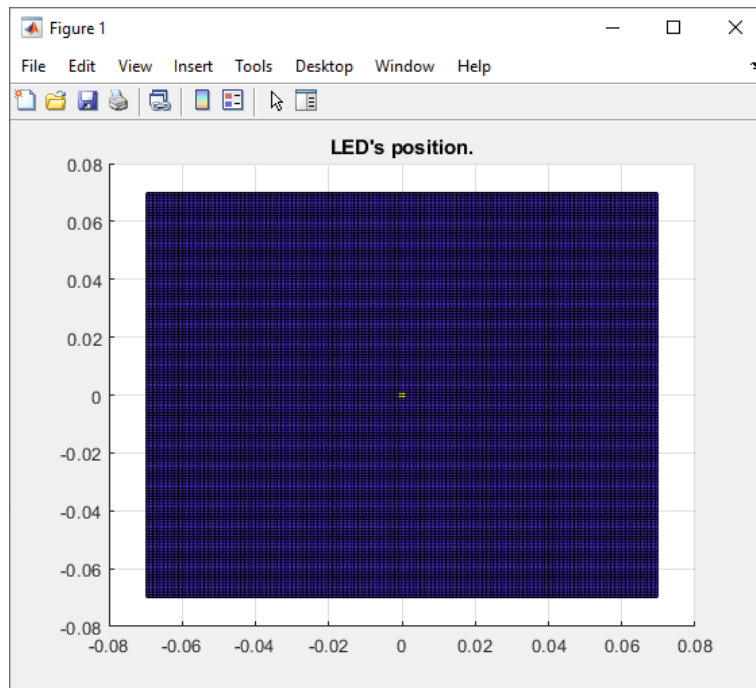


Figure 4.59 LED's position

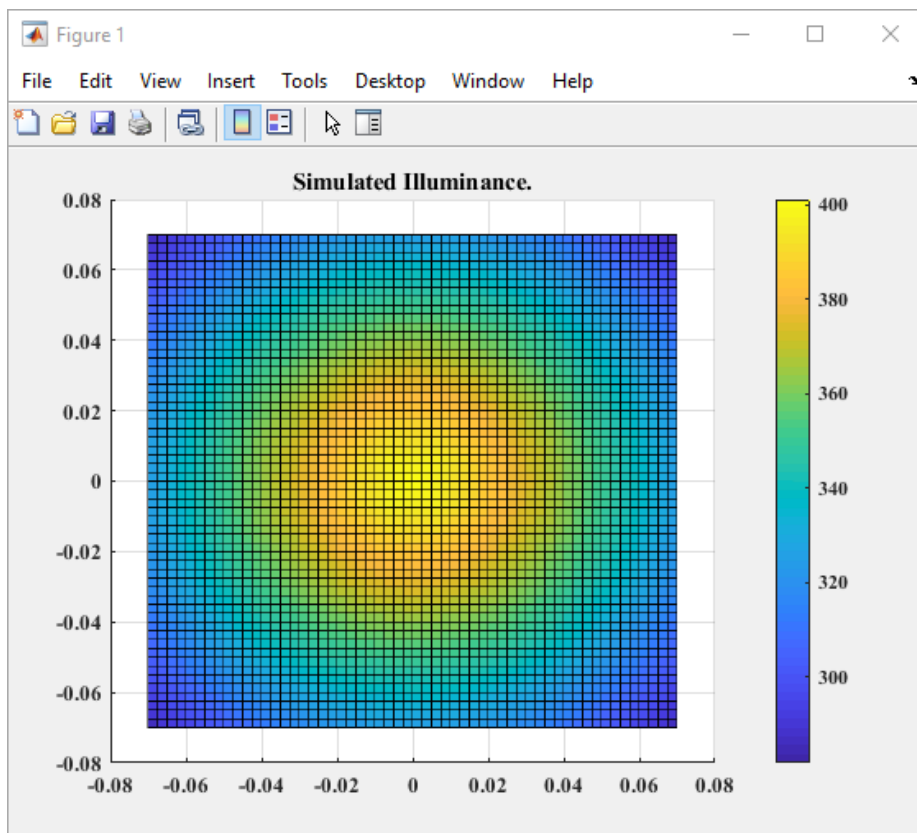


Figure 60 Simulated Illuminance

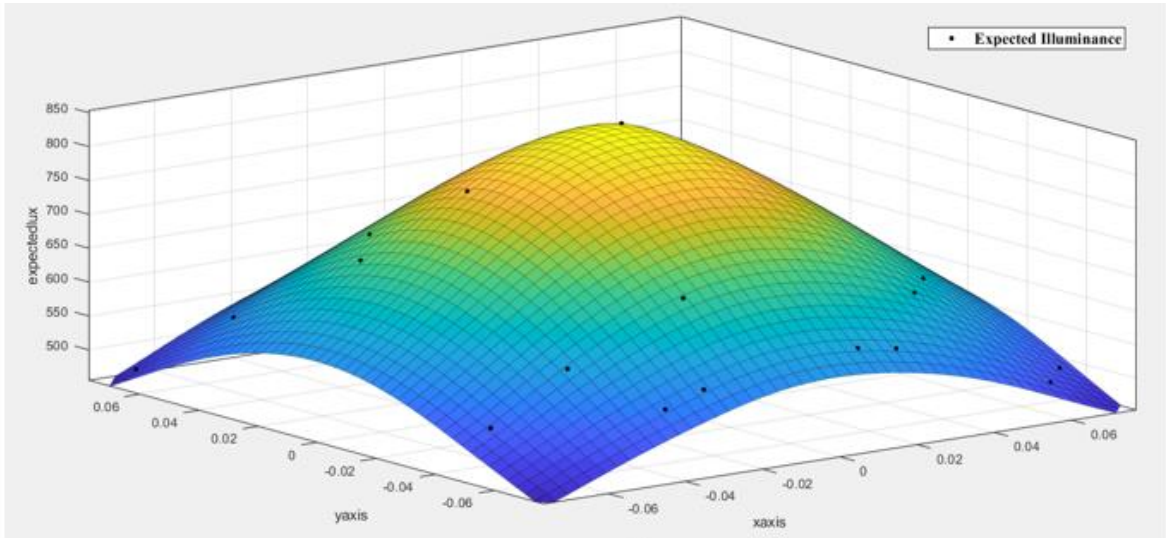
Subsequently, a table of values is presented through which the expected illuminance values are compared with the finally measured values, along the test plane.

x	y	z	Measured Lux	Expected Lux
0.01	0.01	0.21	832	834.3107
0.01	0.05	0.21	738	687.4279
0.01	0.07	0.21	663	597.4749
0.02	0.01	0.21	815	806.0242
0.02	0.05	0.21	726	674.531
0.02	0.07	0.21	660	587.9516
0.03	0.01	0.21	797	770.4785
0.03	0.05	0.21	710	654.2717
0.03	0.07	0.21	637	572.6806
0.04	0.01	0.21	764	730.4172
0.04	0.03	0.21	700	691.8659
0.04	0.05	0.21	689	628.094
0.04	0.06	0.21	652	591.1003
0.04	0.07	0.21	602	552.5191
0.044	0.065	0.21	595	562.115
0.05	0.01	0.21	726	687.4279
0.05	0.02	0.21	665	674.531
0.05	0.04	0.21	621	628.094
0.05	0.05	0.21	666	597.4979
0.05	0.07	0.21	597	528.4392
0.06	0.01	0.21	700	642.7664
0.06	0.05	0.21	627	563.8746

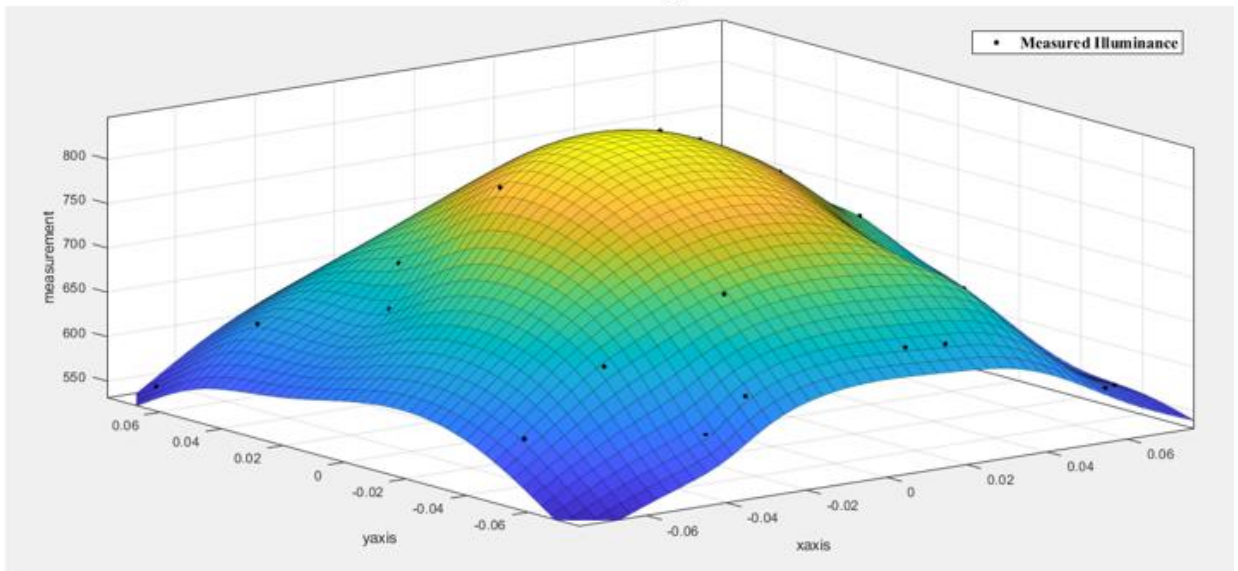
0.06	0.07	0.21	581	501.4419
0.07	0.01	0.21	657	597.4979
0.07	0.05	0.21	599	528.4392
0.07	0.06	0.21	568	501.4419
0.07	0.07	0.21	545	472.4795

TABLE XIV Measured -Expected Illuminance - Single LED Topology.

In the following graphs, the results obtained by the algorithm for the expected Illuminance given that a LED -with the specifications used in the previous experiments- is placed are shown in comparison, as well as the measurements that were finally obtained are depicted. More specifically, the results obtained after comparing the simulation and the measurements are presented graphically in Fig. 4.6. Fig. 4.7 shows the contour plots for the same conditions.

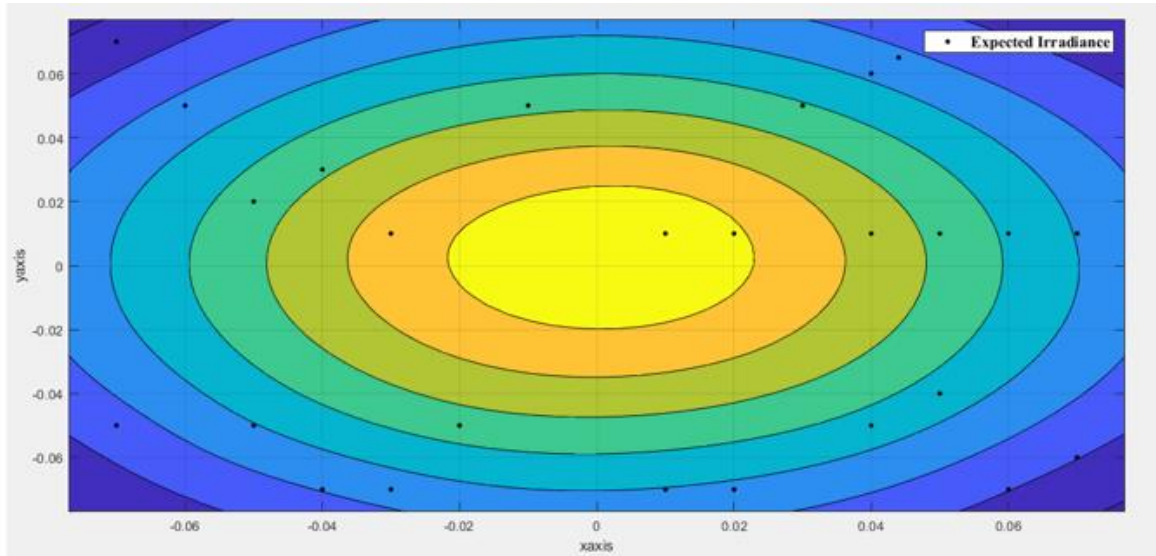


(a)

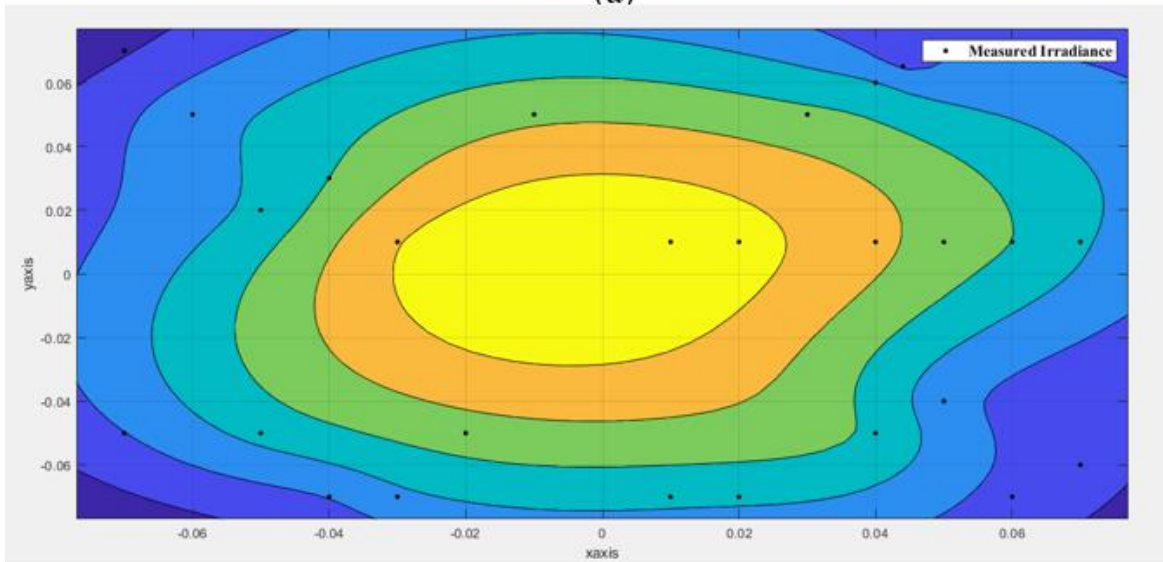


(b)

Figure 61 Comparison of Illumination curves. (a) Expected Illumination curve, (b) Measured Illumination curve.



(a)



(b)

Figure 62 Comparison of contour graphs. (a) Expected Irradiance contour graph, (b) Measured Irradiance contour graph.

4.3 2x2 matrix measurements

For reasons mentioned in the previous chapter, different sets of measurements and predictions were made for the Illuminance. Based on the results extracted by the already analyzed algorithm, it was decided to study the arrangement, where the LEDs are placed squarely.

The algorithm was confronted with the following assumptions throughout the simulation test in order to determine the optimum (appropriate) LED placement. The placement points of the light sources are shown in Fig. 4.8 and the results from modeling the Illuminance and arranging the LEDs in a square configuration are shown in Fig. 4.9.

The dimensions of the of the surface is 18 x 18 cm, at a distance of 31 cm of the Square LED array. The LEDs' positions are marked in the graph with red dots, too. In addition, the 2 x 2 square LED array was chosen with the LEDs distanced at 18 cm, setting $\theta=1.0471975512$ rad, $m=1.1407$ and the Radiometric Flux at 442 mW.

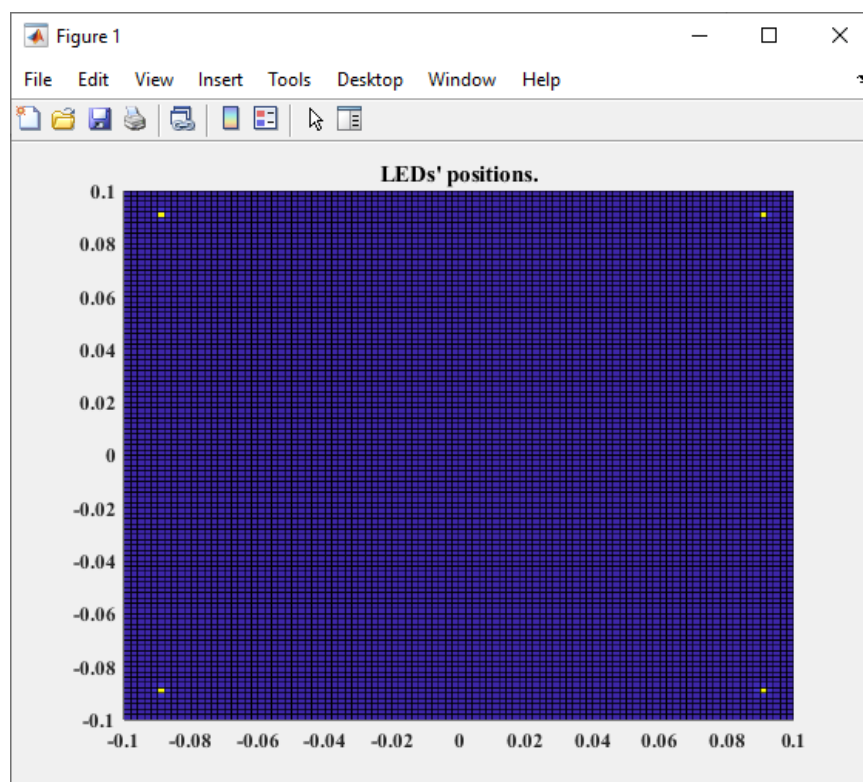


Figure 63 LEDs positions.

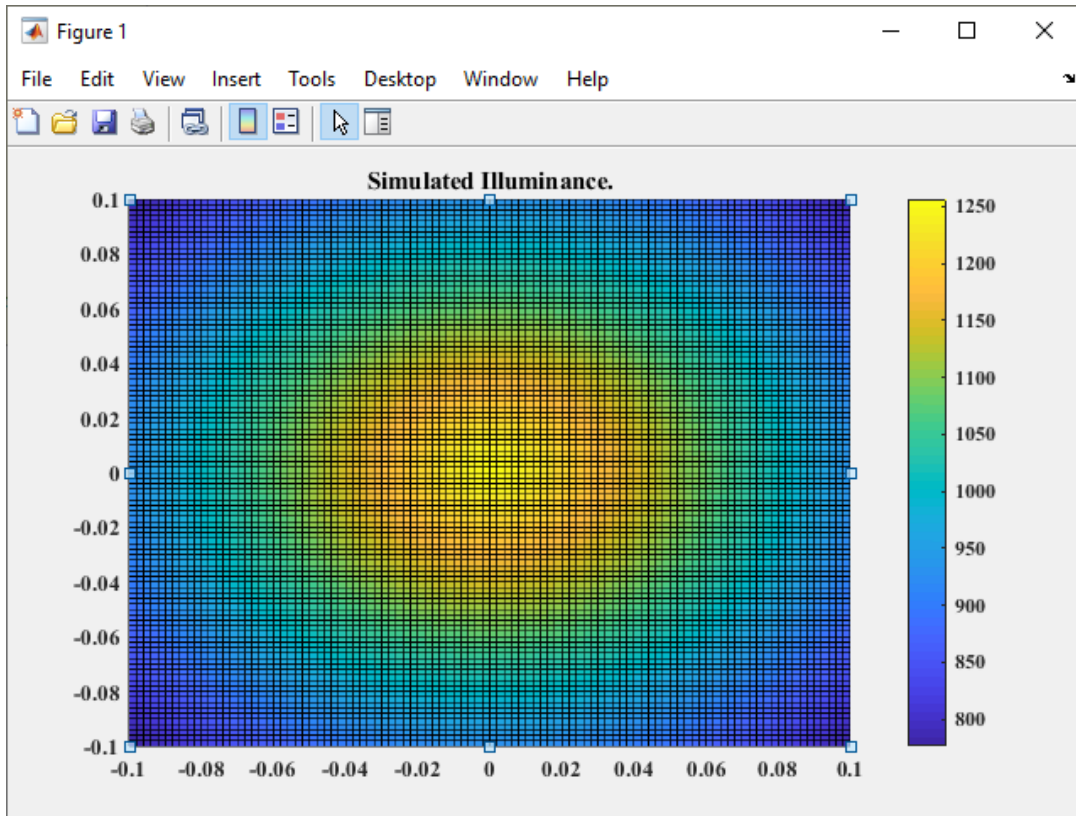


Figure 64 Simulated Illuminance.

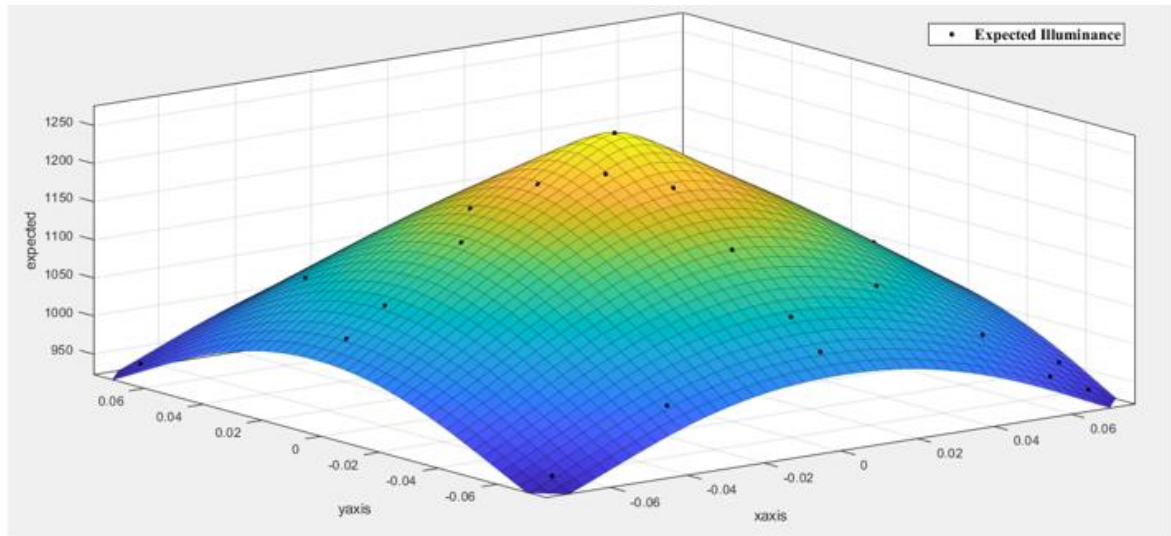
Subsequently, a table of values is presented through which the expected illuminance values are compared with the finally measured values, along a test plane.

x	y	z	Measured Lux	Expected Lux
0	0	0.31	1183	1258.7
0	0.02	0.31	1181	1207.5
0	0.04	0.31	1172	1147.4
0	0.06	0.31	1157	1080.4
0	0.07	0.31	1144	1044.9
0	-0.02	0.31	1174	1207.5
0	-0.04	0.31	1152	1147.4

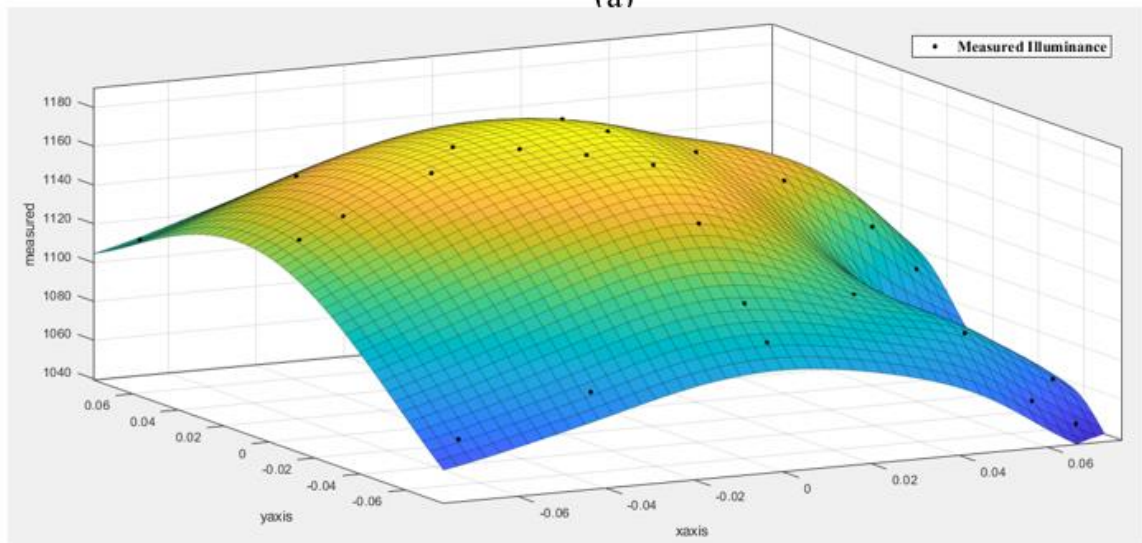
0	-0.06	0.31	1119	1080.4
0	-0.07	0.31	1103	1044.9
0.02	0	0.31	1168	1207.5
0.04	0	0.31	1149	1147.4
0.06	0	0.31	1121	1080.4
0.07	0	0.31	1097	1044.9
-0.02	0	0.31	1178	1207.5
-0.04	0	0.31	1170	1147.4
-0.06	0	0.31	1152	1080.4
-0.07	0	0.31	1142	1044.9
0.02	0.03	0.31	1165	1159.9
0.04	0.06	0.31	1126	1037.7
-0.03	0.01	0.31	1177	1173.5
-0.05	0.04	0.31	1154	1066.5
-0.01	-0.01	0.31	1177	1223.5
-0.04	-0.07	0.31	1086	1006.7
0.06	-0.01	0.31	1083	1077.5
0.03	-0.05	0.31	1113	1086.4
0.05	-0.06	0.31	1093	1016
0.06	-0.07	0.31	1060	963.9871
-0.07	-0.07	0.31	1068	938.5533
0.07	-0.06	0.31	1065	963.9871
0.07	-0.07	0.31	1046	938.5533
0.07	0.07	0.31	1078	938.5533
-0.07	0.07	0.31	1113	938.5533

TABLE XV Measured -Expected Illuminance - Square LED Topology.

More specifically, the results obtained after comparing the simulation and the measurements are presented graphically in Fig. 4.10. Fig. 4.11 shows the contour plots for the same conditions.

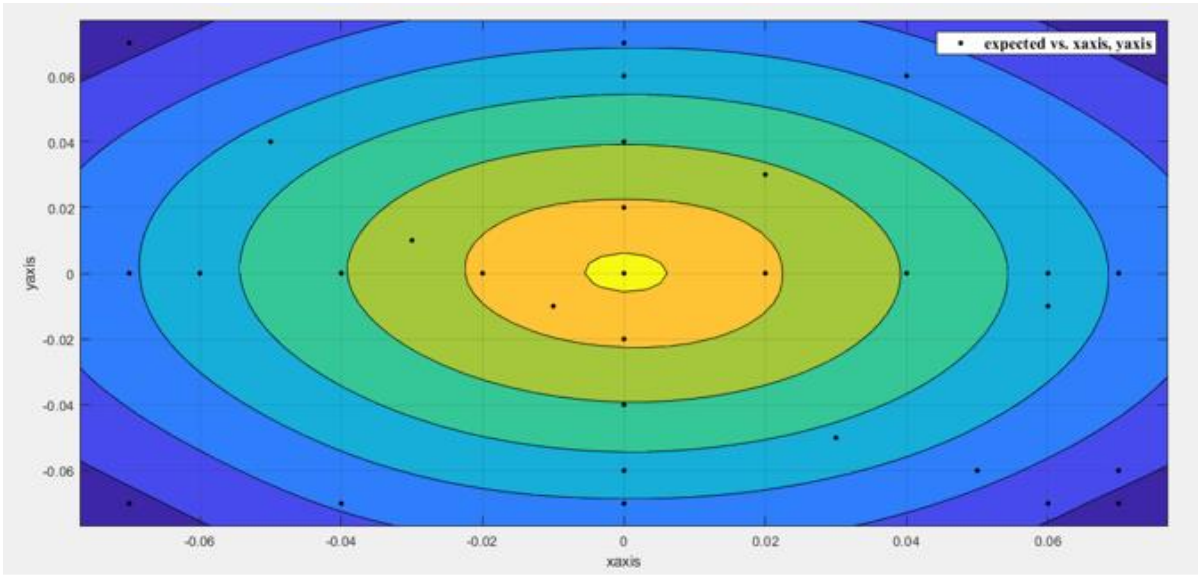


(a)

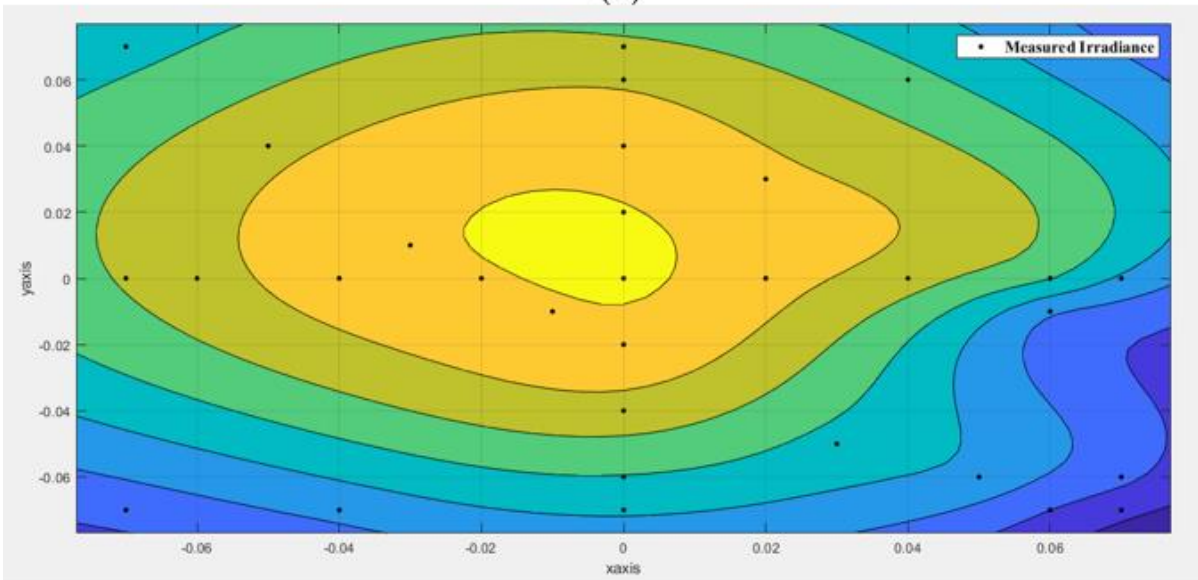


(b)

Figure 65 Comparison of Illumination curves for the 2x2 LED array. (a) Expected Illumination curve, (b) Measured Illumination curve.



(a)



(b)

Figure 66 Comparison of contour graphs for 2x2 LED array. (a) Expected Irradiance contour graph, (b) Measured Irradiance contour graph.

5 Evaluation and interpretation of results

5.1 Evaluation

The way an LED or an LED array distributes light towards the photoluminescent surface is one of the most crucial requirements that must be taken into account throughout both the design and development of the application. Next the ways of evaluating the results are mentioned.

5.1.1 Uniformity of illumination distribution

The illumination of an area is produced by the lighting, according to the definition of light uniformity. When uniformity of illumination is examined, we commonly refer to the ratio of minimum illumination. Uniformity comes as a result from the following formula:

$$U_1 = \frac{E_{min}}{E_{average}}$$

$$U_2 = \frac{E_{min}}{E_{maximum}}$$

(34)

Where U and E, stands for uniformity and illuminance respectively.

5.1.2 ΔE

For quantifying the non – homogeneity of illumination, the percentage of irradiance variation ΔE over a region of the illuminated area is [35]:

$$\Delta E = \frac{E_{max} - E_{min}}{E_{max}}$$

(35)

where, E_{max} and E_{min} are the maximum and the minimum values of irradiance [W/m^2] in the entire test plane.

5.1.3 R (Ratio)

Furthermore, the minimum – to – maximum Irradiance ratio across the illuminated region, is also a method for measuring lighting uniformity, where [35]:

$$R = \frac{E_{min}}{E_{max}}$$

(36)

where, E_{max} and E_{min} are the maximum and the minimum values of irradiance [W/m^2] in the entire test plane.

6 Conclusion

LEDs are gaining more and more ground compared to the use of halogen lamps (or any other light source). This significant turn of interest in the light emitting diode is due to their lifespan and low power consumption.

In this thesis, concepts related to natural and artificial light sources were analyzed. Emphasis was given to light simulators, their architecture, and their characteristics. Then, the light emitting diodes, as light sources, their efficiency, and their operating parameters were analyzed. was carried out, modeling of a multi-source light simulator and a large range of topologies is presented, where the irradiance distribution can be calculated, through a system of analytical equations.

Detailed design guidelines for a light simulator are provided, whose main criterion is the minimization of non-Uniformity. Through these guidelines it is possible to achieve the stabilization of the distribution of Irradiance over a test plane with specific dimensions. All the above findings were tested and verified in a light simulator – experimental setup.

7 Future Work

Aiming at achieving the upgrade – evolution of the already existing study, this work is intended to be the starting point of a series of works.

Initially, it is expected that optics will be mounted in the next work, in order to test light sources with different viewing angles (FWHM). The purpose is both to examine light sources with a small or large viewing angle as well as to examine their co-operation.

It is also intended to reanalyze all previous topologies, in this case adding optimization features such as inclined plane. a corresponding study is expected to be done in a sufficient range of slopes to satisfy further functions of both the light simulators and the models themselves.

Finally, based on the conclusions drawn from the present work, it is intended to use dimming LEDs in the center of the area defined in the design instructions, for the complete smoothing of the uniformity.

APPENDIX

Appendix I

Inverse Square Law

The inverse square law will be obeyed by any point source whose influence extends infinitely in all directions. This is entirely based on geometric factors. The strength of the source divided by the surface area of the sphere gives the intensity of influence at any given radius, r [40].

The inverse square law, which has a fundamentally geometric origin, is applicable to a wide range of physical phenomena. The inverse square law applies to all point sources of gravitational force, electric field, light, sound, or radiation.

In this study, the radiation propagation was examined. A point source of radiation, whether in Roentgens, rads, or rems, can be described by the following relationship, as it is one of the domains that obeys the general inverse square law. Applying the inverse square law, all exposure measurements will decrease.

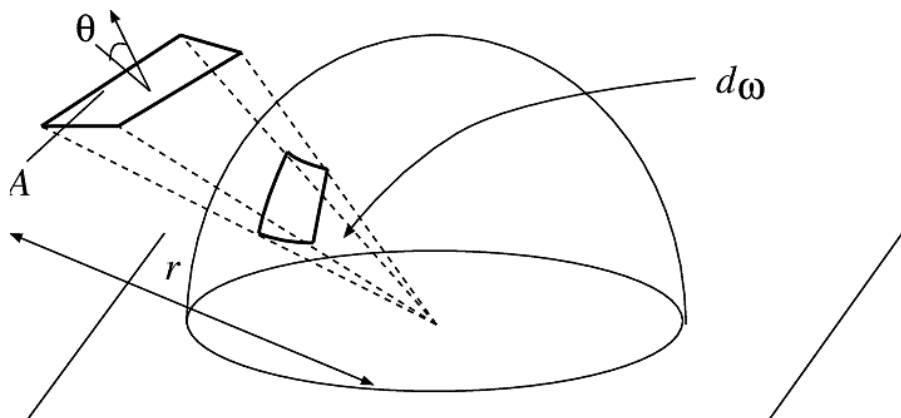


Figure 67 Solid angle

The intensity at surface of sphere is given by the following formula:

$$\frac{S}{4\pi r^2} = I$$

(37)

Which means that the energy twice as far from the source is spread over four times the area, hence one – fourth the intensity (Fig. AI.2).

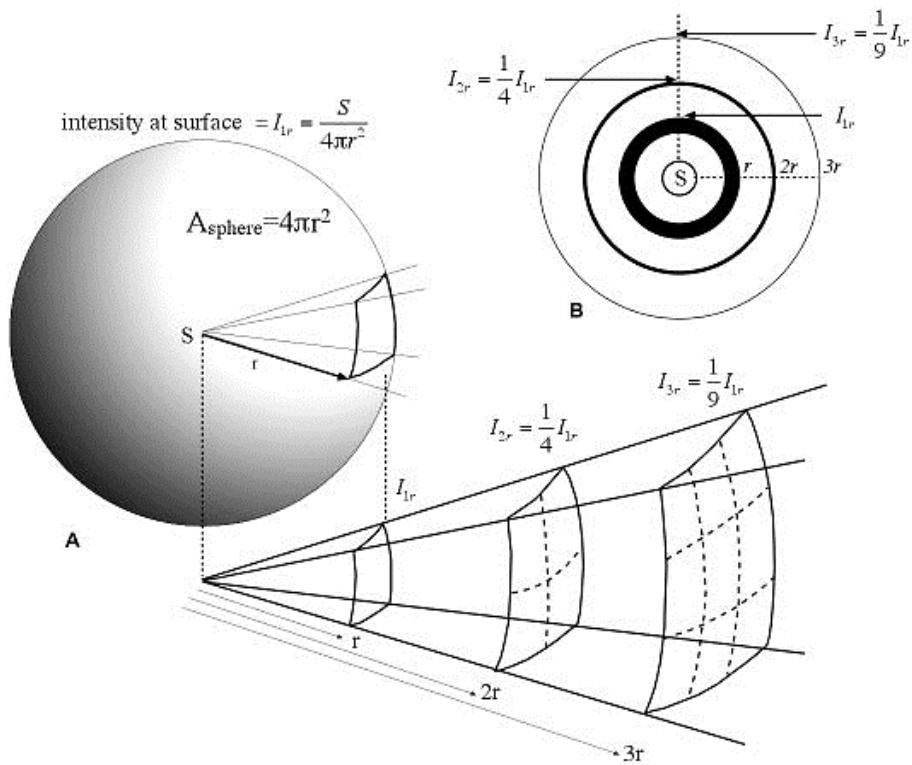


Figure 68 Inverse Square Law [41]

Appendix II

Turning Points [42]

A stationary point at which the gradient (or the derivative) of a function change sign, so that its graph does not cross a tangent line parallel to x – axis, is called the turning point.

Thus, a turning point is a critical point where the function turns from being increasing to being decreasing (or vice versa), i.e., where its derivative changes sign.

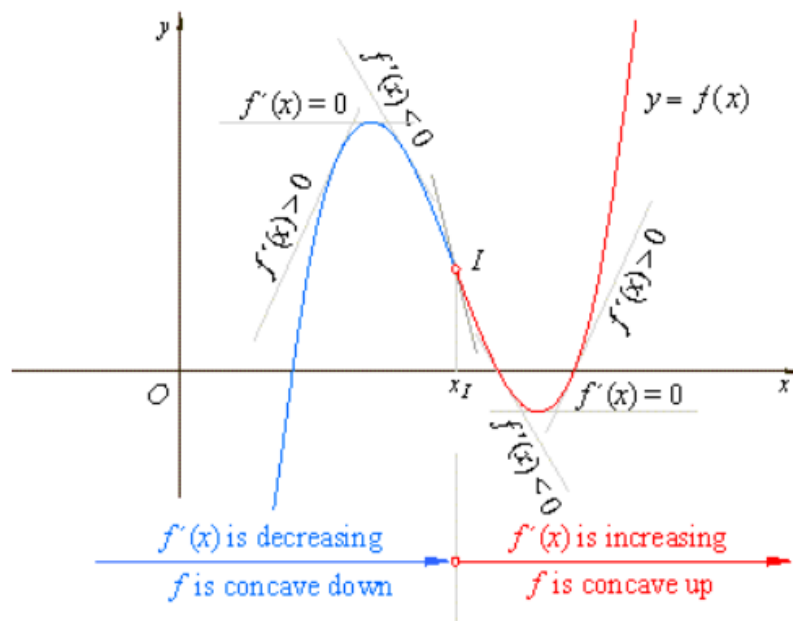


Figure 69 Turning Points

A local (or relative) maximum is a point where the function turns from being increasing to being decreasing, i.e., where its derivative changes sign from positive to negative.

Thus, if the derivative of a function is decreasing over an interval, the graph of the function is concave down.

A local (or minimum) is a point where the function turns from being decreasing to being increasing, i.e., where its derivative changes sign from negative to positive.

BIBLIOGRAPHY

- [1] S. S. Siva Ramakrishna Madeti, "Monitoring system for photovoltaic plants: A review," *Renewable and Sustainable Energy Reviews*, pp. 1180-1207, January 2017.
- [2] J. S. N. M. H. M. Mahbubur Rahman, "Global modern monitoring systems for PV based power generation: A review," *Renewable and Sustainable Energy Reviews*, pp. 4142-4158, February 2018.
- [3] M. G. M. M. M. A. M. A. Ala Al-Fuqaha, "Internet of Things: A Survey on Enabling Technologies, Protocols, and Applications," *IEEE Communications Surveys & Tutorials*, pp. 2347-2376, 15 June 2015.
- [4] NREL Transforming Energy, [Online]. Available: <https://www.nrel.gov/pv/cell-efficiency.html>.
- [5] PowerFilm, [Online]. Available: https://gr.mouser.com/datasheet/2/1009/Electronic_Component_Spec_Sheet_Cla_77DEA84523C82-1658524.pdf.
- [6] G. Stark, "Britannica," [Online]. Available: <https://www.britannica.com/science/light/Early-particle-and-wave-theories>. [Accessed 24 October 2022].
- [7] "Britannica," [Online]. Available: <https://www.britannica.com/science/color/Geometrical-and-physical-optics>.
- [8] Kalmbach Media, "Astronomy," 06 February 2020. [Online]. Available: <https://astronomy.com/magazine/ask-astro/2020/02/what-elements-does-the-sun-contain>.
- [9] LibreTexts, "GEOSCIENCES," [Online]. Available: [https://geo.libretexts.org/Bookshelves/Meteorology_and_Climate_Science/Book%3A_Fundamentals_of_Atmospheric_Science_\(Brune\)/06%3A_Atmospheric_Radiation/6.05%3A_The_Solar_Spectrum](https://geo.libretexts.org/Bookshelves/Meteorology_and_Climate_Science/Book%3A_Fundamentals_of_Atmospheric_Science_(Brune)/06%3A_Atmospheric_Radiation/6.05%3A_The_Solar_Spectrum).
- [10] National Aeronautics and Space Administration, "NASA," March 2013. [Online]. Available: <https://imagine.gsfc.nasa.gov/science/toolbox/emspectrum1.html>. [Accessed

24 October 2022].

- [11] Vebantu , [Online]. Available: <https://www.vedantu.com/physics/light-sources>.
- [12] Wikipedia, [Online]. Available: https://en.wikipedia.org/wiki/Solar_irradiance.
- [13] A. H. Charles Q. Choi, "Space.com," © Future US, Inc. Full 7th Floor, 130 West 42nd Street, New York, NY 10036., 21 April 2022. [Online]. Available: <https://www.space.com/57-stars-formation-classification-and-constellations.html>. [Accessed 24 October 2022].
- [14] S. Lawal, "The New York Times," 10 February 2020. [Online]. Available: <https://www.nytimes.com/2020/02/10/climate/lightning-africa-climate-change.html>.
- [15] Tnuda Center, "Tnuda," 28 February 2016. [Online]. Available: [https://www.tnuda.org.il/en/physics-radiation/infrared-visible-light-and-soft-ultraviolet-radiation-%E2%80%93-introduction/artificial#Light%20Emitting%20Diode%20\(LED\)%20lamps](https://www.tnuda.org.il/en/physics-radiation/infrared-visible-light-and-soft-ultraviolet-radiation-%E2%80%93-introduction/artificial#Light%20Emitting%20Diode%20(LED)%20lamps). [Accessed 25 October 2022].
- [16] Arend, "AREND INVESTING LIGHT," [Online]. Available: <https://arendlighting.com/lighting-efficiency/?lang=en>.
- [17] Enlitech, "Enlitech," [Online]. Available: <https://enlitechnology.com/blog/pv/ss-x-solar-simulator/solar-simulator-01/>.
- [18] Thames Radio Optics, "Thames Radio Optics," [Online]. Available: <https://www.radio-optics.com/en-US/Light-Sources/Incoherent-Light-Sources/Solar-Simulators/Class-AAA-Solar-Simulators.aspx?ID=50#>.
- [19] G2V, "G2V, Engineer the Sun," [Online]. Available: <https://g2voptics.com/iec-60904-9-2020/>.
- [20] D. Y. Ohno, OSA Handbook of Optics, Volume III Visual Optics and Vision, Chapter for Photometry and Radiometry, 1999.
- [21] A. Batista-Leyva, "Radiometry and Photometry: Two Visions of One Phenomenon," *REVISTA CUBANA DE FÍSICA*, 2019.

- [22] C.-C. S. Ivan Moreno, "Modeling the radiation pattern of LEDs," *Optic Express*, 2008.
- [23] "wikipedia," [Online]. Available:
https://en.wikipedia.org/wiki/CIE_1931_color_space#CIE_standard_observer.
- [24] LUMINUS Devices, "Luminus," [Online]. Available:
<https://luminusdevices.zendesk.com/hc/en-us/articles/4403685063437-What-do-CCT-CIE-and-SPD-mean-in-LED-lighting->.
- [25] [Online]. Available: <https://sites.google.com/site/frcrphysicsnotes/electromagnetic-radiation>.
- [26] Conservation Mart, "Conservation Mart," [Online]. Available:
<https://www.conservationmart.com/blog/index.php/what-does-high-cri-mean/>.
- [27] LEDinside, [Online]. Available:
https://www.ledinside.com/knowledge/2012/9/basic_characteristics_light_sources_20120917.
- [28] microstar, "LEDs VS Traditional light sources," [Online]. Available:
<https://www.microstarlight.com/led-lighting-vs-traditional-light-sources/>.
- [29] M. S. Cengiz, "Efficiency relationship of LED parameters in solid state lighting," *JOURNAL OF SCIENCE AND TECHNOLOGY*, vol. 1, no. 1, 2019.
- [30] Δ. Κολοβός, *Μελέτη Συστήματος Ελέγχου LEDs*.
- [31] [Online]. Available: <https://en.wikipedia.org/wiki/OLED>.
- [32] Sera, "SERATEchnologies," [Online]. Available: <https://www.seratechnologies.com/>.
- [33] C. -. C. S. Ivan Moreno, "Three-dimensional measurement of light-emitting diode radiation pattern: A rapid estimation," *Measurement Science and Technology*, 2009.
- [34] [Online]. Available: https://en.wikipedia.org/wiki/Full_width_at_half_maximum.
- [35] I. Moreno, "Configurations of LED arrays for uniform illumination," *The international Society for Optical Engineering*, 2004.

- [36] M. A.-A. R. I. T. Ivan Moreno, "Designing light-emitting diode arrays for uniform near-field irradiance," *Applied Optics*, 2006.
- [37] G. D. C. K. I. M. Vasiliki Naskari, "Design and implementation of an indoors light simulator," Ioannina, Greece, 2022.
- [38] X. & Σ. Λ. 2. Κουτσός, "Σχεδίαση και ανάπτυξη συστήματος αξιολόγησης επιδόσεων Φ/Β στοιχείων. Πτυχιακή εργασία. Αρτα: Τ.Ε.Ι. Ηπείρου. Σχολή Τεχνολογικών Εφαρμογών. Τμήμα Μηχανικών Πληροφορικής Τ.Ε.," [Online]. Available: <https://apothetirio.lib.uoi.gr/xmlui/handle/123456789/13049>.
- [39] Luminus Device, *Luminous Devices, SST - 20 - W Product Datasheet*, 2020.
- [40] [Online]. Available: <http://hyperphysics.phy-astr.gsu.edu/hbase/Forces/isq.html>.
- [41] [Online]. Available: <http://www.csun.edu/science/books/sourcebook/chapters/15-geometric-principles/inverse-square.html>.
- [42] ", " [Online]. Available: <http://www.nabla.hr/CL-IntroToFunctAC.htm>.
- [43] "wikipedia," [Online]. Available: https://en.wikipedia.org/wiki/Color_rendering_index.

